ASSESSMENT OF URBAN ROAD RUNOFF POLLUTION AND TREE-BASED REMEDIATION METHODS

LIN YINGHONG

PhD

The Hong Kong Polytechnic University

2026

The Hong Kong Polytechnic University

Department of Civil and Environmental Engineering

Assessment of Urban Road Runoff Pollution and Tree-Based Remediation Methods

Lin Yinghong

A Thesis Submitted in Partial Fulfilment
of the Requirements for the Degree of
Doctor of Philosophy

August 2025

CERTIFICATE OF ORIGINALITY

I hereby declare that this thesis is my own work and that, to the best of my knowledge and belief, it reproduces no material previously published or written, nor material that has been accepted for the award of any other degree or diploma, except where due acknowledgment has been made in the text.

(Signed)

LIN Yinghong (Name of student)

ABSTRACT

Urban stormwater runoff is a major nonpoint source of pollution, posing significant challenges to urban water quality management due to its diffuse origins, episodic nature, and complex pollutant mixtures. Rapid urbanization has intensified these challenges, particularly in high-density cities such as Hong Kong, where extensive impervious surfaces facilitate the rapid transport and direct discharge of untreated pollutants into receiving waters. Urban road runoff is a critical contributor to this problem, carrying diverse contaminants—including nutrients, heavy metals, pathogens, organic matter, and emerging pollutants such as microplastics (MPs)—that threaten aquatic ecosystems and public health through eutrophication, toxicity, and bioaccumulation. However, the characteristics, interactions, ecological risks, and effective mitigation of multi-pollutant road runoff, especially MPs, remain insufficiently understood in compact urban environments.

This study integrates large-scale field characterization with nature-based mitigation to advance the understanding and management of urban road runoff pollution in Hong Kong. First, stormwater runoff from six representative urban road sites was monitored across 11 rainfall events over 17 months (2021–2022). A total of 32 water quality parameters—including MPs, nutrients, heavy metals, conventional indicators, and microbial contaminants—were analyzed to characterize pollutant dynamics, identify dominant sources and interactions, and assess ecological risks.

Results revealed that microplastic (MP) concentrations in road runoff were particularly elevated during the initial stage of rainfall events. The median MP abundance in road runoff (185 particles L^{-1}) was 4.6 times higher than that in natural rainwater (40 particles L^{-1}). Polyethylene (PE), polypropylene (PP), and polystyrene (PS) were the dominant polymers, with fragments being the most common shape, and more than 60% of MPs measuring smaller than 300 μm. Risk assessment using the Polymer Risk Index (PRI) classified most road sites as pollution classes II–III (PRI = 13.3–138.0), indicating moderate to high ecological risks. MP abundance was significantly influenced by seasonal variability, highlighting urban roads as a major source of MP pollution and underscoring the importance of controlling initial runoff.

In addition, contaminant levels in road runoff were markedly higher than those in natural rainwater; notably, *E. coli* concentrations exceeded rainwater levels by more than four orders of magnitude. Concentrations of organic matter, suspended solids, nutrients, pathogens, and metals exceeded the Water Pollution Control Ordinance (WPCO) objectives in Hong Kong by several to dozens of times. A pronounced first-flush effect was observed for chemical oxygen demand (COD), total suspended solids (TSS), zinc (Zn), and MPs. MPs were positively correlated with pH, *E. coli*, phosphate (PO_4^{3-}), and nitrate nitrogen (NO_3^-–N), and negatively correlated with dissolved oxygen (DO) and iron (Fe), suggesting that MPs may act as vectors for nutrients and pathogens under oxygen-depleted, biologically enriched conditions. Pollutant concentrations varied with land use and season, with higher levels on residential roads and winter peaks for COD, chloride (Cl^-), Zn, Fe, and TSS. Ecological risk assessment indicated very high metal-related risks, primarily driven by lead (Pb) and nickel (Ni), as well as moderate-to-high polymer risks associated with polyvinyl chloride (PVC) and polymethyl methacrylate (PMMA).

Building on these findings, tree-based remediation methods were designed and evaluated to mitigate key road runoff pollutants. A total of 24 banyan tree box filters with different media compositions and six filter columns without trees were constructed and tested through 12 simulated rainfall events over 16 months (2023–2025). The tree box systems demonstrated high and consistent pollutant removal performance, achieving mean removal efficiencies exceeding 90% for NH_4^+–N, PO_4^{3-}, and Cu, and above 80% for Cr, Zn, and Fe. Compared with unvegetated filter columns, tree boxes exhibited substantially enhanced nitrate removal, underscoring the critical role of tree roots in nutrient retention and transformation. Pollutant removal was strongly influenced by pH dynamics and seasonal variability, reflecting root-mediated biogeochemical regulation. Functional media mixtures, particularly sand–granular activated carbon and sand–biochar, further enhanced nutrient and metal removal. Sustained tree growth under polluted runoff conditions confirmed the long-term viability and ecological compatibility of the system.

Overall, this research demonstrates that urban road runoff represents a significant multi-pollutant and ecological risk in high-density cities, while tree-based remediation methods offer a sustainable, resilient, and multifunctional approach for urban stormwater pollution control.

By integrating comprehensive pollutant characterization with field-scale remediation, this study provides new insights into multi-pollutant dynamics, first-flush behavior, and vegetation-driven treatment mechanisms, supporting the development of effective and space-efficient stormwater management strategies for compact urban environments.

Keywords: Urban road runoff; Stormwater pollution; Microplastics; Heavy metals; First flush effect; Ecological risk assessment; Tree-based remediation methods; Bioretention systems; Sustainable stormwater management; High-density cities; Hong Kong

ACKNOWLEDGMENTS

First and foremost, I would like to express my deepest gratitude to my supervisor, Professor Yuhong Wang, for providing me with the opportunity to pursue my Ph.D. at The Hong Kong Polytechnic University. His invaluable guidance, unwavering support, and continuous encouragement have been instrumental throughout my academic journey. He was always available for insightful discussions and helped me navigate the various challenges encountered during my research. Without his mentorship and dedication, this thesis would not have been possible. His guidance has made a lasting impact on my academic and personal development.

I would also like to extend my sincere appreciation to the University Research Facility in Chemical and Environmental Analysis (URF-CEA) at The Hong Kong Polytechnic University for their technical support in Raman spectroscopy analysis. I am also deeply thankful to Professor Kar-Hei Fang and Dr. Yuen-Wa Ho from the Department of Food Science and Nutrition at The Hong Kong Polytechnic University for their invaluable guidance and assistance in microplastic testing.

My heartfelt thanks go to my group members and colleagues in our lab for their generous help with sample collection, as well as their academic collaboration and personal support. I have truly enjoyed working with them and deeply appreciate their unique strengths and camaraderie. I am also thankful to all the staff and students in the Department of Civil and Environmental Engineering for creating a stimulating and supportive research environment.

Lastly, I would like to express my deepest gratitude to my family for their unconditional love and unwavering support. Their belief in me has been a constant source of motivation and strength throughout this journey.

TABLE OF CONTENTS

CHAPTER 1. INTRODUCTION

1.1 Research Background

Currently, urban land occupies only 0.69% of Earth's total surface area (Zhao et al., 2021), yet approximately 58% of the global population—over 5 billion people—resides within these urban regions (UN, 2024). This rapid urbanization has placed significant pressure on freshwater resources and exacerbated urban water pollution. As urban populations, infrastructure, and industries become increasingly interconnected, urban waters are burdened by pollutants from diverse sources, including residential wastewater, industrial discharges, and stormwater runoff from impervious surfaces (EPA, 2024). Among these sources, stormwater runoff, typically classified as non-point source pollution, represents a significant challenge for water quality management due to its diffuse distribution, episodic nature, and varied pollutant composition. The widespread expansion of impervious surfaces such as roads, pavements, and rooftops has substantially increased runoff volumes during rainfall events. This runoff readily mobilizes and transports a wide range of contaminants, which are often discharged directly into rivers, lakes, or coastal waters without treatment, thereby significantly contributing to the degradation of urban aquatic environments (Cho et al., 2023; Gomes & Wai, 2020).

Previous studies have shown that these contaminants pose significant risks to both aquatic ecosystems and human health, with each pollutant group presenting distinct ecological and toxicological concerns. For instance, excessive nutrients such as nitrogen (N) and phosphorus (P) can trigger eutrophication, which leads to algal blooms, reduced dissolved oxygen levels, and the subsequent degradation of aquatic habitats (Smith et al., 2020). Toxic heavy metals such as lead (Pb), chromium (Cr), arsenic (As), zinc (Zn), cadmium (Cd), copper (Cu), and nickel (Ni) have been widely recognized for their adverse effects on human and environmental health. These metals are associated with a range of serious health conditions, including carcinogenicity, neurotoxicity, and reproductive dysfunction (Ahmed et al., 2022; Briffa, Sinagra, & Blundell, 2020; Taka et al., 2022; Xue, Zhao, & Liu, 2020). In parallel, microplastics (MPs) have recently emerged as a new class of urban contaminants of growing concern.

Defined as plastic particles smaller than 5 mm in diameter (EU, 2023), MPs are characterized by their small size, chemical persistence, and resistance to environmental degradation. These properties enable MPs to adsorb and transport toxic substances across aquatic systems. Once introduced into the environment, MPs can be ingested by aquatic organisms and bioaccumulate along the food chain, ultimately posing significant ecological risks and potential health threats to humans (Ding et al., 2022; W. Huang et al., 2021; Rico et al., 2023; Senathirajah et al., 2021).

Urban roadways have emerged as one of the most significant sources of stormwater runoff pollution in urban environments. Previous studies have demonstrated that pollution from urban road runoff is highly complex and diverse, involving strong interrelationships among various pollutants. A wide range of contaminants has been identified in road runoff, including heavy metals (e.g., Zn, Cu, Pb, Ni, Cd), organic matter indicators (e.g., COD), suspended solids (SS), nutrients (e.g., nitrogen and phosphorus), polycyclic aromatic hydrocarbons (PAHs), and pathogens such as *E. coli* (Aryal et al., 2010; Hwang et al., 2016; Kayhanian et al., 2012). Notably, total metal concentrations have been found to correlate strongly with total organic carbon (TOC) and suspended solids (Helmreich et al., 2010). These pollutants primarily originate from the accumulation of vehicular residues, atmospheric deposition, tire and brake wear particles, and other anthropogenic activities (Cho et al., 2023; Du et al., 2019; Lee et al., 2020; V. C. Shruti et al., 2021; Treilles et al., 2021). However, the concentrations and composition of these pollutants are influenced by a variety of factors, including geographical conditions, rainfall characteristics, seasonal variations, land use types, and traffic density (Codling et al., 2020; Wang et al., 2013; Wicke et al., 2021). Therefore, targeted investigations of urban road runoff pollution should consider the specific characteristics of each city. Recent research has highlighted the importance of exploring the correlations between emerging contaminants such as microplastics (MPs) and co-occurring pollutants, including nutrients, heavy metals, and organic matter, to better understand their interactions and cumulative environmental impacts.

Urban road runoff is also highly dynamic and event-driven. One critical phenomenon is the first flush effect (FFE), wherein a disproportionately high load of pollutants is transported during the early stages of rainfall. This initial runoff typically contains elevated concentrations of pollutants such as total suspended solids (TSS), Zn, and Cu, imposing acute stress on aquatic environments in a short period (Chebbo, 1999; Hathaway et al., 2012b; Kayhanian & Stenstrom, 2021; Saget, Chebbo, & Bertrand-Krajewski, 1996; Wang, Feng, & Min, 2023). Consequently, managing the first flush has become a critical aspect of source control strategies. Traditional practices include the design of road inlet grates and pre-treatment structures to intercept and filter out particulate matter and associated pollutants before they enter the storm drain system. These interventions help reduce pollutant loads at the source and improve the overall effectiveness of downstream stormwater management systems.

To further address the challenges posed by multiple pollutants in urban stormwater runoff, a range of management frameworks have been developed, including Low Impact Development (LID), Best Management Practices (BMPs), Water Sensitive Urban Design (WSUD), Sustainable Urban Drainage Systems (SUDS), and the Sponge City concept (Fletcher et al., 2015; Liao et al., 2013; Liu, Jia, & Niu, 2017). These strategies aim to integrate green infrastructure or retrofit existing grey infrastructure to reduce runoff volume and improve water quality. However, several limitations remain. In high-density urban environments, space constraints often restrict the implementation of large-scale green infrastructure. However, limitations such as spatial constraints in dense urban environments, system clogging, high maintenance requirements, and limited sustainability often compromise their effectiveness. Additionally, their performance significantly varies depending on local geographic, climatic, and anthropogenic factors, highlighting the need for site-specific adaptation and validation.

In response to the limitations of conventional stormwater management approaches, Nature-Based Solutions (NBS) have emerged as more adaptive, resilient, and sustainable alternatives for urban stormwater control (Almenar et al., 2021; Kabisch, Frantzeskaki, & Hansen, 2022). NBS are defined as approaches inspired by or derived from natural processes to address environmental challenges while providing ecological and social benefits (Cohen-Shacham et al., 2016). These solutions aim to enhance ecosystem services through renewable natural processes, reducing dependency on non-renewable interventions (Maes & Jacobs, 2017). In urban stormwater management, NBS integrate natural components such as vegetation, soils, and hydrological processes into engineered systems to mimic and restore natural water cycle functions like infiltration, filtration, evapotranspiration, and pollutant attenuation (Raymond et al., 2017). Biofilters, especially tree box filters that combine engineered filter media with vegetation, have attracted increasing attention for their multifunctionality. These systems effectively reduce runoff volumes and improve water quality through physical filtration, chemical adsorption, and biological uptake (Adegun et al., 2021). Urban roadside trees significantly contribute to these biofilter systems, providing multiple benefits including mitigating urban heat islands, reducing flooding, and enhancing pollutant removal. Tree box filters offer compact, scalable, and site-specific solutions that deliver additional ecological benefits, such as increased urban biodiversity, improved microclimate regulation, and enhanced environmental livability.

Hong Kong represents a typical example of a high-density subtropical metropolis characterized by abundant annual rainfall. With an average annual precipitation of approximately 2,400 mm, it is among the highest in the Asia-Pacific region. The city's coastal location and mountainous topography further increase its vulnerability to tropical cyclones and intense summer rainfall events, frequently resulting in urban flooding. Consequently, there exists significant potential for stormwater harvesting and recycling within Hong Kong. Moreover, the urban drainage infrastructure in Hong Kong employs separate systems for stormwater and sewage, allowing stormwater runoff to bypass centralized treatment facilities and discharge directly into nearby water bodies. The spatial and temporal variability of rainfall events, coupled with the diffuse nature of non-point source pollution, makes the effective control of stormwater pollution particularly challenging.

1.2 Problem Statements

Despite growing attention to urban stormwater pollution, several critical challenges remain unresolved, particularly regarding road runoff in high-density urban environments.

Firstly, the characteristics, dynamic behaviours, and ecological risks of MPs—as emerging contaminants in urban road runoff—remain poorly understood. Limited research has investigated how MP abundance and composition vary with land-use types, seasonal changes, and hydrological conditions during rainfall events. This knowledge gap hampers accurate environmental risk assessment and the formulation of effective pollution control strategies.

Secondly, most existing studies focus predominantly on individual pollutant classes, such as nutrients or heavy metals. There is insufficient research addressing the co-occurrence and interactions of multiple pollutants, particularly involving MPs, in urban runoff. Such complex interactions are rarely incorporated into existing runoff models, significantly constraining our understanding of pollutant dynamics and cumulative ecological risks under real-world urban conditions. Furthermore, integrated analyses of pollutant loading dynamics and associated ecological risks for multiple pollutants in urban road runoff remain largely unexplored.

Thirdly, although Nature-Based Solutions (NBS)—such as tree-box bioretention systems—are increasingly recognized as sustainable approaches for urban stormwater management, their real-world effectiveness in treating diverse pollutants remains insufficiently validated. Specifically, the impacts of engineered filter media (e.g., sand, biochar, granular activated carbon) on pollutant removal efficiency, system resilience, and long-term performance are not adequately understood. Additionally, empirical evaluations of ecological co-benefits associated with tree-based NBS, including tree growth performance and adaptation to seasonal variations, are limited.

Finally, Hong Kong offers a unique context for urban stormwater research due to its high urban development density, subtropical climate, frequent heavy rainfall, and distinct separation between stormwater and sewage systems. While these characteristics create both challenges and opportunities for implementing localized NBS, few integrated studies have comprehensively assessed pollutant dynamics, first flush phenomena, and the effectiveness of NBS under Hong Kong's specific urban and environmental conditions.

1.3 Research Aim and Objectives

This study aims to comprehensively investigate the characteristics, ecological risks, dynamic behaviour, and mitigation strategies of MPs and other co-occurring pollutants in urban road runoff under different rainfall events. Eleven rainfall events were monitored between February 2021 and September 2022 across six urban road sites in Hong Kong. A total of 32 stormwater quality indicators—including MPs, nutrients, heavy metals, and conventional parameters—were analyzed to identify key pollutants and assess their interactions and ecological risks, with a particular focus on the early-stage (first flush) runoff. Based on these findings, 24 tree-box filters incorporating different filter media groups (e.g., sand, biochar, granular activated carbon) were designed and constructed. The system's pollutant removal efficiency, seasonal resilience, and tree growth performance were evaluated over 12 simulated rainfall events conducted between December 2023 and April 2025.

The specific objectives of this study are as follows:

1. To investigate the characteristics, dynamic behaviours, and ecological risks of MPs in urban road runoff across various surfaces in Hong Kong, and to evaluate their variation under different influencing factors, including land use types, seasonal conditions, locations, and pavement materials.
2. To identify key stormwater pollutants and analyze their interrelationships, potential sources, and transport mechanisms across 32 stormwater quality parameters. This includes assessing pollutant characteristics under different environmental conditions (e.g., land use types and seasonal variations), evaluating associated ecological risks, and quantifying pollutant loading dynamics.
3. To design and implement a tree-based Nature-Based Solution (NBS) for stormwater treatment, based on the identified levels of key pollutants. The system's pollutant removal performance and ecological co-benefits (e.g., vegetation growth, seasonal adaptability) will be comprehensively evaluated.

1.4 Report Organization

This research is structured into seven chapters, logically divided into three major parts to reflect the progression from problem identification and pollutant characterization to the development and assessment of mitigation strategies.

Part I: Identification of research problem, objectives, and methodology

Chapter 1 introduces the background, research problems, objectives, and overall structure of the study.

Chapter 2 presents a comprehensive literature review, summarizing current knowledge and research gaps related to urban road runoff pollution. It covers the characteristics of multi-pollutants, the dynamics of the first flush effect, and recent developments in urban stormwater management, with a particular focus on Nature-Based Solutions (NBS).

Chapter 3 details the research methodology, including study area selection, sampling strategy, analytical methods, statistical tools, first flush analysis, and risk assessment frameworks.

Part II: Characterization and dynamics of urban road runoff pollutants

This section aims to deepen understanding of the types, behaviors, and ecological risks associated with pollutants in urban road runoff.

Chapter 4 investigates the characteristics, dynamic behavior, influencing factors, and ecological risks of MPs in urban road runoff across different road sites.

Chapter 5 explores the characteristics and interrelationships among multiple pollutants and identifies key pollutants in urban road runoff, and assesses the environmental impacts (e.g., land use, seasonal variance). This chapter also assesses the dynamic behavior and potential ecological risks of these key pollutants.

Part III: Mitigation strategies for urban road runoff pollution

This section introduces and evaluates a practical solution to mitigate road runoff pollution using tree-based NBS.

Chapter 6 details the design, implementation, and performance evaluation of a tree-box filter system tailored for urban stormwater treatment. It examines pollutant removal efficiency, system resilience across seasons, and associated ecological co-benefits.

Chapter 7 summarizes the key findings of the study, discusses its broader implications, and provides recommendations for future research and practical applications in urban stormwater management.

CHAPTER 2. LITERATURE REVIEW

2.1 Current Research on Urban Stormwater Pollution

2.1.1 Sources and pathways of urban road runoff pollution

With rapid urbanization, stormwater runoff has become a major contributor to urban water pollution (Björklund et al., 2018; Lee et al., 2007; Sartor & Boyd, 1972). Urban water pollution primarily originates from two sources: point source pollution and non-point source pollution. Point source pollution refers to any clearly identifiable source from which pollutants are directly discharged, such as factories and wastewater treatment plants. In contrast, non-point source pollution is generated from diffuse sources, primarily rainfall or snowmelt flowing over impervious surfaces, which mobilizes accumulated pollutants and transports them into nearby water bodies such as rivers, lakes, and coastal zones.

As point source pollution has become increasingly well-managed through advances in treatment technologies, non-point source pollution, particularly stormwater runoff, has emerged as a significant threat to urban water bodies (Ballo et al., 2009; Gomes & Wai, 2020; Lee & Bang, 2000; Petrucci et al., 2014). For example, Hong Kong employs separate systems for urban sewage and stormwater drainage. During rainfall events, pollutants that accumulate on impervious urban surfaces are mobilized and often discharged directly into the stormwater drainage network without prior treatment. Figure 2.1 illustrates the urban stormwater drainage process in Hong Kong. Major drainage tunnels on Hong Kong Island intercept stormwater from upland areas and divert it directly into the sea. In contrast, street-level runoff in densely populated lowland zones—where most high-rise residential and commercial buildings are located—is typically conveyed through underground storm drains and discharged untreated into nearby rivers and coastal harbors. These low-lying urban districts, characterized by high-intensity anthropogenic activities, are particularly vulnerable to stormwater pollution, posing substantial ecological and public health risks.

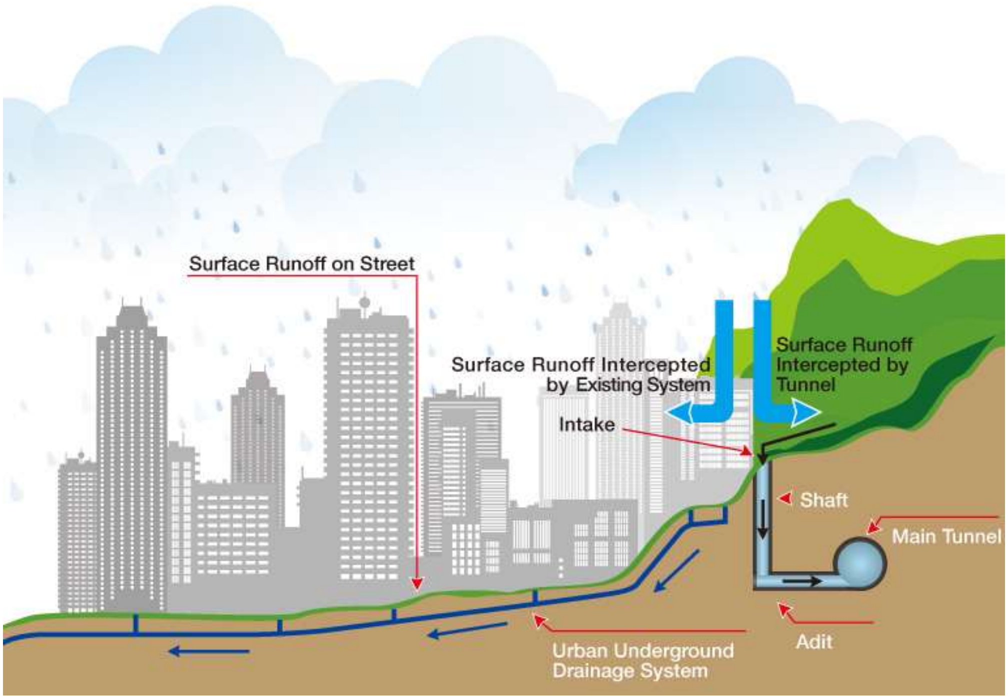

Figure 2.1. The process of urban stormwater drainage in Hong Kong (figure source: https://www.dsd.gov.hk/others/HKWDT/eng/background.html).

Concerns regarding the impact of urban stormwater runoff on water quality can be traced back to the mid-20th century. Pioneering studies by Åkerlindh (1950) and Weibel, Anderson and Woodward (1964) focused primarily on conventional pollutants, including total suspended solids (TSS), chemical oxygen demand (COD), biochemical oxygen demand (BOD), heavy metals (e.g., Cd, Cr, Cu, Ni, Pb, Zn), and nutrients such as nitrogen and phosphorus species. In the 1980s, large-scale initiatives like the U.S. Nationwide Urban Runoff Program (NURP) were implemented to assess stormwater quality across various land use types (Division, 1982). As urban landscapes have evolved, emerging classes of contaminants have gained attention, particularly organic micropollutants and microplastics (MPs). Compounds such as polycyclic aromatic hydrocarbons (PAHs), phthalates, bisphenol A (BPA), and alkylphenols (APs) are now commonly detected in urban runoff, reflecting the growing influence of industrial activities, vehicular emissions, and polymer degradation (Gasperi et al., 2014; Müller et al., 2019; Zgheib, Moilleron, & Chebbo, 2012).

A growing body of research has investigated the sources of pollutants in urban stormwater runoff. Müller et al. (2020) summarized atmospheric deposition, anthropogenic activities, and drainage surfaces as the three primary contributors to stormwater pollution (Figure 2.2). Among these sources, urban roads serve as critical pathways linking pollutant generation sites to receiving water bodies. Vehicular traffic is one of the most significant contributors, producing runoff pollutants through exhaust emissions, fluid leaks, brake and tire wear, road surface abrasion, and vehicle washing. Common contaminants found in road runoff include trace metals, total suspended solids (TSS), and organic matter. Numerous studies have shown that road runoff generally exhibits poorer water quality than roof runoff, especially in terms of TSS, total phosphorus (TP), and COD (Hu et al., 2020; Zhang et al., 2013). Furthermore, the type of road construction material influences pollutant loadings. For instance, asphalt surfaces tend to release higher concentrations of COD and total organic carbon (TOC) compared to concrete surfaces (Drapper, Tomlinson, & Williams, 2000). Additionally, road pavement materials and surface degradation can significantly contribute to elevated levels of TSS, TP, and COD in stormwater runoff.

These findings suggest that urban road runoff is a major non-point source of stormwater pollution and a significant driver of urban water quality degradation. Understanding its characteristics, pollutant composition, and influencing factors is essential for developing effective stormwater management strategies.

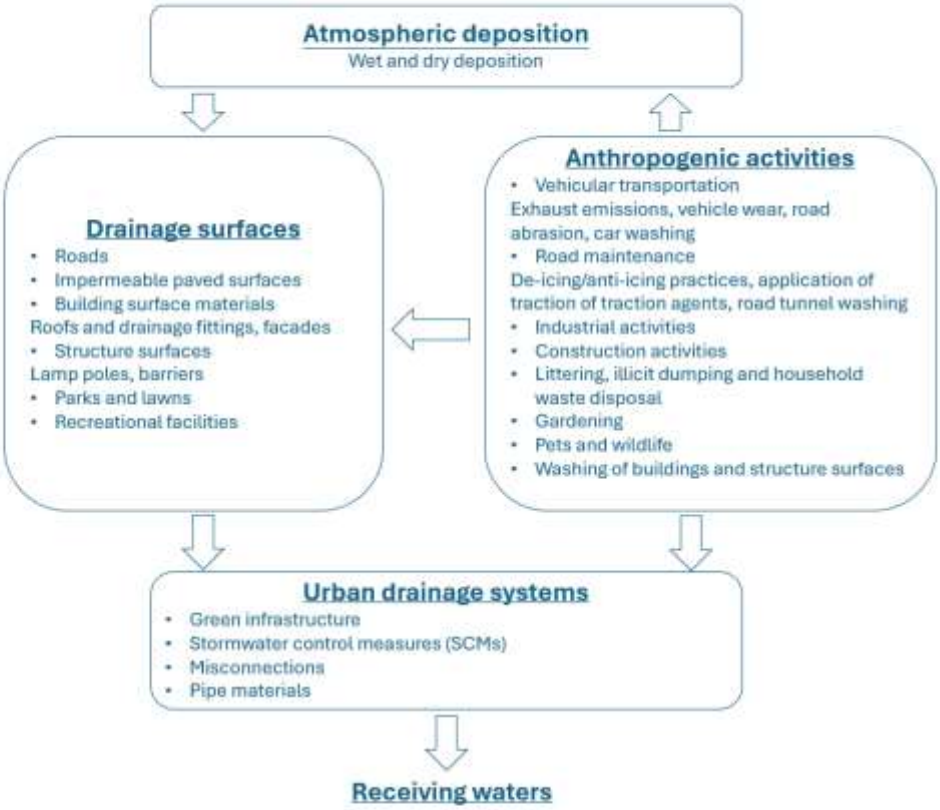

Figure 2.2. The main source categories and pollution transport pathways of urban stormwater pollution sources (Müller et al., 2020).

2.1.2 Characterization of multiple pollutants in urban road runoff

Stormwater pollutants in road runoff were complicated and highly variable. General contaminants were found from stormwater runoff on urban roads, mainly including sediments and suspended solids (SS), nutrients, heavy metals, and organic substances. Among these, heavy metals such as cadmium (Cd), chromium (Cr), copper (Cu), iron (Fe), lead (Pb), nickel (Ni), and zinc (Zn) have received considerable attention due to their toxicity and persistence in the environment (Huber, Welker, & Helmreich, 2016). These metals primarily originate from the chemical components of tire wear, vehicle parts and components, traffic signs, fuel and lubricating oils, and road metallic structures (Aryal et al., 2010; Hwang et al., 2016; Kayhanian et al., 2012). Sediments and SS are major components of road runoff, originating from pavement wear, exhaust emissions, and road construction activities (Aryal et al., 2010; Barbosa, Fernandes, & David, 2012). Notably, strong correlations have been observed between SS concentrations and nutrient levels, particularly nitrogen and phosphorus (Chua et al., 2009). In addition, organic pollutants such as polycyclic aromatic hydrocarbons (PAHs), polychlorinated biphenyls (PCBs), and volatile organic compounds (VOCs) were found in urban runoff. These compounds have raised significant concerns due to their toxicity and persistence (Kayhanian et al., 2012; Ngabe, Bidleman, & Scott, 2000). Their sources include incomplete fossil fuel combustion, tire abrasion, vehicle exhaust emissions, and degradation of asphalt pavements (Barbosa, Fernandes, & David, 2012; Björklund, 2011). Numerous studies have confirmed that these contaminants, including nutrients, heavy metals, and organic substances, can cause severe environmental impacts and pose substantial ecological risks to receiving water bodies (Brezonik & Stadelmann, 2002; Davis, Shokouhian, & Ni, 2001; Färm, 2002; Lee et al., 2004; Ngabe, Bidleman, & Scott, 2000).

Recently, microplastic (MP) pollution in urban stormwater runoff has emerged as a significant environmental concern. Land-based sources are considered the primary contributors, accounting for approximately 80% of total MP inputs (Browne, 2015; Yonkos et al., 2014). Microplastics are defined as plastic particles smaller than 5 mm in diameter (Wagner et al., 2014). Due to their small size and resistance to degradation, MPs are difficult to remove once dispersed in the environment. Figure 2.3 shows the sources, transport pathways, and environmental fate of microplastics in urban stormwater runoff. MPs are commonly discharged into rivers and oceans via urban drainage systems, where they can be ingested by aquatic organisms, leading to degraded water quality and adverse impacts on aquatic ecosystems and human health (Ahmad et al., 2025). Previous studies have demonstrated that MPs pose significant threats to aquatic organisms, including cetaceans, marine mammals, and turtles (Andrady, 2011; Clapham, Young, & Brownell Jr, 1999; Laist, 1997; Mascarenhas, Santos, & Zeppelini, 2004; Tanaka & Takada, 2016). MPs can also act as vectors for toxic chemicals, facilitating their transport through the environment and enhancing their bioavailability, thus contributing to chemical hazards in aquatic ecosystems (Besseling et al., 2017; Koelmans et al., 2016; Tanaka et al., 2015). Alarmingly, studies have identified MPs in the human body, likely entering through the food web, indicating potential risks to human health (Rochman et al., 2015; Wright & Kelly, 2017).

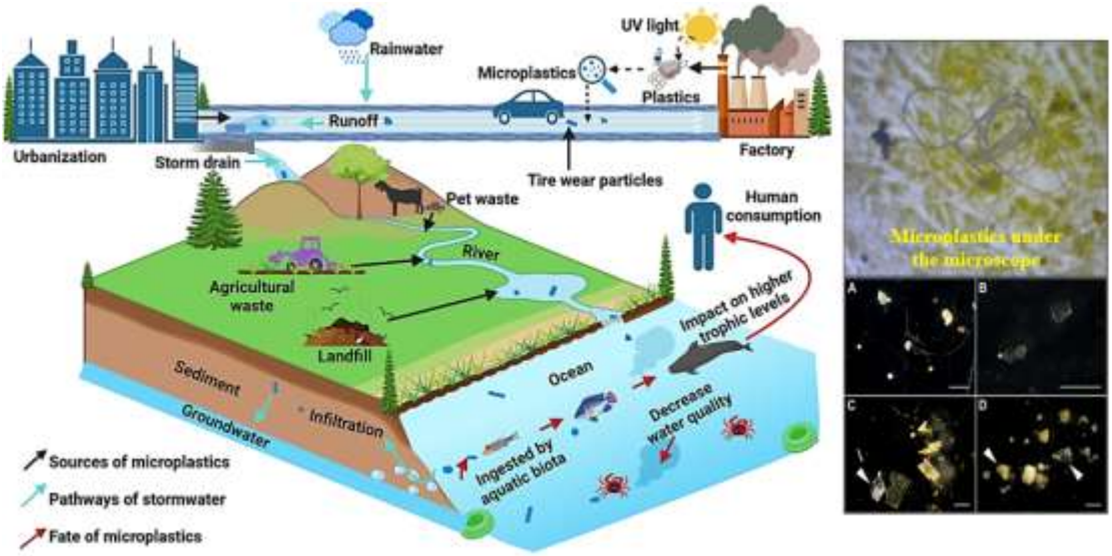

Figure 2.3. Sources, transport pathways, and environmental fate of microplastics in urban stormwater runoff. Images in this figure are adapted from Ahmad et al. (2025) and Wagner et al. (2014).

Studies have reported the presence of abundant MPs in urban road runoff, with common types including polypropylene (PP), polyethylene (PE), polystyrene (PS), and polyethylene terephthalate (PET) (Stang, Mohamed, & Li, 2022; Sugiura et al., 2021; Zhang et al., 2022). In urban environments, road surfaces are a major source of MPs, originating from tire and road wear particles, atmospheric deposition, automotive components, and road markings (Österlund et al., 2023). Moreover, previous studies have demonstrated that suspended solids (SS) and MPs in stormwater runoff act as important vectors for toxic chemicals, facilitating their transport into natural ecosystems and contributing to chemical hazards (Aryal et al., 2010; Besseling et al., 2017; Koelmans et al., 2016).

Several studies have investigated MP pollution in rivers and wastewater treatment facilities in Hong Kong (Cheung, Hung, & Fok, 2019; Fok & Cheung, 2015; Mak et al., 2020). For example, Mak et al. (2020) conducted surveys at four sewage treatment works, including both wastewater and stormwater drainage points, and found high concentrations of MPs, particularly polyethylene (PE) and polypropylene (PP). However, studies focusing on MP pollution from urban road runoff with different land uses in Hong Kong are still lacking, even though Hong Kong has a typical high-density functional zone.

Various environmental factors can significantly influence the pollution levels of stormwater runoff. Numerous studies have demonstrated that land use patterns play a critical role in determining both the type and concentration of pollutants in urban runoff. For example, Lee and Bang (2000) conducted a comprehensive study on stormwater runoff characteristics across nine watersheds in the cities of Taejon and Chongju, Korea, from June 1995 to November 1997. Their findings revealed that pollutant mass loading rates followed the order: high-density residential areas > low-density residential areas > industrial areas > undeveloped urban areas. Similarly, Wang et al. (2013) analyzed the event mean concentrations (EMCs) of stormwater runoff pollutants across six land use types—urban traffic roads (UTR), residential roads (RR), commercial areas (CA), concrete roofs (CR), tile roofs (TRoof), and campus catchment areas (CCA). Their results showed that EMCs of total suspended solids (TSS) and chemical oxygen demand (COD) were significantly higher in runoff from urban traffic roads than from other land use types. These studies highlight the substantial variability in pollutant types and concentrations across different urban contexts, largely driven by variations in land use, human activities, and seasonal conditions.

To further investigate spatial variations in stormwater quality, this study conducted a comparative analysis of urban road runoff in two representative countries—Germany and China—located in Europe and Asia, respectively. Table 2.1 summarizes representative studies on stormwater quality in urban road runoff conducted in both countries. The table includes details such as research locations, sampling periods, and the types of pollutants analyzed. It should be noted that this table does not represent an exhaustive review of all stormwater-related literature. Instead, the selected studies were included based on the following criteria: (1) The study focused specifically on urban road runoff, excluding roof runoff or other urban surface runoff sources; (2) Only English-language publications were considered; studies published exclusively in German or Chinese were excluded; (3) the study included sufficient research information such as sampling sites, sampling period, the detailed sampling methods, and sufficient investigated data. As shown in Table 2.1, a variety of stormwater pollutants have been identified in urban road runoff across multiple cities in Germany (e.g., Munich, Hamburg) and China (e.g., Beijing, Shenzhen, Chongqing). These studies encompassed a wide range of sampling sites, road types, and land use categories. Key water quality indicators commonly examined in both countries include total suspended solids (TSS), pH, and heavy metals such as cadmium (Cd), chromium (Cr), copper (Cu), nickel (Ni), lead (Pb), zinc (Zn), and manganese (Mn). In Germany, particular emphasis was placed on the levels of total organic carbon (TOC) and electrical conductivity (EC), reflecting concerns related to organic matter and ionic composition. In contrast, studies conducted in China focused more on chemical oxygen demand (COD) and nutrient pollutants, specifically total nitrogen (TN) and total phosphorus (TP), highlighting concerns about eutrophication and organic pollution.

Based on the findings summarized in Table 2.1, the mean concentrations of various stormwater quality parameters in urban road runoff in China (CHN) and Germany (DEU) are presented in Figure 2.4. Overall, pollutant levels in road runoff from China were generally higher than those observed in Germany. For example, the mean concentration of total suspended solids (TSS) in Chinese road runoff was approximately 244.58 mg/L, which exceeded the corresponding value reported for Germany (approximately 173.70 mg/L). Heavy metal concentrations in road runoff are of particular concern in both countries. Zinc (Zn) was the dominant heavy metal detected in road runoff in both China and Germany. The mean Zn concentration in Chinese road runoff reached 578.36 μg/L, compared with 338.78 μg/L in Germany. In addition, the concentrations of cadmium (Cd), chromium (Cr), copper (Cu), and manganese (Mn) in road runoff were consistently higher in China than in Germany. Notably, the mean concentration of Cr in China (502.33 μg/L) was substantially higher than that reported in Germany (11.19 μg/L). One possible explanation for these pronounced differences is the higher population density and traffic volume in China, which may result in greater accumulation of pollutants on road surfaces. In contrast, the mean concentration of lead (Pb) in German road runoff (80.78 μg/L) was higher than that observed in China (41.89 μg/L). This discrepancy may reflect differences in automotive manufacturing practices and material usage, as Pb remains a component of certain vehicle-related materials.

In addition to heavy metals, nutrient pollution in Chinese road runoff was also of concern. Mean concentrations of TN and TP were approximately 9.18 mg/L and 0.56 mg/L, respectively, indicating potential risks for eutrophication in downstream water bodies. The mean pH value of Chinese stormwater runoff (8.22) was slightly higher than that in Germany (7.23), possibly reflecting differences in local environmental conditions and chemical compositions. In summary, factors such as traffic density, automotive industry practices, road maintenance and materials, rainfall characteristics, and local policies and regulations significantly influence the pollutant profiles of urban road runoff in different countries.

Despite increasing attention to urban runoff pollution, few studies have systematically investigated the interrelationships among multiple pollutant classes, particularly under dynamic hydrological conditions. The potential synergistic interactions between emerging contaminants such as MPs and conventional pollutants such as heavy metals and nutrients are still poorly understood. This gap hinders the development of accurate pollutant transport models and comprehensive ecological risk assessments. Therefore, a thorough analysis of pollutant profiles—encompassing co-occurrence patterns, correlations, and shared transport pathways—is essential to deepen our understanding of urban runoff dynamics and support the design of integrated, multi-pollutant stormwater management strategies, particularly in high-density urban environments. Additionally, the quantity and quality of urban runoff pollutants face severe challenges because they are influenced by multiple factors that determine flow rate, timing, and pollutant concentrations. These factors include rainfall characteristics (e.g., pattern, intensity, and volume), the number of antecedent dry days, traffic density, land use types, regional geographic and geological conditions, infrastructure maintenance practices, and the design of the urban drainage system (Chui, Mar, & Horner, 1982).

Table 2.1. The representative studies of stormwater quality indicators in urban road runoff in Germany and China.

Lists	Locations	Stormwater quality indicators	Sampling period	Sampling sites	Sample collection	Values of concentrations	References
D1	Munich, DEU	PH, EC, TSS, Cd, Cr, Cu, Ni, Pb, Zn	2017-2019	highly trafficked road	Active-automatic	Median values	Rommel, Stinshoff and Helmreich (2021)
D2	Munich, DEU	PH, EC, TSS, Cd, Cu, Ni, Pb, Zn, Na, DOC, TOC	2 years	traffic road	Active-automatic	Median values	Helmreich et al. (2010)
D3	Munich, DEU	PH, EC, TSS, Cu, Pb, Zn, Na, TOC	1year	traffic road	Active-automatic	Median values	Hilliges, Schriewer and Helmreich (2013)
D4a	Hamburg, DEU	Cd, Cr, Cu, Ni, Pb, Zn, Mn	1986-1987	street in an industrial area	Active-automatic	Mean values	Dannecker, Au and Stechmann (1990)
D4b	Hamburg, DEU	Cd, Cr, Cu, Ni, Pb, Zn, Mn	1987	thoroughfare	Active-automatic	Mean values	Dannecker, Au and Stechmann (1990)
D4c	Hamburg, DEU	Cd, Cr, Cu, Ni, Pb, Zn, Mn	1987	small streets in residential areas	Active-automatic	Mean values	Dannecker, Au and Stechmann (1990)
C1	Beijing, CHN	TSS, COD, BOD_5, TN, TP	2004-2005	traffic road	Active-automatic	Median values	Yufen et al. (2008)

C2	Chongqing, CHN	PH, TSS, COD, TN, TP	2010-2011	traffic road nearing commercial buildings and residential housing	Manual	Mean values	Zhang et al. (2013)
C3a	Shenzhen, CHN	TSS, COD, NH_4-N, TP	2018	Arterial road	Manual	EMCs	Liu et al. (2019)
C3b	Shenzhen, CHN	TSS, COD, NH_4-N, TP	2018	road in the residential area	Manual	EMCs	Liu et al. (2019)
C3c	Shenzhen, CHN	TSS, COD, NH_4-N, TP	2018	road in the industrial area	Manual	EMCs	Liu et al. (2019)
C4a	Beijing, CHN	Cd, Cr, Cu, Mn, Pb, Zn	2015-2018	Heavy traffic roads in commercial areas	Manual	Median values	Du et al. (2019)
C4b	Beijing, CHN	Cd, Cr, Cu, Mn, Pb, Zn	2015-2018	light traffic road in the residential area	Manual	Median values	Du et al. (2019)
C5a	Beijing, CHN	TSS, COD, NH_4-N, NO_3-N, TP, Cu, Fe, Mn, Pb, Zn	2012-2014	road in the residential area	Manual	EMCs	Shen et al. (2016)

C5b	Beijing, CHN	TSS, COD, NH_4-N, NO_3-N, TP, Cu, Fe, Mn, Pb, Zn	2012-2014	main traffic road	Manual	EMCs	Shen et al. (2016)

Note: EMCs = Even mean concentrations

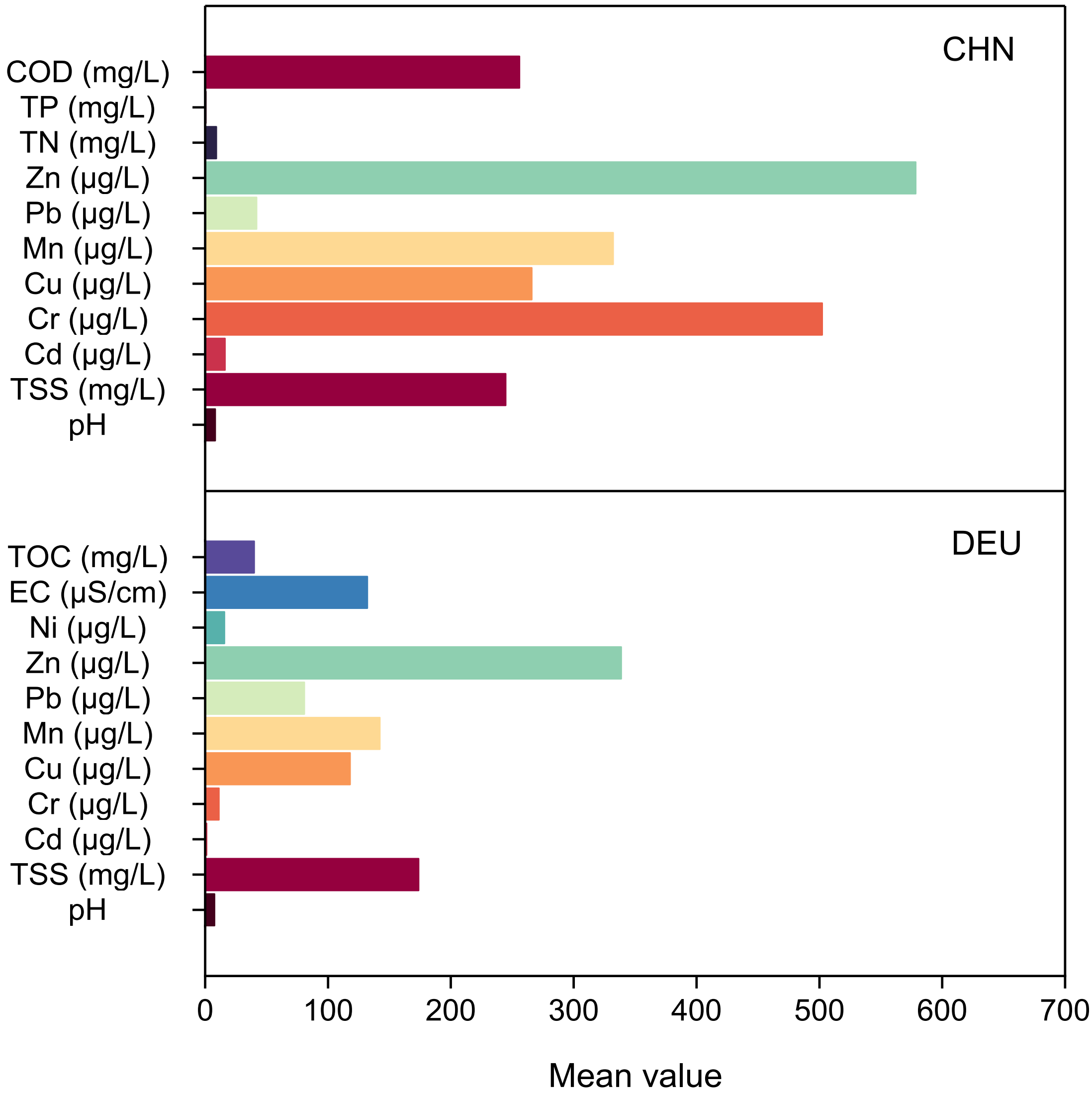

Figure 2.4. Comparison of mean concentrations of various stormwater quality parameters observed in urban road runoff between China (CHN) and Germany (DEU).

2.1.3 First flush phenomenon in urban road runoff

Pollutant levels in urban roadway runoff are dynamic and event-driven influences during different rainfall events. Road surfaces are major accumulation areas for a variety of pollutants that can be altered by flow mechanisms in accordance with varying rainfall characteristics. Numerous studies have demonstrated that pollutant concentrations in stormwater runoff vary across different rainfall events, with the highest levels typically observed during the initial stage of runoff—a phenomenon commonly referred to as the first flush (Gan et al., 2008; Wang et al., 2013; Zhang et al., 2010; Zhao, Shan, & Yin, 2007). The first flush phenomenon refers to the disproportionate transport of pollutants during the early stages of a rainfall event, where a significant portion of the total pollutant load is rapidly mobilized and discharged in the initial runoff volume (Peter et al., 2020). This effect is of particular concern in urban environments, where impervious surfaces such as roads and pavements accumulate various contaminants between storm events. When rainfall begins, these accumulated pollutants are quickly washed off and carried into drainage systems, leading to short-term spikes in pollutant concentrations and posing acute risks to receiving water bodies (Hathaway et al., 2012b; Saget, Chebbo, & Bertrand-Krajewski, 1996).

In a given rainfall event, the first flush significantly affected contaminant constituents of stormwater runoff. Previous studies have shown that contaminants such as total suspended solids (TSS), heavy metals (e.g., Zn, Cu, Pb), nutrients (e.g., TN, TP), and organic matter (e.g., COD) are often present in significantly higher concentrations during the initial phase of runoff (Aryal et al., 2010; Kayhanian et al., 2012). Figure 2.5 shows the precipitation, flow rate, and water quality variation of combined sewer overflows (CSO) for the 2nd and 3rd rainfall events investigated by Kim, Yur and Kim (2007). The peak concentration of pollutants always happens in the initial runoff (also called first flush), the contaminant constituents in descending order of suspended solids> organics >nutrients (Kim, Yur, & Kim, 2007). The intensity and timing of the first flush effect are influenced by multiple factors, including rainfall characteristics (e.g., intensity, duration), antecedent dry period, road surface conditions, traffic volume, and land use types.

To quantitatively assess the first flush phenomenon and pollutant loading dynamics, many studies have adopted metrics such as the First Flush Effect (FFE) and the dimensionless mass–volume (M(V)) curve. These approaches provide a standardized framework for evaluating how pollutants are distributed across the runoff volume during rainfall events and for identifying whether specific pollutants exhibit early-stage loading behavior. Both tools are widely applied in research and practical stormwater engineering.

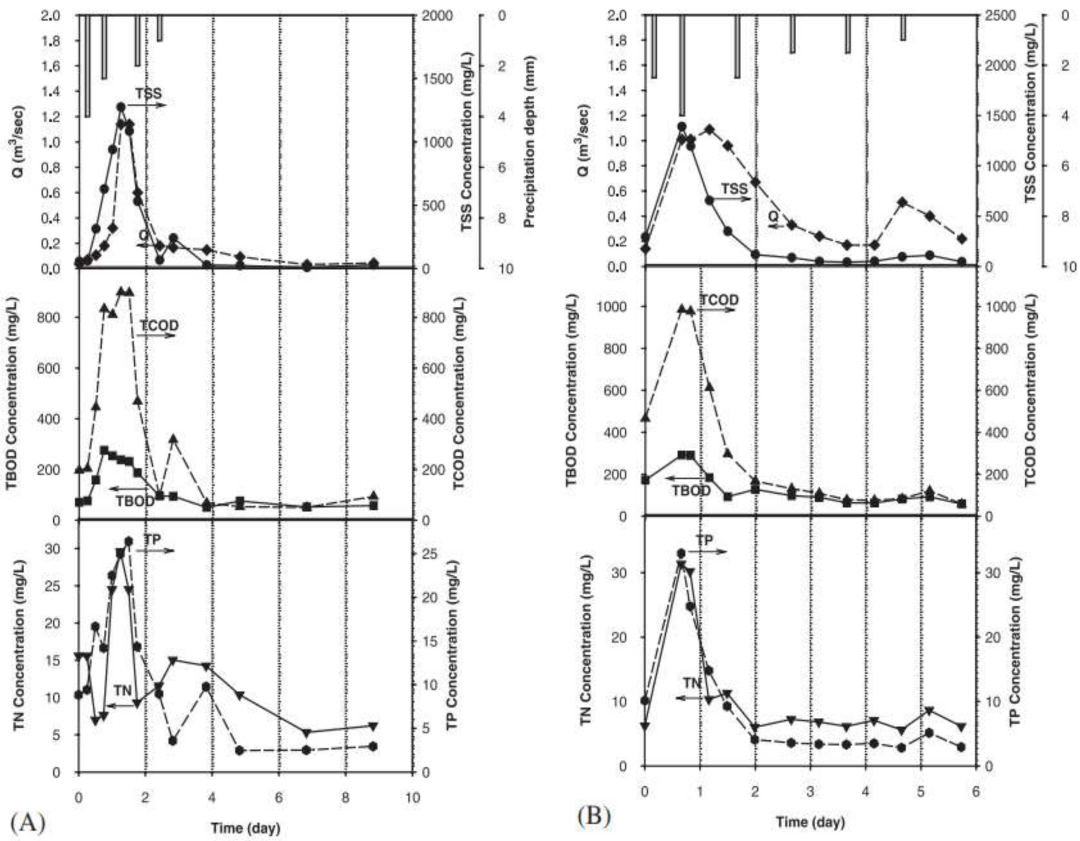

Figure 2.5. Precipitation, flow rate, and TSS (top), TCOD and TBOD (middle), TN and TP (bottom) for (A) 2nd rainfall event; (B) 3rd rainfall event. Figure adapted from Kim, Yur and Kim (2007).

The First Flush Efficiency (FFE) is a quantitative index that describes the intensity of the first flush effect by measuring the proportion of total pollutant mass transported within the initial fraction of runoff volume. In contrast, the dimensionless M(V) curve is a graphical method that plots the cumulative fraction of pollutant mass (M) against the cumulative fraction of runoff volume (V). When the M(V) curve lies above the 45° bisector, it indicates a strong first flush, where pollutants are concentrated in the early stages of runoff. Conversely, curves below the bisector suggest delayed or uniformly distributed pollutant release (Figure 2.6). This method allows for intuitive comparisons of pollutant behavior across different rainfall events and pollutant types (Deletic, 1998; Hathaway et al., 2012b; Mamun, Shams, & Nuruzzaman, 2020). However, the variability in first flush strength across diverse urban environments remains a key challenge in developing generalized stormwater management strategies. Furthermore, limited research has been conducted on the first flush behavior and pollutant loading dynamics of emerging contaminants such as MPs, particularly under dynamic hydrological conditions.

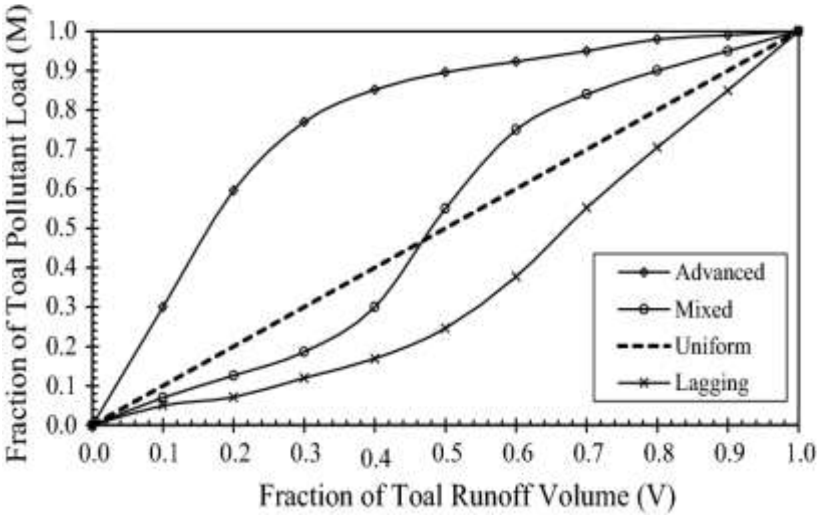

Figure 2.6. Concept of M(v) curve for typical loading characteristics of runoff. Figure adapted from Mamun, Shams and Nuruzzaman (2020).

2.2 Current Research on Urban Stormwater Treatment Strategies

2.2.1 Overview of existing applications for urban stormwater management

Since the 1970s, countries such as Germany, the United States, the United Kingdom, Japan, and Singapore have begun addressing issues related to urban waterlogging and stormwater pollution (Fletcher et al., 2015). Tsihrintzis and Hamid (1997) provided a comprehensive summary of the sources, impacts, and management strategies for typical urban non-point source pollution, as illustrated in Figure 2.7. Urban pollutants primarily originate from impervious surfaces across various land use zones, including residential, commercial, industrial, and highway areas, as well as educational institutions and open spaces such as parks. These contaminants degrade surface and groundwater via runoff and infiltration, harming aquatic ecosystems (e.g., fish kills, reduced biodiversity) and posing risks to human health.

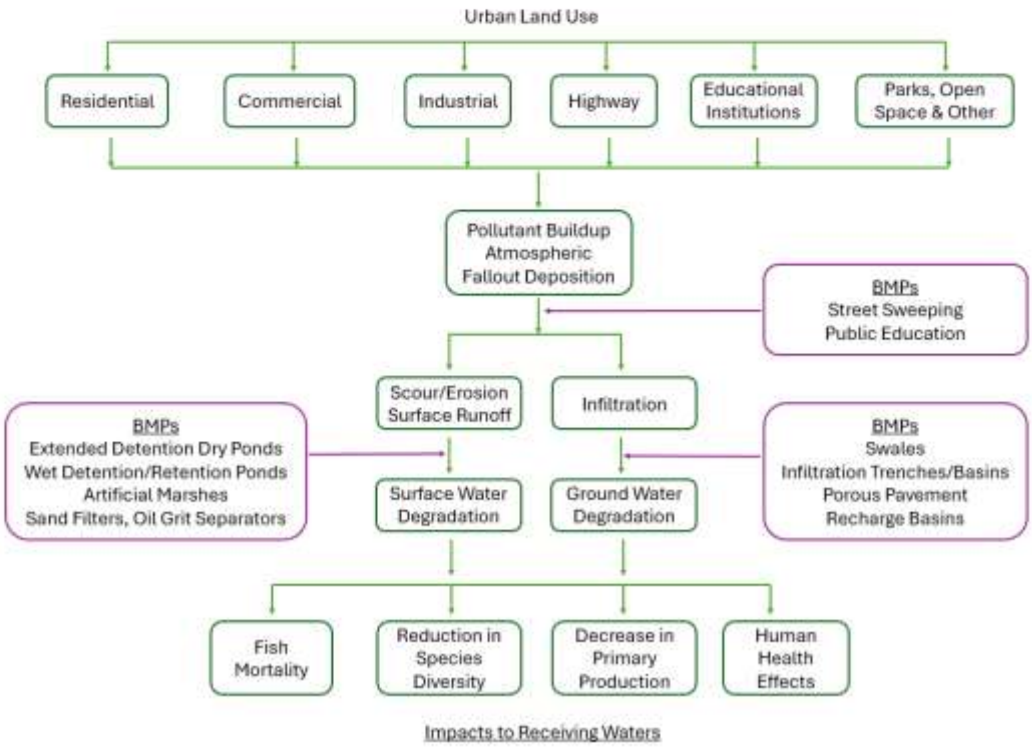

Figure 2.7. Sources, impacts, and management of urban runoff pollution. Figure adapted from Tsihrintzis and Hamid (1997).

Based on the mechanisms of urban stormwater pollution, a range of stormwater management practices have been proposed to reduce peak flow rates and runoff volumes, thereby effectively mitigating urban stormwater pollution. These approaches include policy and regulatory measures, strategic planning, source control, end-of-pipe measures, and the implementation of Best Management Practices (BMPs) (Barbosa, Fernandes, & David, 2012). In the early stages of development, source control emerged as an effective strategy to reduce peak runoff and pollutant loads entering the drainage system by addressing the pollutants at their point of origin (German et al., 2005). Common early source control methods included street sweeping, catch basin cleaning, elimination of illicit discharges, reduction of impervious surfaces, infiltration trenches, dry wells, and sand filters (Pratt, 1995). However, many of these practices encountered challenges such as clogging, limited treatment capacity, and sustainability concerns. To address these limitations at larger urban scales, BMPs were subsequently introduced. BMPs aim to manage both runoff volumes and pollutant loads before they reach receiving water bodies, using a combination of structural and non-structural techniques

(Shoemaker et al., 2000). BMPs encompass source control, intermediate conveyance control, and end-of-pipe treatment. Representative BMPs include constructed wetlands, vegetated swales, and retention ponds.

With the growing understanding of urban stormwater management, advanced approaches such as Low Impact Development (LID), Green Infrastructure (GI), Water Sensitive Urban Design (WSUD), and Sustainable Urban Drainage Systems (SUDS) have been introduced to guide sustainable urban water planning. These methods emphasize minimizing the ecological footprint of urbanization while enhancing the resilience of urban environments to hydrological disruptions. LID tends to achieve hydrological neutrality or mimic natural water cycles by developing urban watersheds to mitigate the interruption of natural hydrological processes (Eckart, McPhee, & Bolisetti, 2017). SUDS, widely implemented in Europe, utilizes a combination of structures and technologies to manage urban runoff and reduce the impact of extreme rainfall events and urban hydrological alteration (Ferrans et al., 2022; Liao et al., 2013). GI represents a landscape planning strategy that integrates ecological networks into urban environments to maximize environmental, social, and economic benefits (Ghofrani, Sposito, & Faggian, 2017). WSUD, predominantly adopted in Australia, promotes urban design principles that align water cycle management with landscape planning to ensure sustainability, livability, and water efficiency. These approaches have been increasingly adopted worldwide, contributing to improved stormwater management outcomes. For example, Singapore's Active, Beautiful, and Clean Waters (ABC Waters) Programme offers a scientific and integrated design model for rainwater collection and drainage distribution. As a result, despite its tropical climate and frequent heavy rainfall, Singapore has experienced minimal urban flooding (Liao, 2019; Xia et al., 2017). Other successful international examples include Potsdamer Platz in Berlin, Green Streets in Portland, USA, and the Ryogoku District in Tokyo, Japan (Sharma & Malaviya, 2021).

Based on these concepts, a wide range of specific techniques and infrastructures have been implemented in field projects to manage urban stormwater. These include constructed wetlands, green roofs, bioswales, sunken green belts, permeable pavements, bioretention tanks, and rain gardens, among others (Eckart, McPhee, & Bolisetti, 2017; Maes & Jacobs, 2017; Shoemaker et al., 2000). These green infrastructure solutions are designed to enhance infiltration, reduce surface runoff, and improve water quality by mimicking natural hydrological processes. Figure 2.8 illustrates examples of such infrastructures currently in use to mitigate urban flooding and stormwater pollution.

The grass swale is a shallow, vegetated channel designed to collect, convey, and discharge stormwater runoff, as illustrated in Figure 2.8a. Vegetation within the swale facilitates the natural purification of rainwater through biological filtration and sedimentation processes. Grass swales are typically implemented along impervious surfaces such as roads and parking lots. This technique is cost-effective, requires relatively low maintenance, and can be seamlessly integrated into the surrounding landscape. However, while grass swales provide temporary storage for runoff, their treatment efficiency and water quality performance can be significantly influenced by seasonal variations (Yan, Chengqing, & Wu, 2008).

The sunken green belt is a type of green infrastructure characterized by a depressed green space situated below the surrounding ground level (Figure 2.8b). It is designed to receive and temporarily store stormwater runoff, utilizing open vegetated areas to reduce surface discharge. These green belts are typically planted with native herbaceous vegetation, which contributes to pollutant removal through natural purification processes such as filtration and phytoremediation (Zhong-hua, 2016). Due to their low construction and maintenance costs, sunken green belts are widely applied in urban environments, including around residential buildings, roadsides, green spaces, and plazas. However, their effectiveness is limited by terrain conditions and seasonal variations, especially when deployed over large areas. Moreover, the storage capacity of sunken green belts is relatively small, making them unsuitable for locations requiring long-term or large-volume rainwater retention (Qiao-ling; Zhang & Li, 2014).

Permeable Pavement Systems (PPSs) are a widely adopted form of green infrastructure (GI), commonly implemented in urban roadways (Figure 2.8c). Common practices include permeable brick pavement, permeable green pavement, and permeable concrete

(Roseen et al., 2012; Sullivan, Thomas, & Rosano, 2018; Xie, Akin, & Shi, 2019). PPSs play a critical role in reducing peak flow and total stormwater runoff volumes (Ahiablame, Engel, & Chaubey, 2012; Dietz, 2007). Unlike conventional pavements, PPSs allow stormwater to infiltrate through porous surface materials and underlying dendritic structures, facilitating timely seepage and mitigating surface runoff (Fassman & Blackbourn, 2010). Additionally, porous pavement is also a water-permeable structural surface that allows precipitation to infiltrate, thereby reducing both runoff volume and flow rates, while also helping to lower surface temperatures (Figure 2.8d). This system provides stable load-bearing surfaces without significantly increasing impervious coverage. Rainwater can infiltrate through the surface pores and be temporarily stored within the sub-base, where finer materials facilitate the removal of certain pollutants via filtration. However, PPSs and porous pavement have limitations. Due to the high porosity of the materials used, their load-bearing capacity is relatively low. As such, they are best suited for light-traffic applications, such as residential roads, parking lots, and recreational areas (Zhong-hua, 2016). Issues such as clogging and maintenance challenges remain significant barriers to widespread application in densely built urban areas.

a. Grass swale b. Sunken green belt

c. Permeable pavements d. Porous pavement

Figure 2.8. Examples of urban stormwater runoff management practices along roads, including (a) grass swale, (b) sunken green belt, (c) permeable pavements, and (d) porous pavement. (Figure sources from: https://pavementnetwork.com/permeable-pavements/; https://www.freshcoastguardians.com/resources/green-strategies/porous-pavement; https://landscape.coac.net/rainwater-harvesting-greenbelt-qianan; https://developersguide.njfuture.org/bmp/grass-swale/).

The concept of the Sponge City has been introduced in China in recent years as an innovative urban stormwater management strategy. It envisions a city that can absorb, store, and purify water by utilizing underground space and mimicking the natural urban hydrological cycle to enable the spatial and temporal redistribution of rainwater (Liu, Jia, & Niu, 2017; Sun et al., 2020). This approach integrates urban buildings, communities, roads, green spaces, and plazas as rainwater carriers, using green infrastructure techniques such as permeable pavements, vegetated swales, sunken green belts, and rain gardens to reshape traditional drainage systems (Wang et al., 2018). The core planning principles—“slow drainage and slow release” and “source decentralization”—aim to both prevent flooding and promote rainwater harvesting.

Empirical studies have demonstrated that Sponge City infrastructures contribute to urban water resource utilization and help alleviate flooding pressures (Li et al., 2019). While the Sponge City framework is a promising direction for sustainable stormwater management, most implementations have primarily emphasized flood control, often overlooking other hydrological processes such as infiltration, evapotranspiration, and water reuse (Xia et al., 2017). Moreover, current practices largely focus on retrofitting spaces adjacent to roadways, with limited attention given to reengineering road structures themselves for multi-functional stormwater management. Consequently, research on integrated stormwater management systems specifically tailored for urban roadways remains limited.

These developments underscore the substantial potential of urban stormwater reuse as a key strategy for sustainable urban environmental planning. However, many of these practices are heavily reliant on infrastructure and face persistent challenges, including clogging, intensive maintenance demands, limited spatial availability, and long-term sustainability concerns. Such limitations are particularly pronounced in high-density urban areas, where space constraints and complex land use patterns hinder the effective implementation of existing green infrastructure solutions.

2.2.2 Development of nature-based solutions in urban stormwater management

With growing recognition of the limitations of conventional stormwater infrastructure, Nature-Based Solutions (NBS) have emerged as a promising paradigm for urban stormwater management. NBS refer to actions that are inspired by, supported by, or built on natural processes to address environmental challenges while providing co-benefits for ecosystems and human well-being, as shown in Figure 2.9 (Cohen-Shacham et al., 2016; Raymond et al., 2017). This concept attempts to improve ecosystem services by increasing investment in renewable natural processes and reducing investment in non-renewable natural processes (Maes & Jacobs, 2017). In the context of urban stormwater management, NBS integrate natural elements—such as vegetation, soil, and hydrology—into engineered systems to mimic the functions of natural water cycles, including infiltration, filtration, evapotranspiration, and pollutant attenuation (Raymond et al., 2017). Several NBS approaches have been conceptualized and implemented globally, often under broader frameworks such as LID, SUDS, WSUD, and GI. A wide variety of NBS technologies have been applied in practice, including rain gardens, bioswales, green roofs, ecological wetlands, and tree-box filters. These systems enhance infiltration, evapotranspiration, and natural filtration, thereby reducing surface runoff and improving water quality.

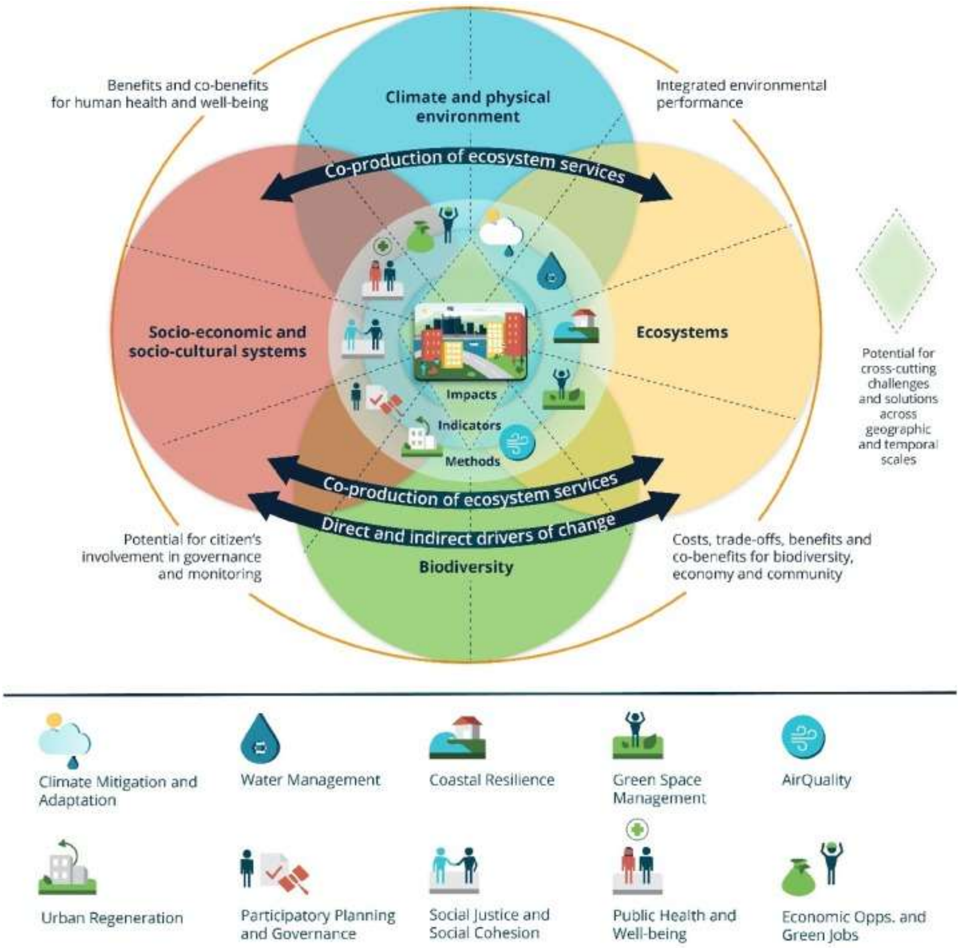

Figure 2.9. The nature-based solutions (NBS) assessment framework. Figure adapted from Raymond et al. (2017).

Trees serve as effective stormwater control measures by integrating seamlessly with soil, the atmosphere, and the surrounding urban landscape, thereby enhancing the quantification and management of urban hydrology (Berland et al., 2017), as shown in Figure 2.10. Among various NBS, tree-based bioretention systems (also known as tree-box filters) have attracted growing interest due to their compact design, suitability for roadside infrastructure, and dual function of supporting tree growth while treating runoff. These systems combine engineered filter media with vegetation to remove pollutants through physical, chemical, and biological processes, while also providing ecosystem services such as shading, cooling, and habitat enhancement (Adegun et al., 2021).

Studies have demonstrated that tree-box systems can effectively remove pollutants such as total suspended solids (TSS), nutrients (N and P), and heavy metals (e.g., Cu, Zn) through mechanisms like physical filtration, adsorption by engineered soil media, microbial degradation, and plant uptake (Ahmed & Borst, 2020; Geronimo, Maniquiz-Redillas, & Kim, 2013). For example, Choi et al. (2013) reported that tree-box filters exhibited enhanced removal of heavy metals, organic matter, and nutrients. The removal efficiency for total heavy metals ranged from 70% to 73%, while satisfactory reductions of particulate matter, organic matter, and nutrients ranged from 60% to 68%. Despite their promising performance, the real-world implementation of tree-box systems remains limited. Key challenges include the selection of appropriate tree species, the optimization of filter media composition, and the adaptation of designs to local climatic and environmental conditions—factors that currently constrain broader adoption and long-term effectiveness.

NBS represent a transformative approach to urban water management by applying natural ecosystem principles to control stormwater runoff while delivering broader environmental and societal benefits. These systems offer flexibility, resilience, and multifunctionality, ranging from pollutant removal to urban greening and climate adaptation. However, despite increasing interest, on-site performance evaluations of NBS remain limited, particularly in high-density urban environments. Many existing studies emphasize system design or hydrological performance but often overlook important ecological co-benefits, such as habitat enhancement, vegetation resilience, and long-term sustainability. Recent research has begun to shift toward integrated assessment frameworks that incorporate hydrological, chemical, ecological, and social dimensions (Raymond et al., 2017). Nevertheless, further studies are needed to (1) quantify the long-term pollutant removal performance of NBS under real-world conditions, (2) optimize system configurations for compact urban spaces, and (3) evaluate their effectiveness in treating multiple types of pollutants simultaneously. While various green infrastructure strategies have been developed under the NBS umbrella, comprehensive reviews specifically addressing road runoff pollution remain scarce. In high-density cities, spatial constraints pose significant challenges to the implementation of conventional green infrastructure, highlighting the need for compact and adaptable NBS designs tailored to the treatment of road runoff.

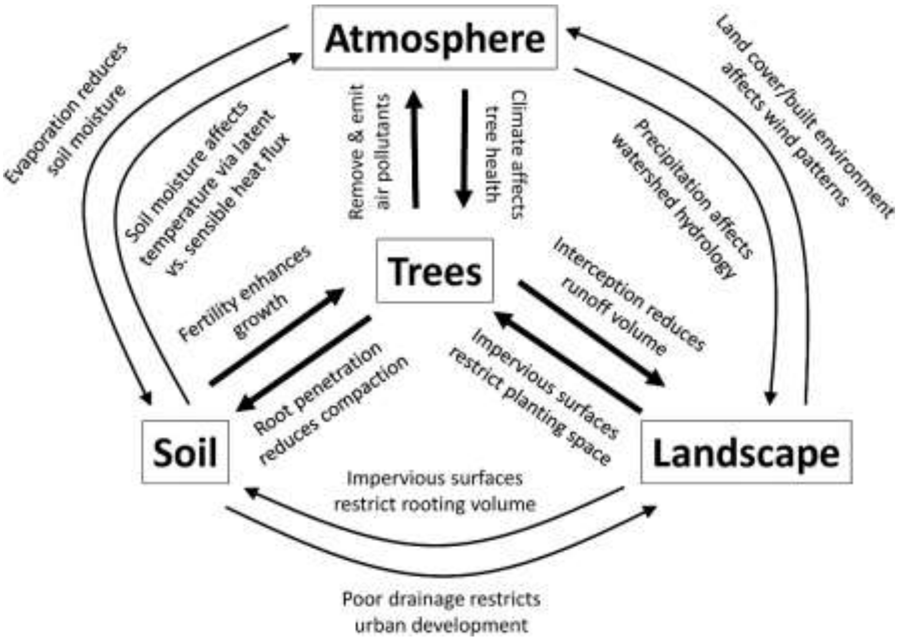

Figure 2.10. Conceptual framework illustrating the role of trees in urban stormwater control measures. Figure adapted from Berland et al. (2017).

CHAPTER 3. RESEARCH METHODOLOGY

3.1 Experimental Framework

A systematic experimental framework was proposed in this study to assess urban stormwater runoff pollution and develop nature-based mitigation strategies. The overall workflow is illustrated in the following flowchart:

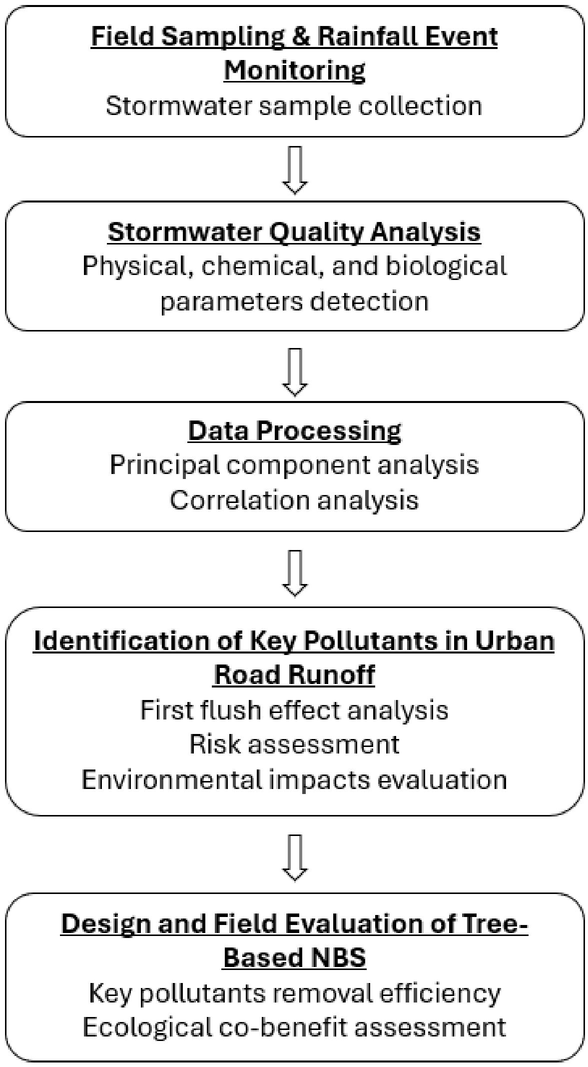

Stormwater samples were collected from various urban road sites across different seasons. A total of 32 physical, chemical, and biological parameters, including TSS, COD, metals, nutrients, Escherichia coli (E. coli), and MPs, were analyzed. Key stormwater quality indicators and potential pollution sources were identified using principal component analysis (PCA) and correlation analysis. Subsequently, first flush effect (FFE) analysis, ecological risk assessment, and statistical methods were employed to further evaluate the dynamic behavior, pollution risks, and influence of environmental factors on pollutant variation during rainfall events. Based on these insights, a tree-based nature-based solution (NBS), specifically tree-box biofiltration systems, was designed and implemented to assess the removal efficiency of stormwater pollutants and the ecological co-benefits provided by the system.

3.2 Study Area

Hong Kong has a subtropical monsoon climate with long and rainy summers. Annual rainfall is approximately 2,200 mm, with around 80% occurring from May to October. This translates to a monthly average of 380 mm during this period. The urban area comprises 25.1% of Hong Kong's total land area and is segmented into residential areas (15.4%), commercial and institutional areas (10.2%), and industrial areas (3.2%). The city has an independent stormwater drainage system separated from the urban sewerage network.

This study focused on the rainfall-runoff from six road locations across different land uses in the districts of Fo Tan and Hung Hom (Figure 3.1). The roads, constructed from concrete and asphalt pavement materials (Table 3.1), are categorized into commercial roads (CR), residential street roads (RSR), and industrial roads (IR). Sampling sites were established beside stormwater drain grates on these six road surfaces, as shown in pictures A-F (Figure 3.1 and Appendix A, Figure A-1). Additionally, natural rainwater (NR) was collected during each rainfall event to serve as a control group, with the collection point situated in the open areas of the roof garden in Block Z at the Hong Kong Polytechnic University.

Figure 3.1. Locations of sampling sites in Hung Hom (A, B, C, and D) and Fo Tan (E and F). NR: Natural rainwater; Sites A and B: Commercial roads; Sites C and D: Residential Street roads; Sites E and F: Industrial roads.

Table 3.1. Information on the sampling sites A-F. The land use types are CR: commercial roads, RSR: residential street roads, and IR: industrial roads.

Site	Location	Road materials	Road width (m)	Road length (m)	Road surface area (m^2)	Land use type
			Hung Hom			
A	Chatham Road South	Concrete	5.5	120	660	CR
B	Baker Street	Asphalt	4.5	12	54	CR
C	Station Lane	Concrete	5.5	40	220	RSR
D	Ming On Street	Asphalt	5.5	71.4	392.7	RSR
			Fo Tan			
E	Wong Chuk Yeung Street	Asphalt	6.75	46.4	313.2	IR
F	Au Pui Wan Street	Concrete	5.5	93.3	513.15	IR

3.3 Sample Collection

We collected road runoff samples from six different road surfaces across 11 rainfall events between February 2021 and September 2022. To balance the research effort and the completeness of research data, we collected samples during the initial 20 minutes of runoff for 9 rainfall events and throughout the entire rainfall period for the other 2 events. For the 9 rainfall events, a total of 54 samples were collected. For the 2 rainfall events, a total of 13 flow-weighted samples were collected (Table 3.2). The duration of each rainfall event exceeded 40 mins, with a mean intensity greater than 2.5 mm/h (n = 11). The intensity data were sourced from the Hong Kong Observatory (Table 3.3).

For the 9 rainfall events, samples were collected using a stainless-steel rain dustpan (Figure 3.2), with 4 consecutive 500 mL samples taken at 5-minute intervals within the initial 20 mins of runoff generation. This resulted in a total of 2 L samples per event for each site. The sample was then mixed in a 2 L pre-cleaned glass bottle for analysis. This 20-minute period was chosen because previous studies demonstrated that peak concentrations of pollutants typically occur within the initial 20 mins of stormwater runoff (Luo et al., 2023).

For the other 2 rainfall events, flow-weighted sampling was conducted to capture the dynamic behavior of pollutants in road runoff. Sampling started with the onset of runoff and continued until the end of the rainfall. We obtained 5–7 consecutive samples at varying intervals: every 5 mins within the first 15 mins, 5 or 10 mins within 15–40 mins, and 15 mins within 40–70 mins of runoff generation. After 70 mins, samples were collected every 30 mins. Each sample volume ranged from 100–500 mL, depending on the flow rate, measured using a flow meter. The same manual collection method was followed.

The initial period of runoff typically has a higher pollutant concentration than the later periods. This initial period is conceptually referred to as the "first flush (Do et al., 2023; Maniquiz-Redillas et al., 2022)". However, the accurate demarcation of the "first flush" requires continuous stormwater sampling and analyzing the cumulative runoff volume and pollutant concentration data. Therefore, samples collected in the 9 rainfall events (20 mins) are referred to as the "initial runoff" in this study.

At the same time of collecting runoff samples from the roads, natural rainwater was collected in each event using passive funnel devices equipped with a stainless-steel funnel and a 2L glass bottle (Do et al., 2023; Shao et al., 2022; Welsh & Sánchez-Murillo, 2020), with collected volumes ranging from 1–2 L. All samples were transported to the lab and stored at 4°C. All pieces of equipment used for sample collection were pre-rinsed with Milli-Q water (Merck, Darmstadt, Germany) to prevent contamination.

Figure 3.2. Pictures of collecting runoff samples on road surfaces during rainfall using a stainless-steel rain dustpan.

Table 3.2. A detailed summary of rainfall events sampled from the selected sites in Hong Kong (Note: The wet season is defined by monthly rainfall exceeding the annual average, while the dry season is defined by the monthly rainfall lower than the annual average (Figure 3.3). Locations of sampling sites are provided in Figure 3.1 and Table 3.1. Meteorological seasons are defined as summer (June–August), autumn (September–November), winter (December–February), and spring (March–May).)

Rainfall events	**Sampling date**	**Meteorological seasons**	**Dry and wet seasons**	**Antecedent dry days**	**Mean rainfall intensity (mm/h)**	**Monitoring points**
1	10/02/2021	Winter	Dry	80	2.5	A–F, NR
2	27/04/2021	Spring	Dry	9	8	A–F, NR
3	25/05/2021	Summer	Dry	1	21.5	A–F, NR
4	04/06/2021	Summer	Wet	2	23.4	A–F, NR
5	03/08/2021	Summer	Wet	1	12	A–F, NR
6	31/08/2021	Summer	Wet	1	3	A–F, NR
7	16/09/2021	Autumn	Dry	8	19.8	A–F, NR
8	07/10/2021	Autumn	Wet	3	41	A–F, NR
9	20/12/2021	Winter	Dry	64	3.1	A–F, NR
10	03/08/2022	Summer	Wet	12	12	A, NR
11	30/09/2022	Autumn	Dry	6	16	C, NR

Table 3.3. The information on rainfall intensity at each site is in the first flush. The initial rainfall intensity was evaluated by the mean intensity during the first 20 minutes of runoff generation.

	Rainfall events										
No.	1	2	3	4	5	6	7	8	9	10	11
Mean rainfall intensity (mm/h)	2.5	8	21.5	23.4	12	3	19.8	41	3.1	12	16
Duration of rainfall (min)	62	90	122	65	115	70	60	135	92	85	60

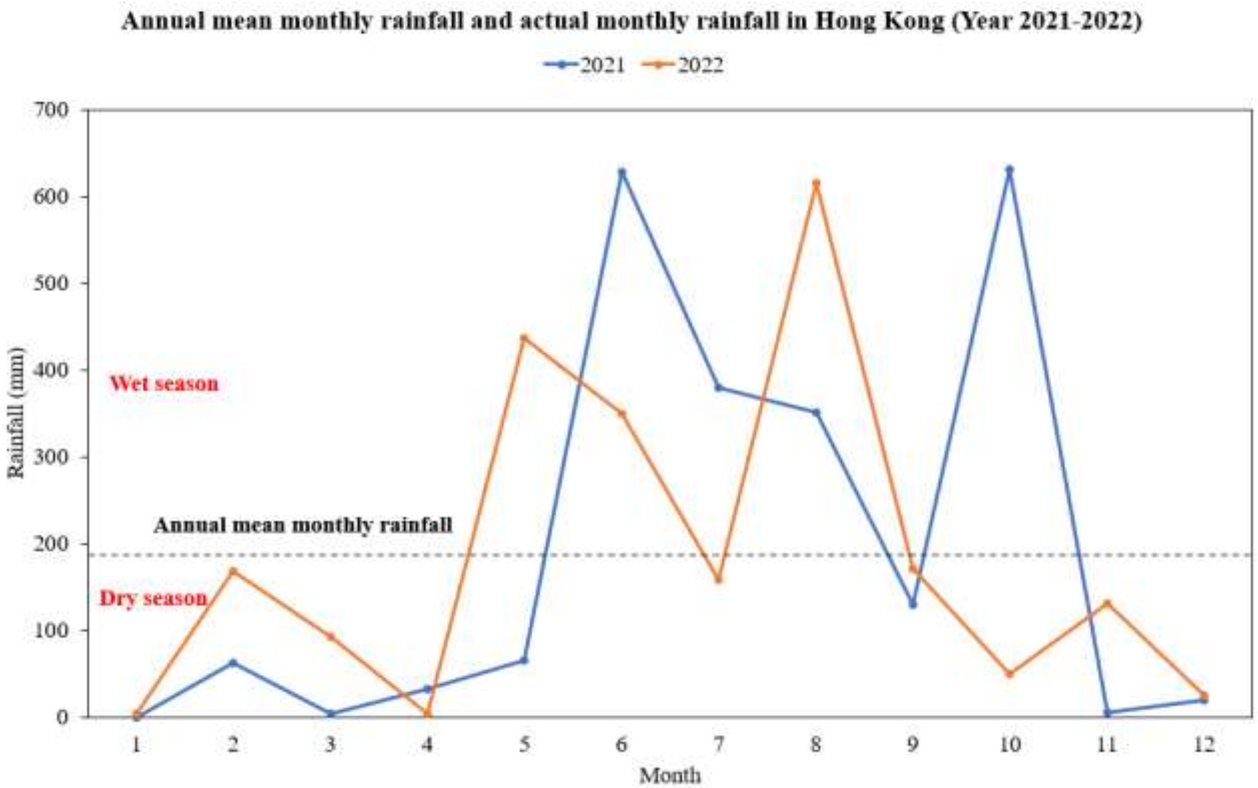

Figure 3.3. Annual mean monthly rainfall and actual monthly rainfall in Hong Kong in 2021 and 2022. The wet season is defined by monthly rainfall exceeding the annual mean, while the dry season is defined by lower than the annual mean monthly rainfall.

3.4 Analytical Methods

3.4.1 Stormwater quality parameters analysis

A comprehensive analysis of 32 stormwater quality parameters was conducted across all collected samples. These parameters encompass a wide range of physical, chemical, and biological indicators, including: temperature, pH, electrical conductivity (EC), turbidity, salinity, total suspended solids (TSS), dissolved oxygen (DO), total alkalinity (TA), hardness, ammonia nitrogen (NH_4^+-N), nitrate nitrogen (NO_3^--N), nitrite nitrogen (NO_2^--N), total inorganic nitrogen (TIN), phosphate (PO_4^{3-}), biochemical oxygen demand (BOD_5), chemical oxygen demand (COD), *Escherichia coli* (*E. coli*), aluminium (Al), arsenic (As), chromium (Cr), cadmium (Cd), lead (Pb), zinc (Zn), copper (Cu), iron (Fe), manganese (Mn), nickel (Ni), fluoride (F^-), chloride (Cl^-), sulfate (SO_4^{2-}), bromide (Br^-), and microplastics (MPs).

The detailed methods for microplastic extraction and identification are described in Chapter 4.2.2, whereas the analytical procedures for the remaining stormwater quality parameters are elaborated in Chapter 5.2.1.

3.4.2 First flush effect analysis

The dimensionless M(V) curves were widely utilized to quantify the occurrence of the first flush phenomenon in stormwater runoff pollution (Perera et al., 2021). These curves represent the distribution of pollutant mass versus volume in stormwater discharge. Specifically, they plot the normalized cumulative runoff pollutant mass (Mi) versus the normalized cumulative runoff volume (Vi) for each time point *t* during a rainfall event (Jensen et al., 2022). The first flush phenomenon is identified when the M(V) curve rises above the 45° bisector at any point during the event (Kong et al., 2021). In this study, we applied the dimensionless M(V) curves to analyze the occurrence of the first flush phenomenon for MPs and key stormwater quality parameters in road runoff. The detailed calculation process is as follows:

Based on the methodology for the M(v) curve described in Hathaway et al. (2012b), we plotted the normalized cumulative pollutant mass at each time t versus the normalized cumulative runoff volume at the same time t to assess the first flush effect. The M(v) curve is calculated as follows:

$$M(v) = \frac{\int_0^v C\big(Q(t)\big)Q(t)dt}{\int_0^{V_{total}} C\big(Q(t)\big)Q(t)dt} \quad (1)$$

Where:

M(v) is the dimensionless cumulative mass ratio (the mass curve);

C(Q(t)) is the concentration of the key stormwater quality parameter as a function of flow rate at time t;

Q(t) is the flow rate at time t;

V_{total} is the total runoff volume for the storm event;

v represents the cumulative volume up to time t.

The cumulative volume v(t) at each time t is obtained by integrating the flow rate over time:

$$v(t) = \int_0^t Q(t')\, dt' \quad (2)$$

The total mass of key stormwater quality parameters discharged during the entire storm event is:

$$M_{total} = \int_0^{V_{total}} C\big(Q(t)\big)Q(t)dt \quad (3)$$

Therefore, for a given volume v, we can calculate the corresponding cumulative mass ratio using:

$$M(v) = \frac{\int_0^v C\big(Q(t)\big)Q(t)dt}{M_{total}} \quad (4)$$

To quantitatively compare first-flush intensities among events and pollutants, we employed a first-flush coefficient, MFF_n, defined as the ratio of the cumulative mass fraction to the cumulative volume fraction at a selected fraction n of the total runoff volume. Values of MFF_n greater than 1 indicate a pronounced first-flush effect, while values close to 1 indicate more uniform pollutant transport (Beom et al., 2021). In this study, we calculated MFF_{20} and MFF_{30} to capture the first-flush behaviours during the initial 20% and 30% of total runoff volume. The choice of these fractions is consistent with prior studies and is particularly relevant for urban runoff, as the early stage of rainfall typically contributes disproportionately to total pollutant loads (Niazkar et al., 2024; W. Zhang et al., 2023).

3.4.3 Pollution load and ecological risk assessment

3.4.3.1 Microplastics

The extent of MP pollution in road runoff and natural rainwater was evaluated using the pollution load index (*PLI*) method (Huang et al., 2023; Pan et al., 2021). The *PLI* equations are as follows,

$$PLI_i = \sqrt{\frac{C_i}{C_{io}}} \tag{5}$$

$$PLI_{Zone} = \sqrt[n]{PLI_1 \times PLI_2 \times \ldots \times PLI_n} \tag{6}$$

Where PLI_i is the pollution load index at each sampling site, C_i is the abundance of MPs monitored in the stormwater at each sampling site, C_{io} is the background abundance of MPs (with a minimum detection value of 10 particles/L used as the background level), and PLI_{Zone} is the regional pollution load index. The classifications of pollution are as follows: class I pollution: $PLI_{\text{Zone}} < 10.0$; class II pollution: $10.0 \leq PLI_{\text{Zone}} < 20.0$; class III pollution: $20.0 \leq PLI_{\text{Zone}} < 30.0$, and class IV pollution: $PLI_{\text{Zone}} > 30.0$ (Huang et al., 2023).

The potential ecological risks of various types of MPs in road runoff and natural rainwater were assessed using the polymer risk index (*PRI*) method (Wang et al., 2024; Xu et al., 2018). This can be quantified by the equation,

$$H = \sum P_n \times S_n \tag{7}$$

Where H is the evaluated polymer risk index at each sampling site, P_n is the percentage of each MP polymer identified at each site, and S_n is the ecological hazard score of the polymer (Table 3.4). This study employs the hazard scores of plastic polymers from Lithner et al., (2011) and Xu et al. (2018). The classifications of pollution are as follows: class I pollution: $H < 10.0$; class II pollution: $10.0 \leq H < 100.0$; class III pollution: $100.0 \leq H < 1000.0$; and class IV pollution: $H > 1000.0$ (Wang et al., 2024).

Table 3.4. Detailed information for microplastic polymers detected in this study includes monomers, monomer hazard level, and score. The hazardous scores follow the hazardous assessment by Lithner, Larsson and Dave (2011) and Xu et al. (2018).

Polymer	Monomer	Monomer hazard level	Score
Nylon 6	ε-caprolactam	I	50
PE	Ethylene	II	11
PET	Ethylene glycol	II	10
PMMA	Methyl methacrylate	IV	1021
Nylon 6,6	Adipic acid	II	47
PP	Propylene	I	1
PS	Styrene	II	30
PVC	Vinyl chloride	V	10551
SAN	Acrylonitrile	V	11521
PMP	4-methyl-pentene	—[a]	—[a]
PMS	Alpha-methyl styrene	—[a]	—[a]
PTFE	Tetrafluoroethylene	—[a]	—[a]

a - = No SIDS Initial Assessment Reports, lack of data

3.4.3.2 Heavy metals

The extent of heavy metals was evaluated using the pollution load index (*PLI*) method (Da Silva et al., 2023; Salazar-Rojas et al., 2023). The *PLI* equations are as follows,

$$CF_i = \frac{C_i}{C_{io}} \tag{8}$$

$$PLI_{site} = \sqrt[n]{CF_1 \times CF_2 \times \ldots \times CF_n} \tag{9}$$

Where CF_i is the contamination factor of substance i; C_i is the concentration of substance i monitored in the stormwater at each sampling site, C_{io} is the background concentration of substance i (the lowest detection concentration in road runoff was served as the background concentration); PLI_{site} is the pollution load index of pollutants at a given sampling site, and n is the number of pollutants considered. The classifications of pollution load levels (Da Silva et al., 2023) are as follows: unpolluted ($PLI_{site} < 1$), moderately polluted ($1 \le PLI_{site} < 3$), highly polluted ($3 \le PLI_{site} < 5$), and very highly polluted ($PLI_{site} > 5$).

The potential ecological risks of heavy metals pollution in stormwater runoff were assessed using the potential ecological risk index (*RI*) model (Farajollahi et al., 2024; Waara & Johansson, 2022):

$$RI = \sum_{i}^{n} Er^{i} = \sum_{i}^{n} Tr^{i} \times CF_{i} \tag{10}$$

Where Er^i is the risk factor, and Tr^i is the toxic response factor for a given substance (e.g., As= 10, Pb= Cu= Ni= 5, Cr= 2, Zn= 1(Yang et al., 2009)). The classifications of heavy metals ecological risk levels (Farajollahi et al., 2024) are as follows: low risk ($RI < 150$), moderate risk ($150 \leq RI < 300$), considerable risk ($300 \leq RI < 600$), and very high risk ($RI > 600$).

3.4.4 Statistical analysis

The abundance of MPs followed a normal distribution. To examine the effects of locations and seasonal variations on MP pollution, a one-way analysis of variance (ANOVA) and a two-sample t-test were conducted. Additionally, Pearson correlation analysis was used to explore the relationships between MP abundance and potential influencing factors. Detailed results are presented in Chapter 4.2.4.

In contrast, a multitude of stormwater quality parameters exhibited non-normal distributions. Non-parametric statistical tests were employed in subsequent analyses. Principal component analysis (PCA)and Spearman rank-order correlation were applied to identify key pollutants and assess interrelationships among multiple parameters. The Mann–Whitney U test and the Kruskal–Wallis H test were used to evaluate the effects of land use and seasonal variation on multi-pollutant distributions. The details can be seen in Chapter 5.2.2.

A significance level of $P < 0.05$ was adopted for all tests. All statistical analyses were performed using IBM SPSS Statistics (IBM Corp., USA).

CHAPTER 4. MICROPLASTIC POLLUTION: CHARACTERISTICS AND ECOLOGICAL RISKS

4.1 Introduction

Global plastic production reached a staggering 400.3 million tons in 2022, with China being the leading producer, contributing 32% of the world's plastic production (Europe, 2023). This growth in plastic production has led to a worldwide surge of microplastic (MP) pollution. Microplastics (MPs), first proposed by Thompson et al. (2004) as microscopic plastic fragments that accumulate in oceans and threaten marine life, are defined as polymer particles smaller than 5mm (Wagner et al., 2014). Recently, the European Union (EU) proposed a more refined definition of MPs: solid polymer-containing particles that may include additives and other substances, with all particle dimensions ≤ 5 mm, and all fiber-like particles ≤ 15 mm with a length-to-diameter ratio of ≥ 3 (EU, 2023).

Public awareness of MPs and their associated hazards has been growing. MPs pose serious threats not only to environments such as oceans, soils, rivers, and lakes, but also to ecosystems and human health (Rico et al., 2023; Shi et al., 2023; Tunali, Adam, & Nowack, 2023; Zhou et al., 2020). MPs can serve as carriers of toxic chemicals in the environment, thereby exacerbating their harmful impacts (Elizalde-Velázquez & Gómez-Oliván, 2021; Rakib et al., 2023; Vo & Pham, 2021). Additionally, MPs have been found in human bodies through food chains (Campanale et al., 2020; Li et al., 2022), with humans potentially ingesting 0.1–5 g of MPs weekly via inhalation and ingestion (Senathirajah et al., 2021).

Current studies have demonstrated that approximately 80% of marine MP pollution originates from land-based sources (Kabir et al., 2020; Xu et al., 2020). Stormwater runoff is a critical pathway transporting diverse land-based pollutants to water bodies through urban drainage systems (Mak et al., 2020; Piñon-Colin et al., 2020). Major sources of urban stormwater pollution include atmospheric deposition, anthropogenic activities, and drainage surfaces (Müller et al., 2020; V. Shruti et al., 2021). These sources are closely related to urban road transportation, such as vehicles, impermeable paved surfaces, and road maintenance activities (Järlskog et al., 2021; Lange et al., 2022; Rosso et al., 2023; Tamis et al., 2021), making road runoff an important source of urban stormwater pollution. However, studies on MP pollution from urban road runoff remain insufficient, even though many studies have highlighted the importance of MP pollution in urban stormwater runoff (Cho et al., 2023; Werbowski et al., 2021; Yano et al., 2021). For instance, most research on stormwater pollution in road runoff has primarily sampled from a limited number of stormwater drains serving large catchment areas (Mak et al., 2020; Zhang et al., 2022). This approach may overlook the actual concentrations and characteristics of MPs in road runoff, as other sources of runoff (e.g., roof runoff) are also discharged into the stormwater drains simultaneously (De Buyck et al., 2021; Müller et al., 2020). Therefore, sampling runoff directly from road surfaces should be adopted to minimize potential errors from these additional sources.

In addition, a rainfall event and the resulting stormwater runoff are a dynamic process. Studies found that the types and concentrations of pollutants in runoff are subject to time variation in such a process. Water quality indicators such as total suspended solids (TSS), chemical oxygen demand (COD), total nitrogen (TN), and total phosphorus (TP) often reveal higher pollutant concentrations at the initial stages of stormwater runoff (Hathaway et al., 2012b; Kayhanian & Stenstrom, 2021; Wang, Feng, & Min, 2023)—a phenomenon referred to as the "first flush (Chebbo, 1999; Saget, Chebbo, & Bertrand-Krajewski, 1996)". Consequently, managing the first flush has become a significant focus in urban stormwater management strategies, including Best Management Practices (BMPs), Sponge City, and Low Impact Development (LID) (Chaudhary, Chua, & Kansal, 2022; Jeung et al., 2019; Perera et al., 2019). Although MPs are widely available in road runoff (Jayalakshmamma et al., 2023; Rosso et al., 2022), research remains limited on the dynamic nature, the first flush phenomenon, and the characteristics of MPs in urban road runoff. This affects the development of effective management practices.

Apart from the time effect, MPs in urban road runoff are also likely affected by factors such as land use, season, and road pavement type. Such influencing factors are not reported in detail in existing studies. Moreover, despite increasing research on the risk assessment of MPs, there is still insufficient understanding of the impacts of MPs in urban road runoff. Particularly missing is the link between the MP characteristics and their risks to ecosystems and human health.

In recognizing the above research gaps, this study aims to analyze the characteristics and ecological risks of MPs in the initial runoff from various urban road surfaces. We also investigated the dynamic behavior and the first flush phenomenon of MPs in road runoff throughout selected entire rainfall events, as well as the potential influencing factors on MP concentration in the runoff. This study was conducted in Hong Kong, a typical densely populated city characterized by high levels of urbanization and plastic consumption. We examined six different roads during 11 rainfall events over a year and used the Raman spectroscopy technique to characterize MPs in the collected water samples. The findings are expected to not only provide valuable insights into MP pollution in urban road runoff—especially for high-density cities but also generate basic data for developing treatment methods for MP removal from road runoff.

4.2 Materials and Methods

4.2.1 Sample collection

Stormwater runoff samples from six road sites and natural rainwater samples across 11 rainfall events were collected between February 2021 and September 2022; the details are in Chapters 3.2 and 3.3.

Preliminary experiments indicated that direct digestion and filtration of the full stormwater samples would cause significant clogging of the filters, so we used and analyzed a 100 mL subsample from the original 2 L stormwater samples for MPs identification using Raman spectroscopy. To ensure representativeness, each sample was thoroughly mixed before subsampling.

4.2.2 Extraction and identification of microplastics

MPs were extracted by using the protocol established by Leung, Ho, Lee, et al. (2021). To remove biological materials, stormwater samples were treated with 10% hydrogen peroxide (H_2O_2) in a 40 °C water bath for 48 hours. The samples were then filtered using a stainless-steel filter membrane with a 50 μm mesh size. For particles smaller than 50 μm, density separation was conducted by adding saturated sodium iodide solution (NaI; density = 1.83 g/mL) to the sample, followed by centrifugation at 1000 rpm for 5 mins. The supernatant (20 mL) was filtered through a stainless-steel filter membrane with a 5 μm pore size.

The MP particles retained on the stainless-steel membrane were identified using a Renishaw inVia Raman microscope (Wotton-under Edge, Gloucestershire, UK). The whole area (Ø=8mm) was scanned using a Leica 10×objective (Wetzlar, Germany) and a 785 nm edge laser (300 mW output power). The Raman spectra were acquired for 10 seconds using a laser power of 0.05–1%. Renishaw WiRE 5.1 software was used for cosmic ray removal and baseline correction of the spectra.

For spectral identification, a non-negative least squares algorithm was used for component analysis, and the spectra were compared against a database (Renishaw Polymeric Materials Database) that includes the 30 most commonly identified plastics in Hong Kong (Ho et al., 2022; Leung, Ho, Maboloc, et al., 2021; Lo et al., 2021; Mak et al., 2020). The polymer type was confirmed if the matching index was above 0.6. For indices between 0.4 and 0.6, the sample spectrum was re-examined visually for matching of characteristic peaks with the standard.

MP particle sizes were measured from stereo images using ImageJ software (Ver. 1.52q). Fiber lengths were measured along the central axis, while the longest dimension was measured for MPs of other shapes. Due to detection limitations, the size distribution of microplastics (MPs) was classified into six ranges for further analysis: 20–100 µm, 100–200 µm, 200–300 µm, 300–500 µm, 500–1000 µm, and 1000–5000 µm.

4.2.3 Quality assurance and quality control (QA/QC)

Comprehensive quality control measures were performed to ensure the accuracy and reliability of MP analysis in this study, including procedural blanks and spike tests (Shruti & Kutralam-Muniasamy, 2023). Procedural blanks (n = 3) involved 1 L of Milli-Q water treated with hydrogen peroxide (H_2O_2), following the same procedure used for the road runoff and rainwater samples. These blanks were analyzed with Raman spectroscopy. For recovery efficiency, spike tests were conducted by adding known quantities of polyethylene (PE) particles to Milli-Q water: 50 particles of 500 µm and 100 particles of 50 µm per L. These spiked samples underwent the same pre-treatment and analytical procedures as the road runoff and rainwater samples to validate the method's efficacy in recovering MPs. The results of these quality control measures are shown in Table 4.1. Additionally, no microplastics were detected in the procedural blanks, confirming the absence of background contamination.

Table 4.1. Procedural blanks and spike test recovery assessments for polyethylene particles of size 50 µm (n = 100) and 500 µm (n = 50).

Trial	**Procedural blank (No. of MPs)**	**Number of recovered particles**		**Recovery rate**	
		500 µm	50 µm	500 µm	50 µm
1	0	48	97	96%	97%
2	0	50	96	100%	96%
3	0	49	98	98%	98%
Average	0	49	97	98%	97%
% deviation	0%	-	-	2.0%	1.0%

4.2.4 Statistical analysis

MP abundance was normalized using a square root transformation. The differences in MP abundance across locations, rainfall events, land uses, and meteorological variations were analyzed using a one-way analysis of variance (ANOVA) test. Differences in MP abundance between road runoff and natural rainwater, as well as between concrete and asphalt pavements, and dry and wet seasons, were assessed using the two-sample t-test. Additionally, a Pearson correlation analysis was conducted to investigate the relationship between MP abundance and rainfall intensity, as well as between MP abundance and antecedent dry days. A significance level of $p < 0.05$ was set for all statistical tests.

4.3 Results and Discussion

4.3.1 Microplastic abundance in the road runoff

MPs were detected in 97.0 % of the 67 stormwater samples collected from the six different road pavements. A median MP abundance of 185 particles/L (range = 0–940 particles/L; Figure 4.1a) was observed in the initial road runoff across the 11 rainfall events. The median MP abundance varied between the six sites, ranging from 140 to 280 particles/L. Our findings are consistent with those of Sugiura et al. (2021), who reported an MP abundance of 292 pieces/L in highway runoff.

Sites C, D, and F exhibited higher median MP abundance (251, 220, and 280 particles/L, respectively) compared to the lower ranges of 140–180 particles/L observed at the other three sites (Figure 4.1a). Despite these differences, no difference in MP abundance was found across the sampling sites (ANOVA test; $p > 0.05$). The higher MP levels at sites C, D, and F may be attributed to their locations near markets and industrial areas with high traffic and population density, where activities such as trading, transporting goods, and cleaning likely contribute to increased MP generation. Notably, no particles were detected at site A during the 4th rainfall event and at site F during the 2nd event. This could be due to variations in rainfall intensity and duration, differences in flow rates and water turbulence, or limitations in sampling and analytical methods. Similar variability in MP abundance has been reported in other studies, with concentrations in stormwater drains ranging from 0 to 3,500 particles per kilogram (Lutz, Fogarty, & Rate, 2021).

MPs were also detected in natural rainwater, with a median abundance of 40 particles/L (Range = 10–260 particles/L) during the 11 rainfall events. This presence is likely due to atmospheric deposition and wind influences (Y. Huang et al., 2021). Strady et al. (2021) similarly reported substantial variation in atmospheric MP deposition in Southeast Asia, ranging from 71 to 917 particles/m^2 per day. While the measurement units and sampling contexts differ between our study and theirs, these findings highlight the significant role of atmospheric deposition in contributing to MP levels in rainwater.

Additionally, a significant difference was found in MP abundance between road runoff and natural rainwater (t-test, $p < 0.05$). Figure 4.1 (b) summarizes the abundance distributions of MPs in the road runoff and rainwater during the 11 rainfall events. Notably, the median MP abundance in road runoff (median = 185 particles/L) is 4.6 times that in rainwater (median = 40 particles/L). The complex urban road environments may lead to greater concentrations of MPs, indicating the significance of terrestrial MP pollution.

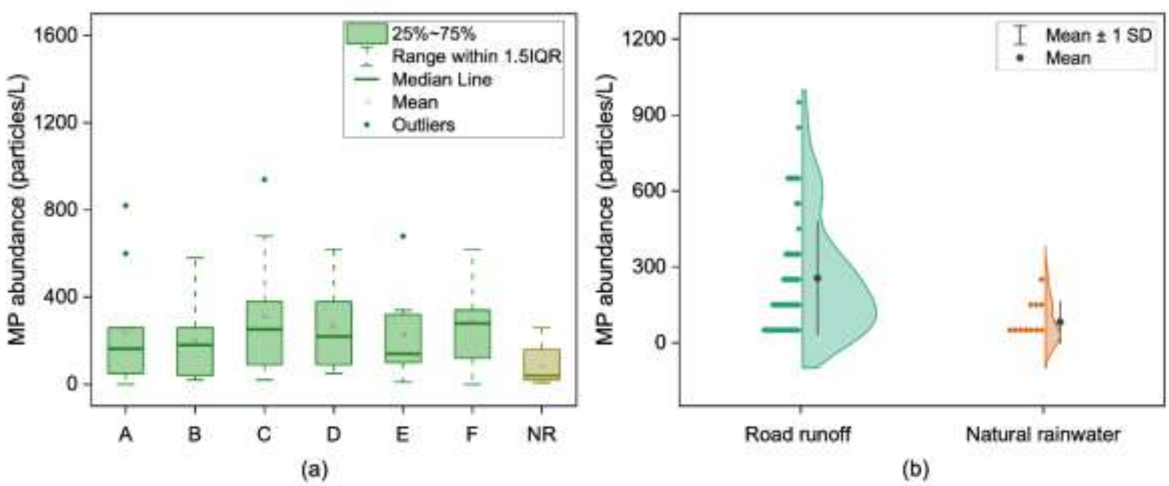

Figure 4.1. Microplastic abundance found in the first flush: (a) MP abundance found at each site (site A–F) and in natural rainwater (NR); (b) The distributions of MP abundance during the 11 rainfall events in the road runoff and natural rainwater.

4.3.2 Dynamic properties of microplastics throughout the rainfall

The temporal changes in MP abundance, flow rates, and dimensionless M(V) curves were examined at sites A and C during the 10th and 11th rainfall events to assess the first flush effect and dynamic nature of MPs in road runoff in Hong Kong (Figure 4.2).

The dimensionless M(V) curves for MPs consistently remained above the 45° bisector throughout the rainfall events, showing a positive first flush phenomenon (Figure 4.2c). However, the degree of first flush effect can vary between rainfall events, likely influenced by multiple factors such as rainfall intensity, traffic flows, and human activities on the roads (Mamun, Shams, & Nuruzzaman, 2020; Tuttolomondo et al., 2020). These findings are consistent with observations by Sun et al. (2023) and Do et al. (2023), indicating a significant MP transport in stormwater runoff. Additionally, we observed that about 80% of the total mass of MPs was carried by the initial 60%-70% of runoff volume in these rainfall events (Figure 4.2c), which typically occurred within the initial 20 mins of runoff generation (Figure 4.3). This indicates that the majority of MPs in road runoff are discharged in the early stages of rainfall.

Furthermore, the dynamic changes of MP abundance in road runoff may be closely linked to the flow rate variations in stormwater runoff. In the 10th rainfall event, the peak MP abundance occurred at the 10th minute of runoff, with 250 particles/L, while in the 11th event, the peak abundance was observed at the 5th minute, with 320 particles/L (Figure 4.2b). The peak MP abundance was observed before the peak flow of the runoff, with a noticeable decline in MP abundance following the peak flow (Figure 4.2a and 4.2b). This pattern suggests that the variations of flow rates significantly influence the mobility of MPs on the roads, similar to trends reported by Treilles et al. (2021), and for other stormwater pollutants like organic contaminants (Peter et al., 2020).

These findings confirm that MP abundance is heavily affected by dynamic hydrological conditions during rainfall events, and the first flush phenomenon is significant for MP transport. This highlights the importance of targeting the initial stages of runoff for effective mitigation and management strategies for MP pollution in urban environments.

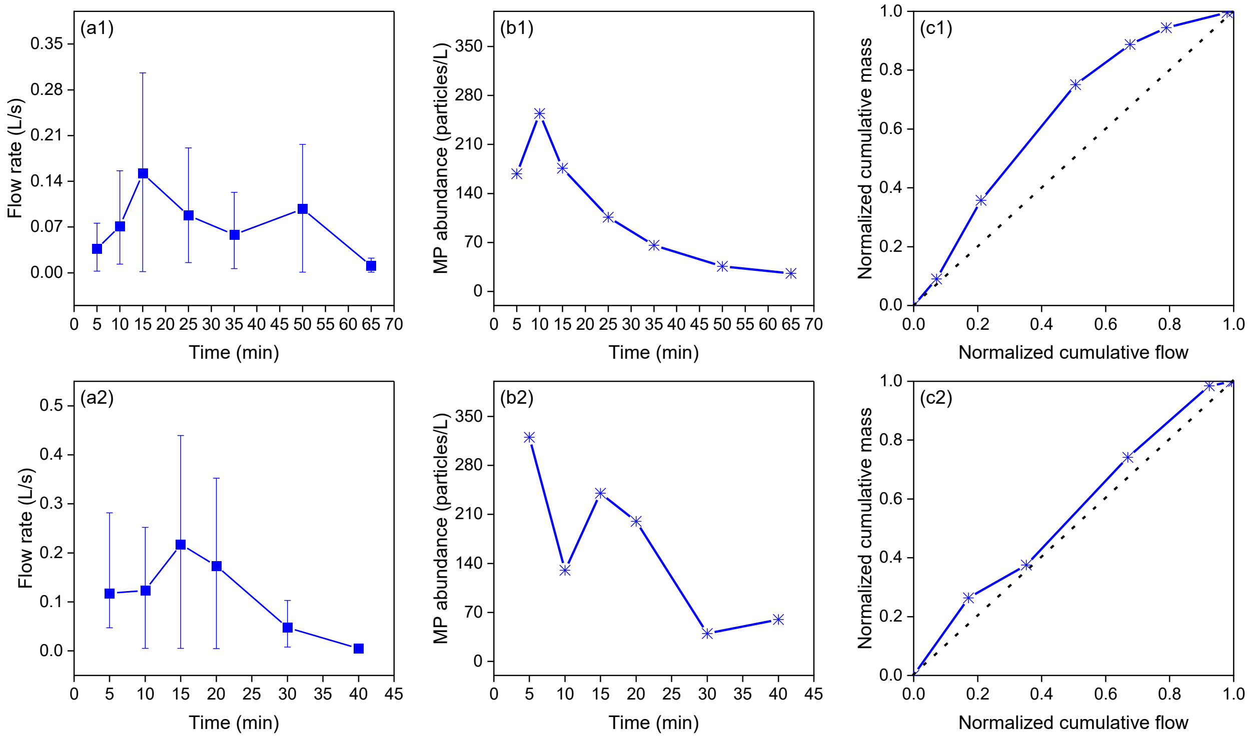

Figure 4.2. Temporal changes of MP abundance, flow rates, and the dimensionless M(V) curves: (a1, b1, c1) Data from site A during the 10th rainfall event; (a2, b2, c2) Data from site C during the 11th rainfall event. Each set includes flow rates (a1, a2), MP abundance (b1, b2), and M(V) curves (c1, c2) for stormwater on road pavements.

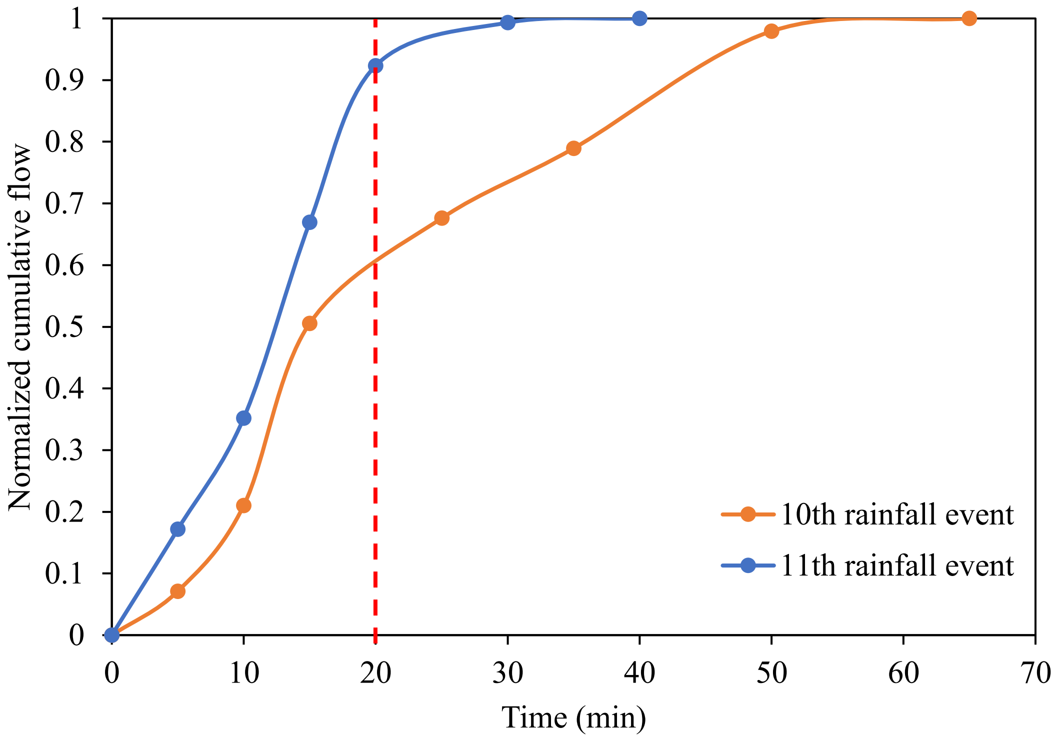

Figure 4.3. The relationship between the normalized cumulative flow and the runoff generation time during these two rainfall events.

4.3.3 Characterization of the microplastics in the road runoff

Eleven polymer types were identified in the road runoff samples, including polypropylene (PP), polyethylene (PE), polystyrene (PS), polyethylene terephthalate (PET), polycaprolactam (Nylon 6), poly (hexamethylene adipamide) (Nylon 6,6), poly (methyl methacrylate) (PMMA), poly(tetrafluoroethylene) (PTFE), poly (vinyl chloride) (PVC), poly(4-methyl-pentene) (PMP), and poly(alpha-methyl styrene) (PMS) (see Appendix B, Table B-1; Figure 4.5). PP, PE, and PS were the most abundant polymer types at each site, accounting for 39.0% (26.0%–65.0%), 36.0% (18.0%–49.0%), and 17.0% (5.0%–25.0%) of all samples, respectively (Figure 4.4a). These findings are consistent with those from previous studies on stormwater runoff conducted in Hong Kong (Mak et al., 2020; Zhang et al., 2022). PE and PP are commonly used in food packaging, reusable bags, pipes, and automotive parts. PS is typically used in building insulation and electronic equipment. These items can easily become deposited on the road surface through vehicle transportation, human activities, and atmospheric deposition.

Moreover, we found that natural rainwater samples mainly contained PP, PE, PS, and PET, whereas a higher diversity of polymer types was detected in road runoff.

The MP samples were classified into four shapes: fragments, films, fibers, and pellets (see Appendix B, Table B-2; Figure 4.6). Figure 4.4 (c) illustrates the percentage of shapes found for different polymer types. Fragments were the most common MP shape, consistent with findings reported by Zhang et al. (2022). In all samples, over 50% of detected particles of Nylon 6, Nylon 6,6, PE, PMP, PP, PS, PTFE were in the shape of fragments. Additionally, PMMA, PE, PP, and PS were detected as films, while PET predominantly appeared as fibers.

The majority of MPs were 20–100 μm (22.8% ± 11.8%), 100–200 μm (39.1% ± 8.4%), 200–300 μm (14% ± 6.3%), and 300–500 μm in size (16.7% ± 6.8%), with the remaining between 500–1000 μm (9.1% ± 7.7%) and 1000–5000 μm (4.8% ± 4.8%, Figure 4.4b; Appendix B, Table B-3). Over 60% of the observed MPs were smaller than 300 μm, which are predominantly PE and PP (Figure 4.4d).

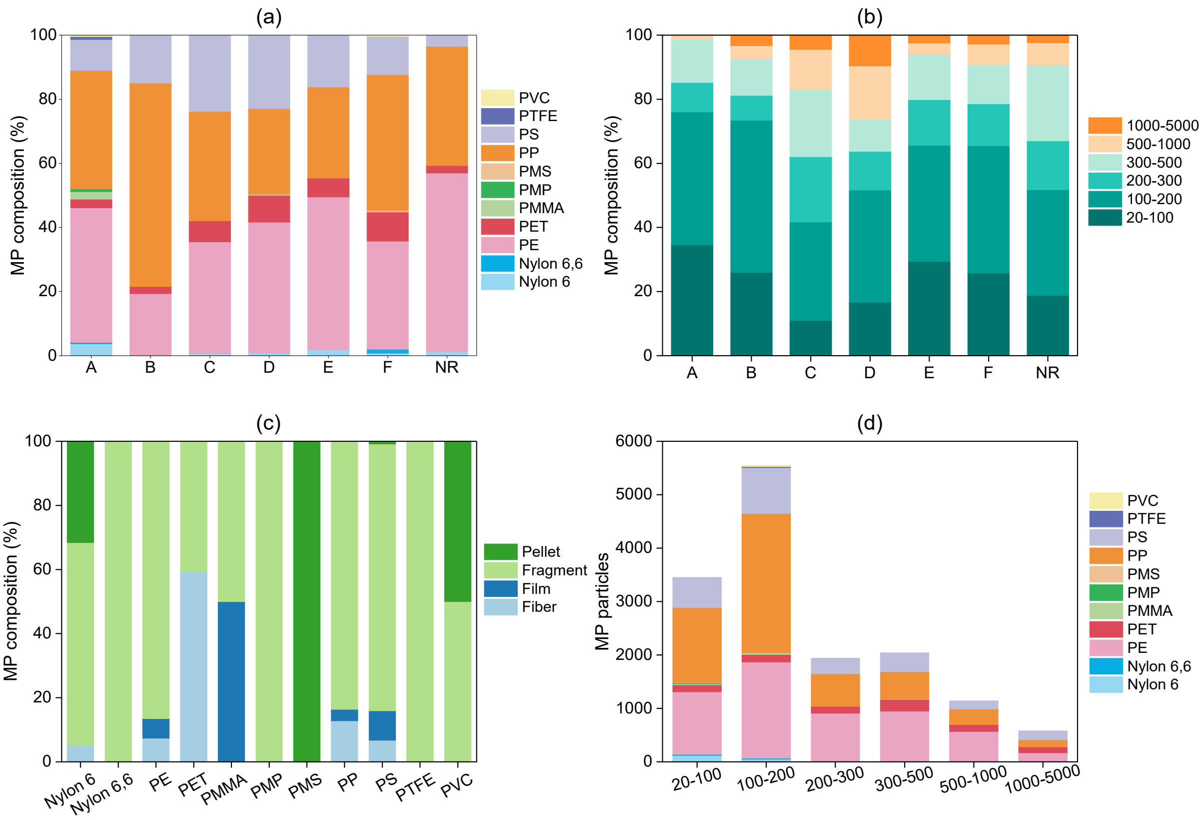

Figure 4.4. The distribution and characteristics of microplastics: (a) the percentage of different polymer types at each site; (b) the percentage of MP size at each site; (c) the percentage of shapes found in different polymers; and (d) the size distribution of different polymers. Note: polypropylene (PP), polyethylene (PE), polystyrene (PS), polyethylene terephthalate (PET), polycaprolactam (Nylon 6), poly (hexamethylene adipamide) (Nylon 6,6), poly (methyl methacrylate) (PMMA), poly(tetrafluoroethylene) (PTFE), poly (vinyl chloride) (PVC), poly(4-methyl-pentene) (PMP), and poly (alpha-methyl styrene) (PMS).

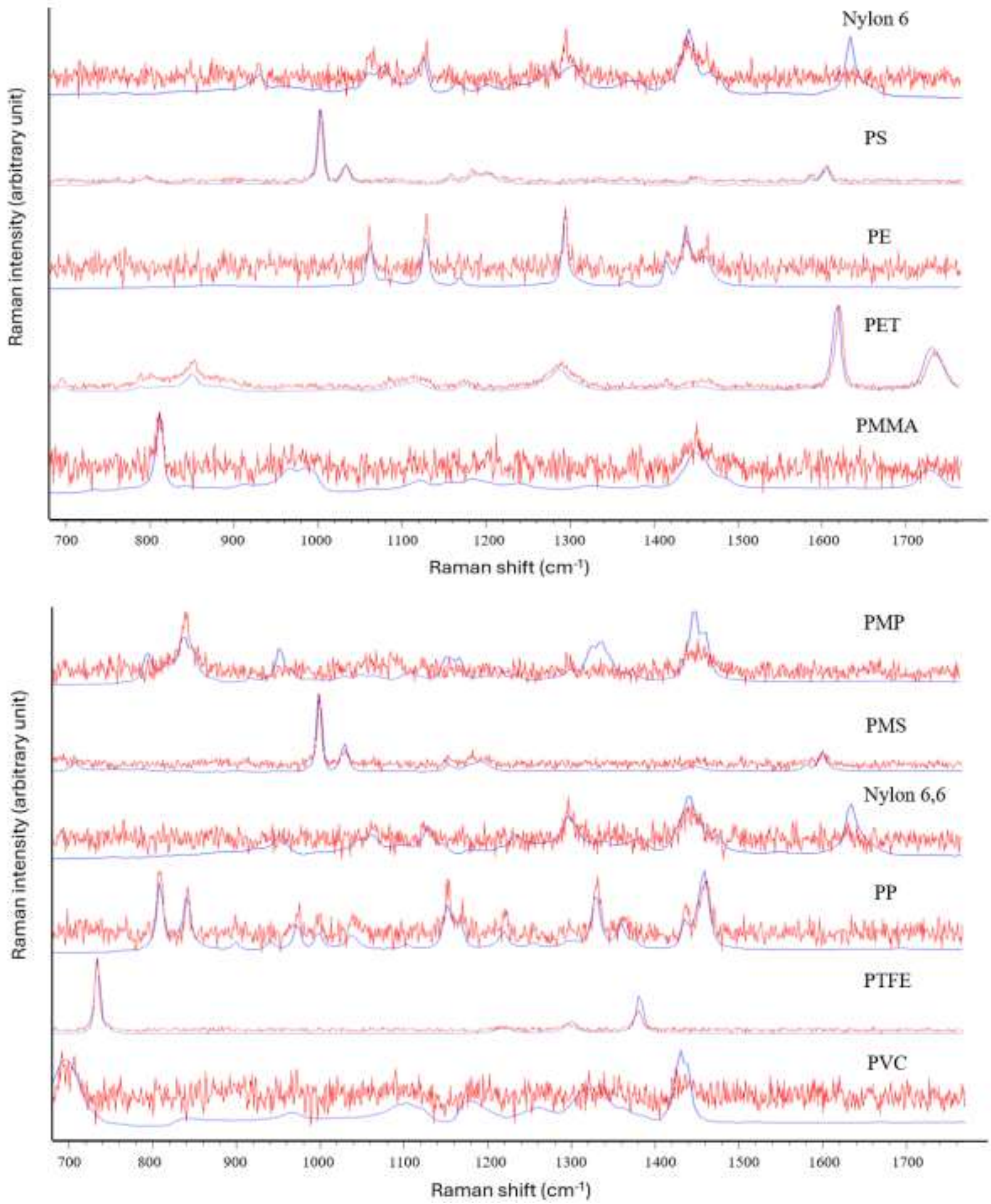

Figure 4.5. Example polymer spectra for the eleven identified polymer types, with red lines for the environmental particles and blue for the reference spectra, including Nylon 6, PS, PE, PET, PMMA, PMP, PMS, Nylon 6,6, PP, PTFE, and PVC. The matching index ranged from 0.41 to 0.97.

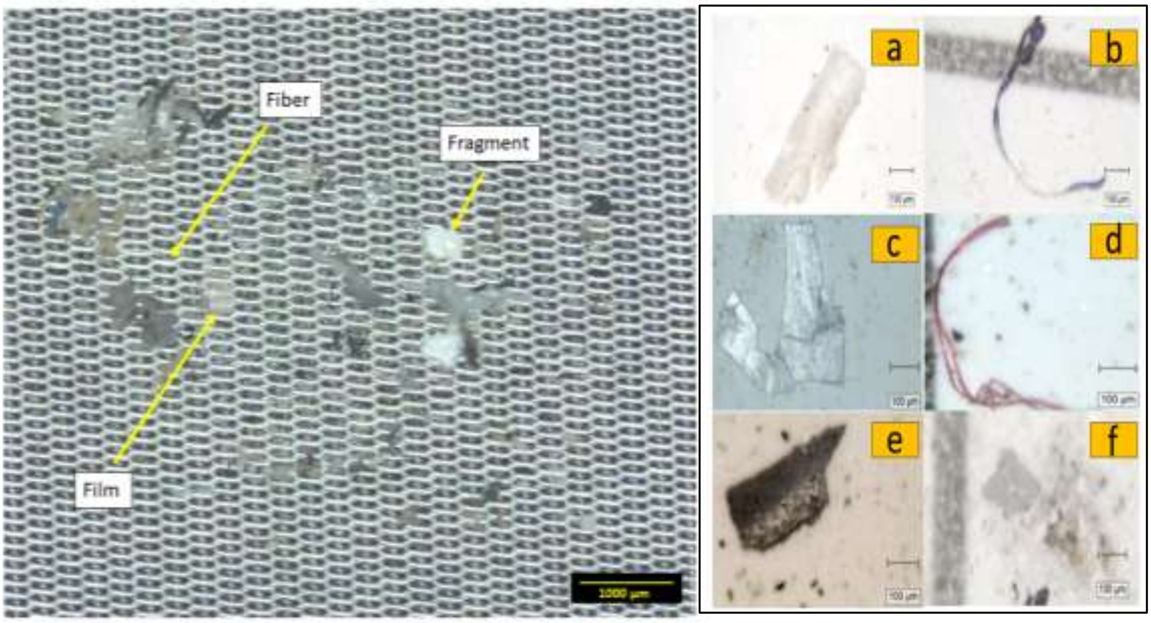

Figure 4.6. An example of microplastic shapes, including fiber, film, and fragments from the stormwater sample collected at site E on 07/10/2021.

4.3.4 Factors affecting microplastic abundance in road runoff

4.3.4.1 Land uses

Figure 4.7a presents the MP abundance in road runoff across various land uses. Residential areas showed the highest median value (245 particles/L), followed by industrial areas (220 particles/L) and commercial areas (165 particles/L). However, the differences in MP abundance between the various land uses were not statistically significant (ANOVA test; $p > 0.05$). The higher MP abundance in residential areas may be attributed to higher population density and traffic flow. Markets in residential areas and plants in industrial areas could further increase MP production. Additionally, rainfall characteristics and road cleaning practices may impact the variation in MP abundance across different land uses (Wei et al., 2023).

4.3.4.2 Meteorological variations

Relationships between MP abundance and meteorological variations were analyzed, including the effects of seasonal changes (e.g., meteorological seasons, dry and wet seasons) and the number of antecedent dry days before rainfall events.

We observed a significant difference in MP abundance between spring and autumn (ANOVA test; $p < 0.05$). The highest median MP abundance was found in autumn (340 particles/L), followed by winter (190 particles/L), summer (180 particles/L), and spring (35 particles/L) (Figure 4.7b). Additionally, the median abundance of MPs in the wet season (260 particles/L) was 2.2 times higher than that in the dry season (120 particles/L) (Figure 4.7d). This seasonal variation may be related to differences in rainfall intensities. We found a strong correlation between rainfall intensity and seasons (Pearson correlation; $p < 0.05$), with lower rainfall intensity typically occurring in spring and the dry season, and relatively higher intensity in autumn and the wet season. Higher rainfall intensity could increase the mobility of MPs in road runoff by washing out more MPs that accumulate on road surfaces. However, our findings did not show a significant direct correlation between rainfall intensity and MP abundance (Pearson correlation; $p > 0.05$; Figure 4.8a), suggesting that other factors such as atmospheric deposition, traffic volume, and human activities may play an important role in influencing MP presence and distribution (Abbasi, 2021; Cho et al., 2023). For instance, regular road cleaning by sanitation workers in urban areas might reduce the quantity of MPs available for transport in runoff, potentially overshadowing the effects of meteorological and seasonal variations alone.

Additionally, we observed that MP abundance after longer antecedent dry days (>50 days; mean = 315 particles/L) was higher than that after shorter antecedent dry days (<10 days; mean = 253 particles/L) (Figure 4.8b), aligning with the findings by Cho et al. (2023). This suggests that longer dry periods may allow for greater accumulation of MPs on road surfaces, which could subsequently be mobilized during rainfall events. These findings emphasize the need to account for both natural factors (e.g., rainfall patterns and atmospheric deposition) and human activities (e.g., road cleaning practices) when assessing MP dynamics in urban environments.

4.3.4.3 Pavement types

The median MP abundance in runoff on concrete pavements was slightly higher than that on asphalt pavements; however, no significant difference in MP abundance was found between the two road types (median = 190 and 180 particles/L, respectively; t-test; $p > 0.05$; Figure 4.7c). Asphalt pavements are rougher than concrete pavements and may retain more MPs, resulting in lower MP abundance in runoff. Additionally, factors such as traffic volume and type, vehicle speed, and pavement age may also affect the retention and transport of MPs on different road pavements (Österlund et al., 2023). Therefore, future studies can investigate the influences of these factors on the fate and transport of MPs in stormwater runoff to better understand the impact of different road types on MP abundance.

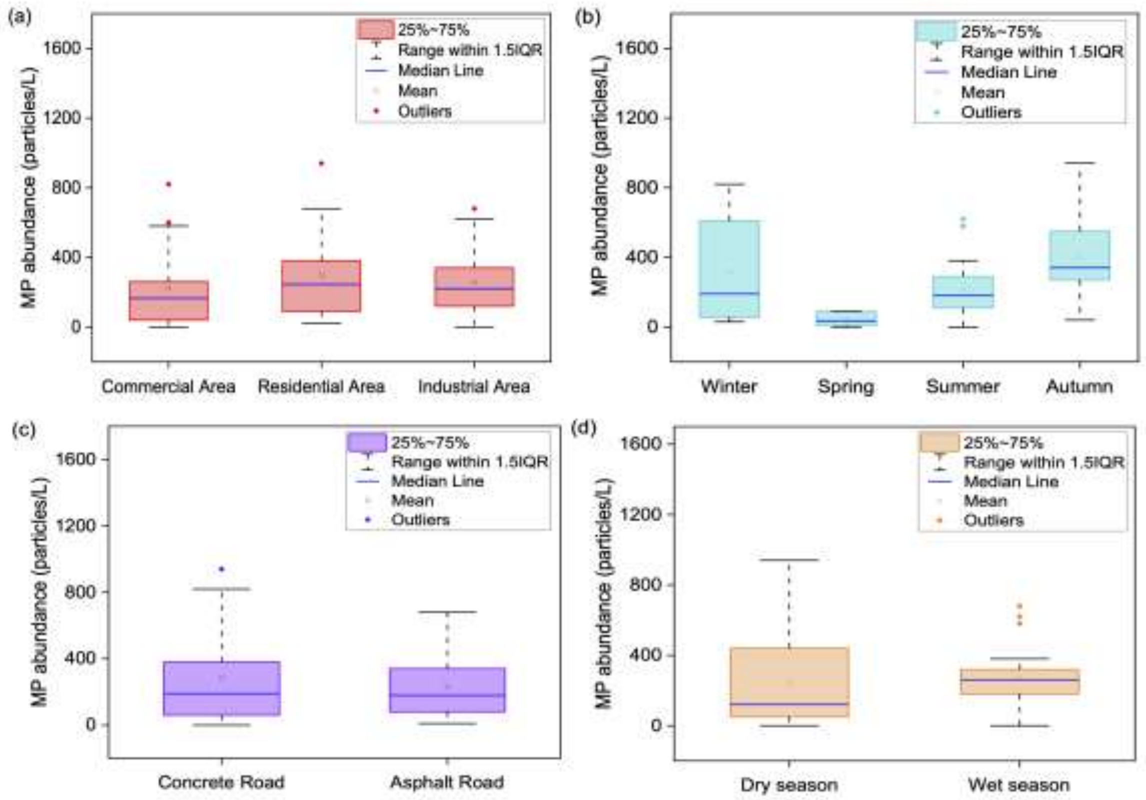

Figure 4.7. MP abundance in the road runoff under the different environmental factors: (a) MP abundance found on the roads with different land uses; (b) MP abundance at each site during different meteorological seasons; (c) MP abundance found on concrete and asphalt roads; and (d) MP abundance at each site in dry and wet seasons.

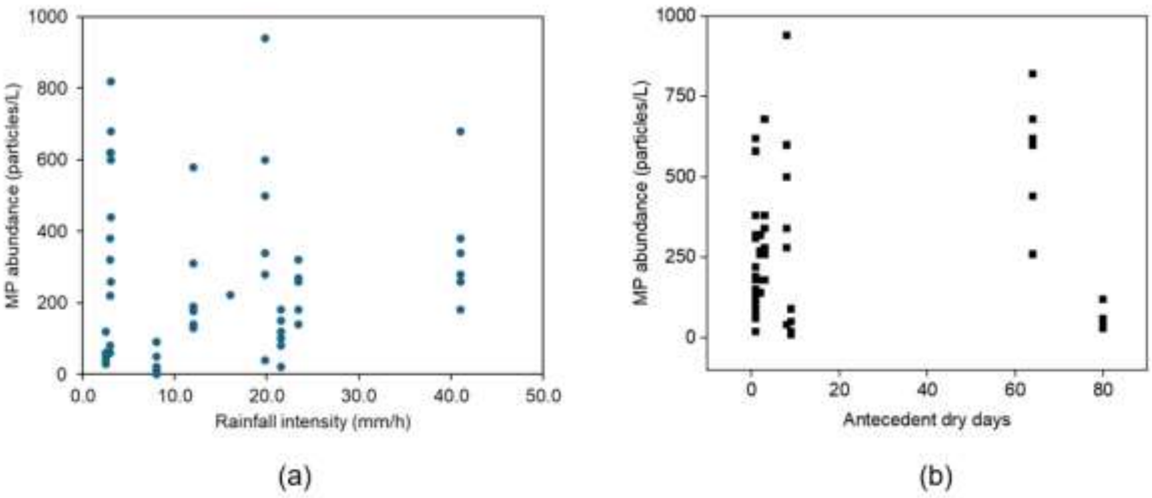

Figure 4.8. (a) The relationship between rainfall intensity and MP abundance; (b) The relationship between the antecedent dry days and MP abundance.

4.3.5 Ecological risk assessments

To assess the ecological and pollution risks of MPs in the study area, both rainwater and road runoff were evaluated using the Potential Load Index (PLI) and Potential Risk Index (PRI) (Figure 4.9; Appendix B, Table B-4). The PLI values in road runoff at each site ranged from 3.4 to 5.2, falling within Class I pollution ($PLI_{Zone} < 10.0$) and indicating relatively low levels of MP pollution load. However, the mean PLI value in road runoff (PLI = 4.2) was 1.7 times higher than that in rainwater (PLI = 2.5), suggesting a greater load of MPs in road runoff compared to rainwater.

Similarly, the PRI values in road runoff ranged from 7.3 to 138.0. The mean PRI value in the initial road runoff (H = 52.5) was significantly higher, being 7.2 times that found in rainwater (H = 7.3). PRI classifications at most road sites (H = 13.3–138.0) fell into categories II and III (10.0 < H < 1000.0), suggesting a moderate to high ecological risk of MP pollution. Notably, the PRI (H) values at sites A (H = 138.0) and F (H = 118.0) were higher than those at the other four sites (H = 7.3–24.5). MPs with high hazard scores for PVC and PMMA were found at sites A and F. These two types of polymers significantly contribute to the elevated ecological risk at the two locations. This is likely linked to the extensive use of plastics in commercial and industrial areas, such as construction materials, pipes, etc. (Kabir et al., 2024). The variability in rainfall intensity also plays an important role in influencing the mobilization of MP abundance and types into runoff, resulting in differing levels of polymer-related risks in road runoff.

The presence of diverse and high concentrations of MPs in road runoff can significantly increase toxicological risks to biological organisms in both aquatic and terrestrial environments when this runoff discharges into urban water bodies or overflows into roadside vegetation. Common polymers detected in the first flush of road runoff, such as PP, PE, PS, PVC, PMMA, PET, and PTFE, are known to be harmful to various organisms. For example, PS particles have been shown to cause liver inflammation in zebrafish (Xu et al., 2021), and PE and PP can exhibit toxic effects on medaka larvae (Pannetier et al., 2020). Other studies indicate that PE, PET, and PP negatively impact the feeding activity and energy reserves of aquatic organisms (S. Du et al., 2021; Silva et al., 2019), while PVC exposure can disrupt the growth of juvenile carp and damage their immune systems (Liu et al., 2023). Moreover, the chemical additives present in these MPs may cause acute toxicity in the early life stages of several marine invertebrates (Ding et al., 2022; W. Huang et al., 2021; Na et al., 2021). Additionally, MPs can interact with other chemical pollutants, exacerbating their toxic effects. For instance, PMMA particles have been found to negatively affect marine diatom growth when interacting with changes in salinity (Dong et al., 2022), and combined exposure to PTFE particles and heavy metals poses a significant threat to plant growth (Kumar et al., 2022).

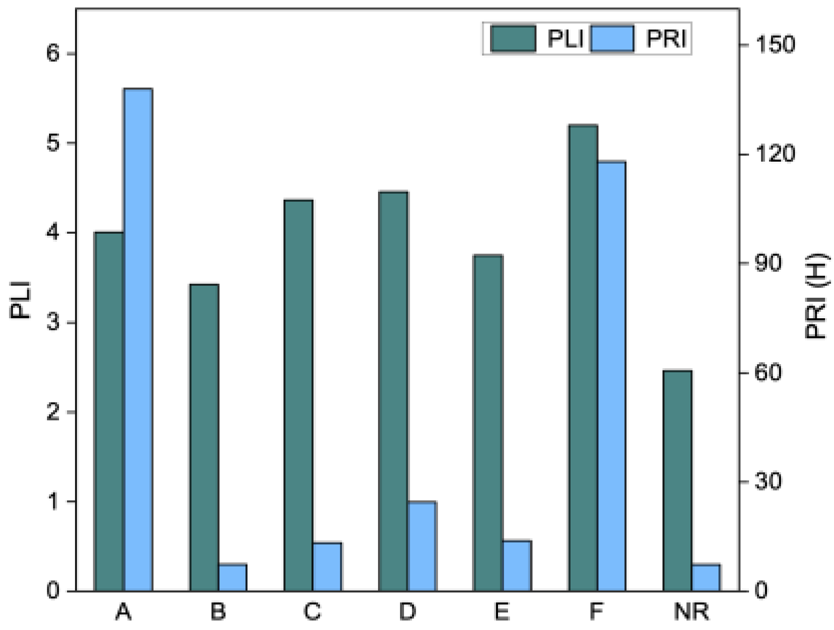

Figure 4.9. The values of the Potential Load Index (PLI) and Potential Risk Index (PRI) for polymers in the initial road runoff at the sampling sites (A–F) and the natural rainwater (NR) in Hong Kong.

4.3.6 Comparative analysis of microplastic levels in rainfall, runoff, and stormwater systems

Figure 4.10 and Table B-4 (Appendix B) present a comparison of MP abundance across different environmental media, including natural rainwater (NR), initial road runoff (IRR), overall road runoff (RR), stormwater drains (SD), stormwater outfalls (SWO), and adjacent harbours (AH) in this study and other literature (Mak et al., 2020; Piñon-Colin et al., 2020; Tsang et al., 2017; Zhang et al., 2022). This comparison is for indicative purposes only due to the different filter mesh sizes adopted in other studies. The mean values of MP abundance were considered for comparison in this study, as mean values were adopted in some previous reporting studies.

The results show that the mean MP abundance in the initial road runoff (IRR) at six sites in our study (201–313 particles/L) is higher than those reported for overall road runoff (RR) (Mexico, 88–289 particles/L), stormwater drains (SD), and adjacent harbors (AH) in Hong Kong from other studies (0.7–20 particles/L). This suggests a decreasing concentration gradient of MPs from the initial stages of runoff to the later stages (remaining runoff), and further through stormwater drains and outfalls, eventually reaching the ocean, likely due to dilution and dispersion effects.

The MP abundance in natural rainwater during the 11 rainfall events in our study shows a large variance (10–260 particles/L). This suggests that rainfall plays a dual role as both a transport mechanism and a contributing source to MP levels in urban stormwater runoff. It captures airborne MPs from sources such as vehicle emissions, industrial processes, and tire wear and washes them down onto urban surfaces. As rainwater containing these MPs flows across roads and other urban surfaces, it contributes to the total MP load in stormwater runoff. This interaction between rainfall and urban surfaces results in an initial surge, where MP concentrations are highest, which is subsequently diluted as the runoff progresses through the drainage system. This finding underscores the importance of focusing on the early stages of stormwater runoff for effective MP management and mitigation strategies in urban areas.

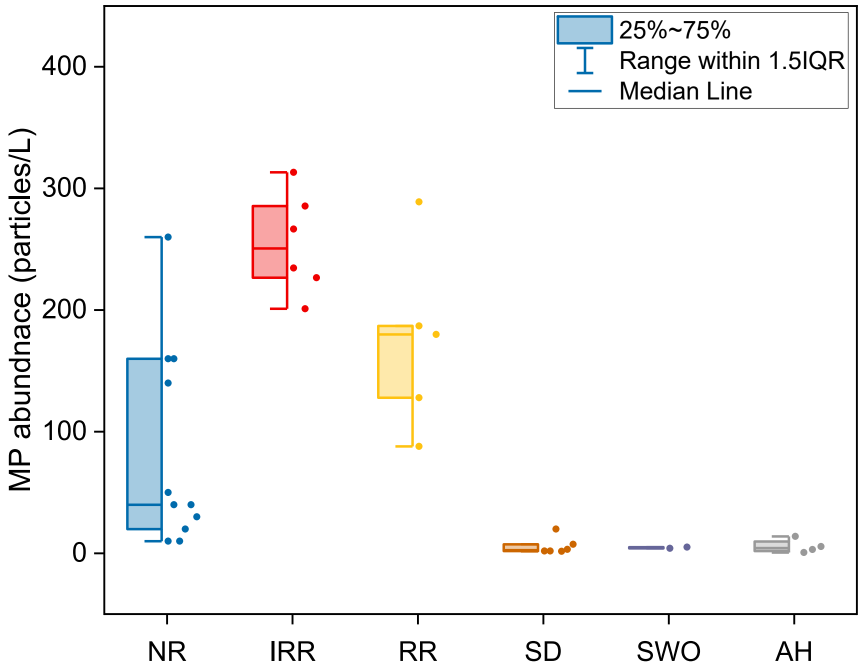

Figure 4.10. Comparison of MP abundance found in natural rainwater (NR), initial road runoff (IRR), road runoff (RR), stormwater drains (SD), stormwater outfalls (SWO), and adjacent harbors (AH) at different sites in Hong Kong and other regions (Mak et al., 2020; Piñon-Colin et al., 2020; Tsang et al., 2017; Zhang et al., 2022).

4.3.7 Future perspective

Controlling MP pollution in the initial road runoff is critically important for protecting aquatic and terrestrial environments. Several strategies may be considered to remove MPs from urban road runoff.

Firstly, runoff diverters and interceptors (Figure 4.11) can be strategically designed and implemented alongside urban roads to prevent initial runoff from entering drainage systems. This would enable the collection and disposal of MPs from stormwater. Secondly, enhanced filtration systems can be integrated into both road and green infrastructure to effectively capture MPs. For example, granular filtration techniques using different media (e.g., quartz sands, glass beads, activated carbon) have demonstrated removal efficiencies of 84%-96% for MPs in water bodies (Stang, Mohamed, & Li, 2022). Advanced membrane filtration, such as dynamic membranes (DM), can effectively capture nano-sized microplastics (Pizzichetti et al., 2023). Additionally, multilayer lattice filtration devices, assisted by vacuum systems, can capture MPs of various sizes in aquatic environments (Y. Zhang et al., 2021). These technologies can be adapted and applied within urban road infrastructure to assist in MP removal.

Moreover, innovative approaches, such as the use of microbial consortia for the biodegradation of MPs, could be employed in green infrastructure like green belts or constructed wetlands. For example, a bacterial combination of *S. maltophilia* and *B. velezensis* has been shown to degrade up to 43.5% of MPs (Xiang et al., 2023), offering a promising bioremediation strategy for removing MPs from road runoff.

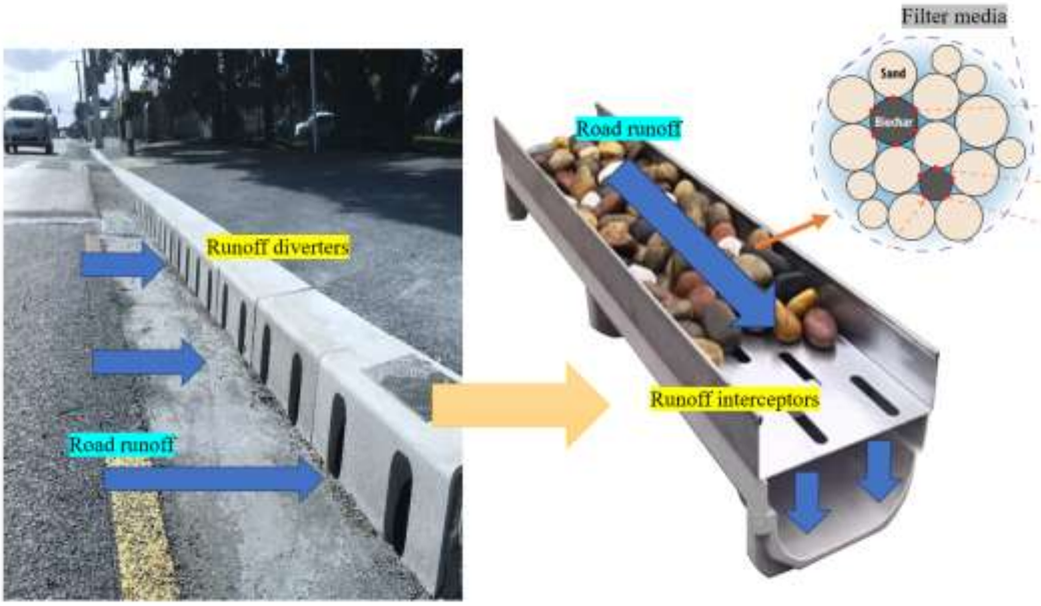

Figure 4.11. An example of the design of runoff diverters and interceptors installed alongside roadways.

4.4 Chapter Summary

By investigating seven sites across 11 rainfall events over more than one year, this comprehensive study provides important insights into the characteristics and ecological risks of MPs in urban road runoff. Overall, MP abundance in the initial road runoff (median = 185 particles/L) was 4.6 times higher than that in rainwater (median = 40 particles/L), demonstrating the significant contribution of urban roads to MP pollution. Eleven polymer types were identified in the road runoff samples, with PE, PP, and PS being the most common. Fragment was the dominant shape of the MPs, and over 60% of the MPs were smaller than 300 μm. In general, MPs in the runoff samples fall within Class II–III pollution levels, reflecting moderate to considerable ecological risks. The presence of polymers with high monomer hazard levels, such as PVC and PMMA, highlights the importance of addressing polymer-specific risks in road runoff.

The study also attempted to investigate the influences of various factors on MP abundance, including land use, seasonal variation, rainfall characteristics, and pavement material. Although there are differences in MP concentration associated with these factors, most of the differences are not statistically significant (except for the seasonal effect). This may be caused by some natural factors (e.g., rainfall characteristics and atmospheric deposition) and human activities (e.g., road cleaning practices). Overall, the results suggest a pressing need to control MP pollution near urban roadways, and effective measures should be targeted at the initial runoff.

CHAPTER 5. MULTI-POLLUTANT CHARACTERIZATION AND INTERRELATIONSHIPS

5.1 Introduction

Previous studies have identified a wide range of pollutants in urban stormwater runoff, including toxic substances, pathogens, chemical contaminants, and microplastics (MPs) (Cho et al., 2023; Du et al., 2019; Lee et al., 2020; V. C. Shruti et al., 2021; Treilles et al., 2021). These pollutants not only contribute to the degradation of urban water quality but also pose significant risks to both ecosystems and human health. The primary sources of these contaminants include atmospheric deposition, anthropogenic activities, and drainage surfaces (Müller et al., 2020). Among these, urban road pavements play a particularly critical role in pollutant transport, with impervious surfaces, vehicular traffic, and road-associated activities acting as major contributors (Järlskog et al., 2021; Lange et al., 2022; Rosso et al., 2023; Tamis et al., 2021). Common road-related activities, such as vehicle operation, road marking application, tire and brake wear, exhaust emissions, as well as street cleaning and maintenance, generate diverse pollutants, including heavy metals, sediments, suspended solids (SS), and MPs (X. Du et al., 2021; Gao et al., 2022; Österlund et al., 2023; Zhao et al., 2022). During rainfall events, stormwater runoff mobilizes these contaminants from road surfaces and often discharges them directly into nearby lakes, rivers, or oceans through urban drainage systems without prior treatment. This unregulated discharge significantly exacerbates urban water pollution.

Numerous studies have demonstrated that both the type and concentration of pollutants in stormwater runoff exhibit significant temporal variation throughout a rainfall event. Rainfall events and the resulting stormwater runoff represent highly dynamic hydrological and chemical processes. Water quality indicators such as TSS, COD, TN, and TP are often found at markedly elevated concentrations during the initial stage of runoff—a phenomenon widely known as the "first flush"(Chebbo, 1999; Saget, Chebbo, & Bertrand-Krajewski, 1996). The first flush phenomenon refers to the disproportionate transport of pollutants in the early portion of stormwater discharge, often carrying a major share of the total pollutant load. This phenomenon has become a central consideration in the design of urban stormwater management systems, particularly within frameworks such as Best Management Practices (BMPs), Sponge City concepts, and Low Impact Development (LID) approaches (Chaudhary, Chua, & Kansal, 2022; Jeung et al., 2019; Perera et al., 2019).

Although many studies have examined individual pollutants or single categories of contaminants in urban runoff, few have investigated the composite contamination framework in which metals, nutrients, organic matter, pathogens, and MPs co-occur, co-vary, and potentially interact during storm events. Existing research has rarely explored how these multi-pollutant interactions evolve dynamically or how they jointly reflect the mixed anthropogenic sources characteristic of compact high-density cities. Moreover, source-tracking approaches have seldom been integrated with multi-pollutant datasets to understand the co-origin and transformation of pollutants across road environments.

To address these gaps, this study introduces an integrated framework that: (i) characterizes composite contamination patterns across a broad suite of pollutants, (ii) identifies multi-source attributions using principal component analysis (PCA)-based pollutant signature analysis, and (iii) links these patterns to ecological risks under compact-city conditions. Accordingly, the objectives of this study are to: (i) systematically investigate and characterize multiple contaminants in urban road runoff;

(ii) analyse their major components, interrelationships, and dynamic behaviours, including MPs, metals, and conventional contaminants; (iii) evaluate the influence of environmental factors, such as city's functional zones and seasonality, on pollutant distribution and dynamics; and (iv) assess the ecological risks associated with pollutant loads in initial road runoff.

We hypothesize that: (1) road runoff in a compact, high-density city such as Hong Kong contains elevated contaminant levels due to intense traffic, human activity, and commercial operations; (2) multiple pollutants exhibit a pronounced first-flush effect, with several contaminants showing strong correlations due to common or overlapping sources; (3) pollutant magnitudes and profiles vary significantly across functional urban zones and seasons; and (4) the pollutant loads in the early-stage urban road runoff pose substantial ecological risks.

Road runoff pollution in high-density cities remains insufficiently characterized, even though such cities accommodate a large and rapidly growing proportion of the global population. By addressing this understudied context, the present work fills an important research gap. The integrated approach advances beyond traditional single-pollutant or single-factor paradigms, offering a more comprehensive conceptual and analytical perspective on urban runoff contamination. The findings are expected to yield critical insights into pollutant characteristics, co-occurrence behaviours, and ecological risks, thereby informing evidence-based stormwater management strategies for densely populated urban regions.

5.2 Materials and Methods

5.2.1 Sample collection

Stormwater runoff samples from six road sites and natural rainwater samples across 11 rainfall events were collected between February 2021 and September 2022. The study area and sampling methods are described in Chapters 3.2 and 3.3.

5.2.2 Stormwater quality parameter detection

Based on previous studies investigating stormwater quality, a total of 32 stormwater quality parameters were selected in this study to comprehensively analyse all collected samples. The rationale for selecting these parameters lies in their demonstrated relevance to the impacts of urban runoff on receiving environments, including water quality deterioration, eutrophication, ecological toxicity, and public health risks. Specifically, the parameters included: (1) Physicochemical properties: temperature, pH, turbidity, TSS, and dissolved oxygen (DO); (2) Nutrients: ammonia nitrogen (NH_4^+–N), nitrate nitrogen (NO_3^-–N), nitrite nitrogen (NO_2^-–N), total inorganic nitrogen (TIN; Sum of NH_4^+–N + NO_3^-–N + NO_2^-–N), and phosphate (PO_4^{3-}); (3) Organic matter indicators: biochemical oxygen demand (BOD_5) and COD; (4) Microbial indicator: *Escherichia coli* (*E. coli*); (5) Metals and metalloids: As, Cr, Cd, Pb, Zn, Cu, Ni, aluminium (Al), iron (Fe), and manganese (Mn); (6) Major ions and ionic strength parameters: electrical conductivity (EC), salinity, total alkalinity (TA), hardness, and major anions (fluoride F^-, chloride Cl^-, sulfate SO_4^{2-}, and bromide Br^-); (7) Emerging contaminants: MPs.

Common analytical methods and limits of quantification (LOQ) for the 32 stormwater quality indicators are provided in Table 5.1.

Table 5.1. Classification of stormwater quality parameters and common analytical methods. Total Inorganic Nitrogen (TIN) is calculated as the sum of nitrate nitrogen (NO_3^-–N), nitrite nitrogen (NO_2^-–N), and ammonium nitrogen (NH_4^+–N); that is, total inorganic nitrogen (TIN).

Category	**Representative Parameters**	**Analytical Methods**	**Limits of Quantification (LOQ)**
(1) Physicochemical properties	Temperature, pH, Turbidity, Total suspended solids (TSS), Dissolved oxygen (DO)	Multiparameter probe; 2100Q Portable Turbidimeter (Turbidity); Gravimetric method (TSS); Electrochemical sensors (pH, DO)	Turbidity: 0.02 NTU TSS: 2 mg/L
(2) Nutrients	Ammonia nitrogen (NH_4^+-N), Nitrate nitrogen (NO_3^--N), Nitrite nitrogen (NO_2^--N), Total inorganic nitrogen (TIN), Phosphate (PO_4^{3-})	Salicylate Method (NH_4^+-N); Cadmium Reduction Method (NO_3^--N); Diazotization Method (NO_2^--N); PhosVer 3 (Ascorbic Acid) Method (PO_4^{3-})	NH_4^+-N: 0.02 mg/L NO_3^--N: 0.1 mg/L NO_2^--N: 0.005 mg/L PO_4^{3-}: 0.02 mg/L

(3) Organic matter indicators	Biochemical oxygen demand (BOD_5), Chemical oxygen demand (COD)	Dilution and incubation method (BOD_5); Dichromate reflux method (COD)	COD: 5 mg/L BOD_5: 2 mg/L
(4) Microbial indicator	*Escherichia coli* (*E. coli*)	The membrane filtration (MF) method	*E. coli:* 1 CFU/100mL
(5) Metals and metalloids	Aluminium (Al), Arsenic (As), Chromium (Cr), Cadmium (Cd), Lead (Pb), Zinc (Zn), Copper (Cu), Iron (Fe), Manganese (Mn), Nickel (Ni)	Inductively coupled plasma–mass spectrometry (ICP-MS)	Al: 0.5 ug/L As: 0.05 ug/L Cr: 0.05 ug/L Cd: 0.005 ug/L Pb: 0.01 ug/L Zn: 0.5 ug/L Cu: 0.05 ug/L Fe: 0.5 ug/L Mn: 0.02 ug/L Ni: 0.05 ug/L
(6) Major ions and ionic strength parameters	Electrical conductivity (EC), Salinity, Total alkalinity (TA), Total hardness, Fluoride (F^-), Chloride (Cl^-), Sulfate (SO_4^{2-}), Bromide (Br^-)	Electrochemical sensors (EC); The PSS-78 method using EC sensors (Salinity); Titrimetric methods (TA, Hardness); Ion chromatography	EC: 0.5µS/cm Salinity: 0.01 ppt TA:1 mg/L CaCO3 Total Hardness: 2 mg/L CaCO3 F^-: 0.01 mg/L Cl^-: 0.02 mg/L

		(IC)	SO_4^{2-}: 0.05 mg/L Br^-: 0.005 mg/L
(7) Emerging contaminants	Microplastics (MPs)	Raman spectroscopy	See Table 4.1

5.2.3 Statistical analysis

Stormwater quality parameters in this study did not meet the assumption of normality. Consequently, non-parametric statistical tests were employed throughout the analysis. Before conducting PCA and correlation analysis, the data were log10-transformed with a unit shift [log10 (x + 1)] to reduce skewness. Subsequently, Z-score standardization was applied to normalize the data and address differences in scale. PCA was then performed to analyse the major components of urban stormwater quality. The Kaiser-Meyer-Olkin (KMO) and Bartlett's tests were employed to assess the appropriateness of the data for PCA. A minimum measure of sampling adequacy (MSA) greater than 0.5 in the KMO test, along with a significant Bartlett's test result ($p < 0.05$), is required to ensure the suitability of the data for factor extraction (Roy et al., 2024). Spearman's rank-order correlation was used to examine associations among multiple stormwater quality parameters. The Mann–Whitney U test was employed to compare pollution levels between road runoff and natural rainwater, while the Kruskal–Wallis H test was applied to assess differences in stormwater parameters across road sites, land-use types, and seasons. A significance level of $P < 0.05$ was adopted for all statistical tests. All analyses were conducted using SPSS Statistics (IBM Corp., Armonk, NY, USA).

5.3 Results and Discussion

5.3.1 Stormwater pollution from urban roads

5.3.1.1 Characterization of stormwater quality in urban road runoff

Table 5.2 presents the statistical characteristics (minimum, maximum, mean, and median) of the 32 stormwater quality parameters measured in road runoff from six sites across 11 rainfall events.

For physicochemical properties, turbidity, and TSS concentrations in urban road runoff were remarkably high. Median concentration of TSS was 141 mg/L, and median turbidity was 68.0 NTU, indicating substantial resuspension of deposited sediments during rainfall events. Elevated TSS levels (max 438 mg/L) are likely associated with roadside urban activities such as bustling pedestrian traffic, as well as road transportation-related factors, including road surface abrasion, tire wear, and vehicular emissions, all of which contribute particulate matter to runoff. The finding is consistent with previous studies that have identified road-related activities as major sources of sediments in urban runoff (Helmreich et al., 2010; Zhao et al., 2022). DO levels were relatively low (median 5.3 mg/L), suggesting a potential risk of oxygen depletion in receiving waters. The pH of road runoff was neutral to slightly alkaline (6.0–8.3), consistent with the buffering effect of road dust and concrete (P. Zhang et al., 2023).

For nutrients, elevated nitrogen species were observed, with NO_3^-–N concentrations reaching up to 26.0 mg/L (mean 9.02 mg/L) and TIN averaging 10.2 mg/L, highlighting roads as important sources of nitrogen in stormwater. PO_4^{3-} concentrations (median 1.32 mg/L) were also relatively high, suggesting a strong eutrophication potential in downstream waters. These nutrient inputs likely originate from urban wastes and atmospheric deposition (Wang et al., 2022).

High levels of organic matter and microbial contamination were also detected in the initial road runoff. COD concentrations were extremely high (median 183 mg/L), suggesting urban road runoff may be enriched in organic pollutants from vehicular emissions, litter, and decomposing materials. *E. coli* concentrations were exceptionally high (median 37,800 CFU/100 mL), which may be influenced by fecal contamination from domestic animals and birds (McKee & Cruz, 2021). In Hong Kong, many roadside wet markets are located in densely populated urban areas and are subject to frequent deliveries and cleaning operations, which may contribute additional waste and pathogen inputs.

Regarding metals and metalloids, concentrations of Fe, Al, Zn, and Cu in the initial runoff were particularly high. Fe exhibited the highest median concentration at 740 μg/L, followed by Al at 729 μg/L, Zn at 141 μg/L, and Cu at 39.5 μg/L. The predominance of Fe and Al likely reflects their high natural abundance in road construction materials and their input from atmospheric dust deposition (Müller et al., 2020). Elevated Zn and Cu concentrations can be attributed to transportation-related sources, including vehicle emissions, tire wear, and brake pad abrasion (Gupta, 2020). Mn and Cr exhibited median concentrations of 28.1 μg/L and 13.6 μg/L, respectively. Pb, Ni, and As were present at comparatively lower concentrations, with medians of 9.08 μg/L, 3.84 μg/L, and 0.97 μg/L, respectively. Cd was detected in only a small number of samples, with a median of 0.06 μg/L. The risks of these metals and metalloids with varying concentrations will be discussed later.

For anions, elevated and highly variable concentrations of Cl^- were observed, with a median of 46.9 mg/L but a maximum value of 2,456 mg/L. Br^- showed a similar pattern, with a median of 0.81 mg/L but a maximum value of 554 mg/L. These high concentrations and large variability may be associated with the frequent use of chloride-and bromide-containing cleaning agents (Gronba-Chyła, 2022) during street washing at wet markets along residential roads in Hong Kong.

For MPs, the median MP abundance in initial road runoff was 185 particles/L, with a maximum of 940 particles/L across the 11 rainfall events (Lin et al., 2024). This is consistent with previous MP pollution studies (Lutz, Fogarty, & Rate, 2021; Sugiura et al., 2021). The diverse polymer composition, predominance of fragments, and high proportion of sub-300 μm particles underscore the important contributions of vehicular wear, road surface weathering, and urban activities to MP pollution in road runoff.

Overall, these results highlight the complex and heterogeneous composition of urban road runoff, reflecting the diverse land-use patterns and dense human activity characteristics of Hong Kong. Collectively, the findings underscore the crucial role of urban roads as major sources and pathways of stormwater pollution.

Table 5.2. Statistical summary (minimum, maximum, mean, and median) of 32 stormwater quality parameters measured in road runoff across six road sites during 11 rainfall events. The number of samples (n) for each parameter was 56. Total Inorganic Nitrogen (TIN) is calculated as the sum of nitrate nitrogen (NO_3^-–N), nitrite nitrogen (NO_2^-–N), and ammonium nitrogen (NH_4^+–N).

Category	Parameters	Unit	Minimum	Maximum	Mean	Median
(1) Physicochemical properties						
1	Temperature	℃	15.2	30.2	21.5	21.2
2	Turbidity	NTU	11.9	276	89.9	68.0
3	Total suspended solids (TSS)	mg/L	19.1	438	159	141
4	pH		6.1	7.6	6.8	6.8
5	Dissolved oxygen (DO)	mg/L	2.0	8.0	5.1	5.3
(2) Nutrients						
6	Ammonia nitrogen (NH_4^+–N)	mg/L	0.1	5.2	0.81	0.53
7	Nitrate nitrogen (NO_3^-–N)	mg/L	0.15	26.0	9.02	9.63
8	Nitrite nitrogen (NO_2^-–N)	mg/L	0.04	1.86	0.35	0.23
9	Total inorganic nitrogen (TIN)	mg/L	1.11	31.6	10.2	10.4
10	Phosphate (PO_4^{3-})	mg/L	0.21	10.1	2.01	1.32

(3) Organic matter indicators						
11	Biochemical oxygen demand (BOD_5)	mg/L	1.5	24.5	17.7	19.6
12	Chemical oxygen demand (COD)	mg/L	16.3	651	200	183
(4) Microbial indicator						
13	*Escherichia coli* (*E. coli*)	CFU/100mL	379	1,030,868	131,037	37,800
(5) Metals and metalloids						
14	Aluminium (Al)	µg/L	48.2	3,601	886	729
15	Arsenic (As)	µg/L	0.24	3.09	1.18	0.97
16	Chromium (Cr)	µg/L	2.6	22.4	13.6	13.6
17	Cadmium (Cd)	µg/L	0.0	1.2	0.12	0.06
18	Lead (Pb)	µg/L	0.11	37.7	11.3	9.08
19	Zinc (Zn)	µg/L	3.39	707	223	141
20	Copper (Cu)	µg/L	8.01	376	68.4	39.5
21	Iron (Fe)	µg/L	8.53	3,981	918	740
22	Manganese (Mn)	µg/L	4.62	182	38.6	28.1
23	Nickel (Ni)	µg/L	0.26	65.1	6.31	3.84
(6) Major ions and ionic strength parameters						

24	Electrical conductivity (EC)	mS/cm	0.04	6.39	0.81	0.29
25	Salinity	ppt	0.03	21.8	0.69	0.13
26	Total alkalinity (TA)	mg/L $CaCO_3$	30.0	170	70.2	67.5
27	Total hardness	mg/L $CaCO_3$	25.8	730	151	84.2
28	Fluoride (F^{-})	mg/L	0.0	5.41	0.50	0.17
29	Chloride (Cl^{-})	mg/L	4.25	2,456	262	46.9
30	Sulfate (SO_4^{2-})	mg/L	0.0	64.6	14.6	10.9
31	Bromide (Br^{-})	mg/L	0.0	554	25.9	0.81
(7) Emerging contaminants						
32	Microplastics (MPs)	Particles/L	0.0	940	255	185

5.3.1.2 Exceedance of urban water quality standards

Initial road runoff in Hong Kong exhibited markedly elevated concentrations of organic matter, nutrients, solids, and pathogens (Table 5.2), significantly exceeding the urban water quality objectives set by the Water Pollution Control Ordinance (HKEPD, 2021).

Specifically, the median COD concentration (183 mg/L) was 6.1 times higher than the WPCO objective of 30 mg/L, while the median BOD_5 concentration (19.6 mg/L) exceeded the standard of 5 mg/L by a factor of 3.9. The median TSS concentration (141 mg/L) was 5.6 times higher than the inland water threshold of 25 mg/L (HKEPD, 2021). The median TIN concentration (10.4 mg/L) was 26 times higher than the WPCO limit of 0.4 mg/L, and PO_4^{3-} (median 1.3 mg/L) exceeded the effluent discharge standard of 1.0 mg/L by 30%. Pathogen levels were also alarmingly high, with *E. coli* counts (median 37,800 CFU/100 mL) surpassing the WPCO limit of 1000 CFU/100 mL by 37.8 times. For metals, the mean Zn concentration (223 μg/L) was 2.2 times higher than the effluent discharge standard of 100 μg/L, while the mean Fe (918 μg/L) exceeded the effluent discharge standard of 600 μg/L by a factor of 1.5.

Collectively, these results highlight the severe pollution burden imposed by initial road runoff, which contributes substantially to the deterioration of urban water quality. These findings demonstrate the urgent need for greater public awareness and emphasize the importance of targeting the initial stages of runoff to develop effective mitigation and management strategies for key pollutants in urban environments.

5.3.1.3 Comparison with natural rainwater concentrations

Figure 5.1 illustrates the mean concentration ratios of 32 parameters in initial road runoff relative to NR across the 11 rainfall events. Most parameters in initial road runoff exhibited significantly higher concentrations than those in NR (Mann-Whitney U test, $P < 0.05$), proving that urban road runoff substantially enriches a wide spectrum of contaminants compared to atmospheric deposition alone. Detailed concentrations of stormwater quality indicators in NR during 11 rainfall events are summarized in Table B-5.

The most pronounced enrichment was observed for *E. coli*, with concentrations more than four orders of magnitude higher in road runoff than in NR. This shows the significant microbial contamination associated with road surfaces, likely originating from animal droppings, litter, and wash-off from roadside wet markets in urban areas. Among inorganic ions, Br^- and Cl^- exhibited an exceptionally high ratio of 1,090 and 198, respectively, reflecting major inputs from road cleaning agents. Elevated ratios were also evident for turbidity and TSS, which were 85.3- and 29.3-fold higher than natural rainwater, highlighting the strong resuspension of particulates accumulated on impervious road surfaces. In terms of metals, Fe, Al, Pb, As, and Cu showed substantial enrichment, with concentrations 139-, 36.7-, 31.8-, 18.0-, and 10.0-fold higher than those in natural rainwater, respectively. These may be attributed to road dust, construction materials, and vehicular wear (e.g., tires, brake pads). In addition, COD, BOD_5, PO_4^{3-}, and NO_2^-–N increased markedly (>10-fold), suggesting enhanced organic pollution and eutrophication potential from road runoff inputs.

By contrast, parameters such as temperature, pH, and DO had ratios close to unity, reflecting limited modification by surface wash-off processes. Collectively, these findings demonstrate that initial road runoff serves as a critical source of microbial, particulate, metal, nutrient, and organic pollutants, which can severely compromise downstream water quality if discharged untreated.

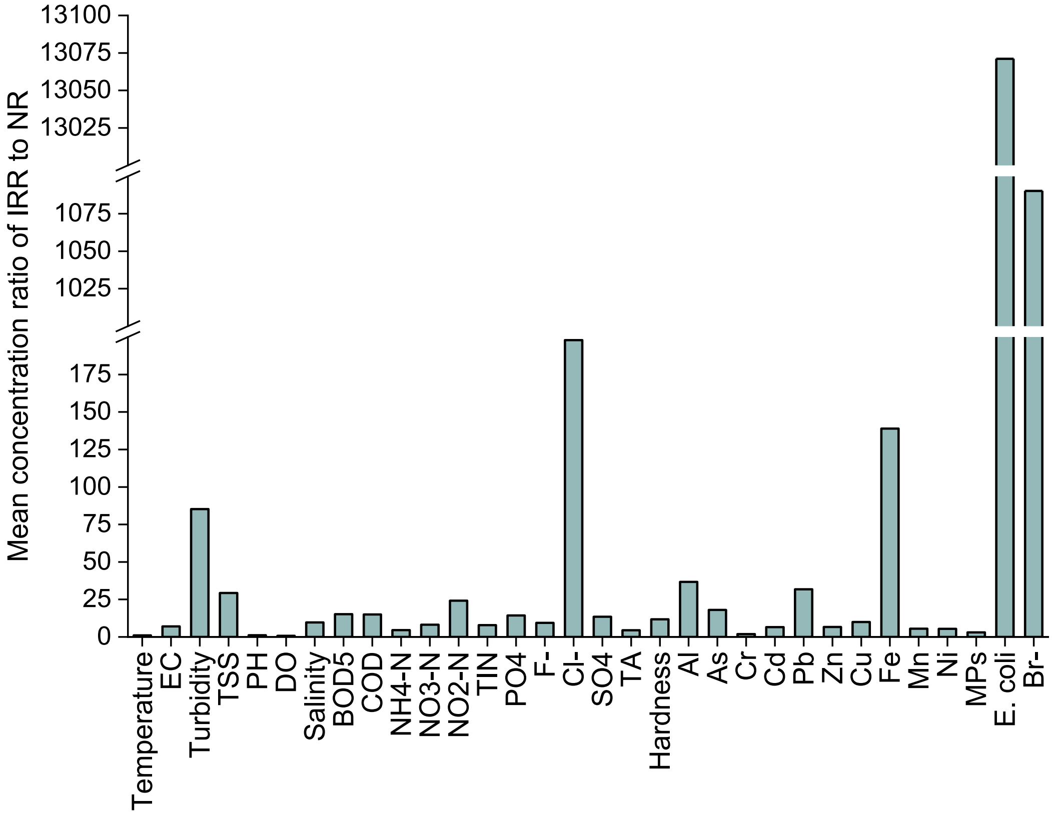

Figure 5.1. Mean concentration ratios of 32 parameters in initial road runoff (IRR) relative to natural rainwater (NR) across 11 rainfall events. Values > 1 indicate higher concentrations in road runoff compared to natural rainwater.

5.3.2. Principal component and correlation analyses of urban road runoff parameters

The major components of urban road runoff across 11 rainfall events were analysed using PCA, as shown in Figure 5.2. In this study, MSA was found to be 0.7 in the KMO test, and Bartlett's sphericity test was significant at an alpha level of 0.05. The KMO and Bartlett's tests suggest the dataset was suitable for PCA.

PCA was performed on the 32 parameters, and seven principal components (PCs) were selected based on eigenvalue criteria (Tripathi & Singal, 2019), covering 75.7% of the total variance (Table B-8). Among these, the first four PCs were the most representative, explaining 61.9 % of the total variance, as shown in Figures 5.2a and 5.2b. Specifically, the first two components (PC1 = 34.1%, PC2 = 12.0%) accounted for 46.1% of the total variance (Figure 5.2a). PC1 exhibited high loadings for Zn, Cu, Mn, Fe, Pb, As, Al, turbidity, and COD, which can be attributed to the mobilization of metals, suspended particles, and organic matter. This suggests runoff co-mobilizes traffic-derived road deposits, with metals migrating predominantly in particulate- and organic-associated forms alongside suspended solids and organic matter. PC2 showed high loadings for EC, Cl^-, PO_4^{3-}, NO_3^-—N, TIN, and hardness, indicating that ions and nutrient-related compounds are key components of urban road runoff. These may be associated with road-cleaning agents, urban waste from wet market activities, and atmospheric deposition. The PC3–PC4 loading plot (Figure 5.2b) explained an additional 15.9 % of the variance. PC3 exhibited high loadings for *E. coli*, suggesting fecal contamination sources from wastewater or open street markets. PC4 was dominated by MPs, pointing to pollution sources related to plastic products, including plastic litter degradation, roadway wear, and synthetic fiber release. Negative loadings for DO reflect its inverse relationship with pollutant levels, as oxygen is typically depleted under high organic and microbial loads. Negative loadings for salinity were likely associated with broader environmental background factors, such as rainfall-driven dilution. These findings might be further modulated by seasonal dynamics and land-use patterns.

Spearman correlation analysis was performed on the 32 stormwater quality parameters (Figure 5.2c). Significant correlations ($p < 0.05$) revealed clusters indicative of shared sources or coupled processes. Metals, including Pb, Zn, and Cu, showed strong positive correlations, pointing to common origins such as brake and tire wear, vehicle emissions, and surface abrasion (Gupta, 2020; Hong et al., 2020; Pradhan, Ram, & Mishra, 2021; Roy et al., 2022). These metals are typical indicators of traffic-related nonpoint source pollution, and their strong co-occurrence suggests synchronized deposition and mobilization during rainfall events. COD and BOD_5 showed significant correlations with metals (Cu, Zn, Mn) and turbidity, suggesting co-transport of metals and organic matter through particulate-associated processes such as surface adsorption and aggregation (Jeong et al., 2020; Luo et al., 2023). Additionally, nutrients (TIN) were positively correlated with metals (Fe, Mn, Zn, Cu, Pb), reflecting co-adsorption of nutrients with particulate-bound metals in sediments, as well as shared anthropogenic inputs such as road washing, sewage overflows, and market effluents.

MPs exhibited positive correlations with Ph, *E. coli*, PO_4^{3-}, and NO_3^-—N, suggesting association with biologically active or nutrient-rich urban runoff. Under neutral-to-alkaline conditions, MPs may remain suspended, reducing sedimentation. The co-occurrence with *E. coli*, PO_4^{3-}, and NO_3^-–N indicates that MPs serve as important carriers for nutrients and pathogens in urban road runoff, potentially originating from packaging waste, sanitary products, or littering. In contrast, MPs showed negative correlations with DO and Fe, likely reflecting MP accumulation in stagnant, oxygen-poor zones. This suggests their persistence in surface-active, low-oxygen environments, which are typical of densely urbanized areas.

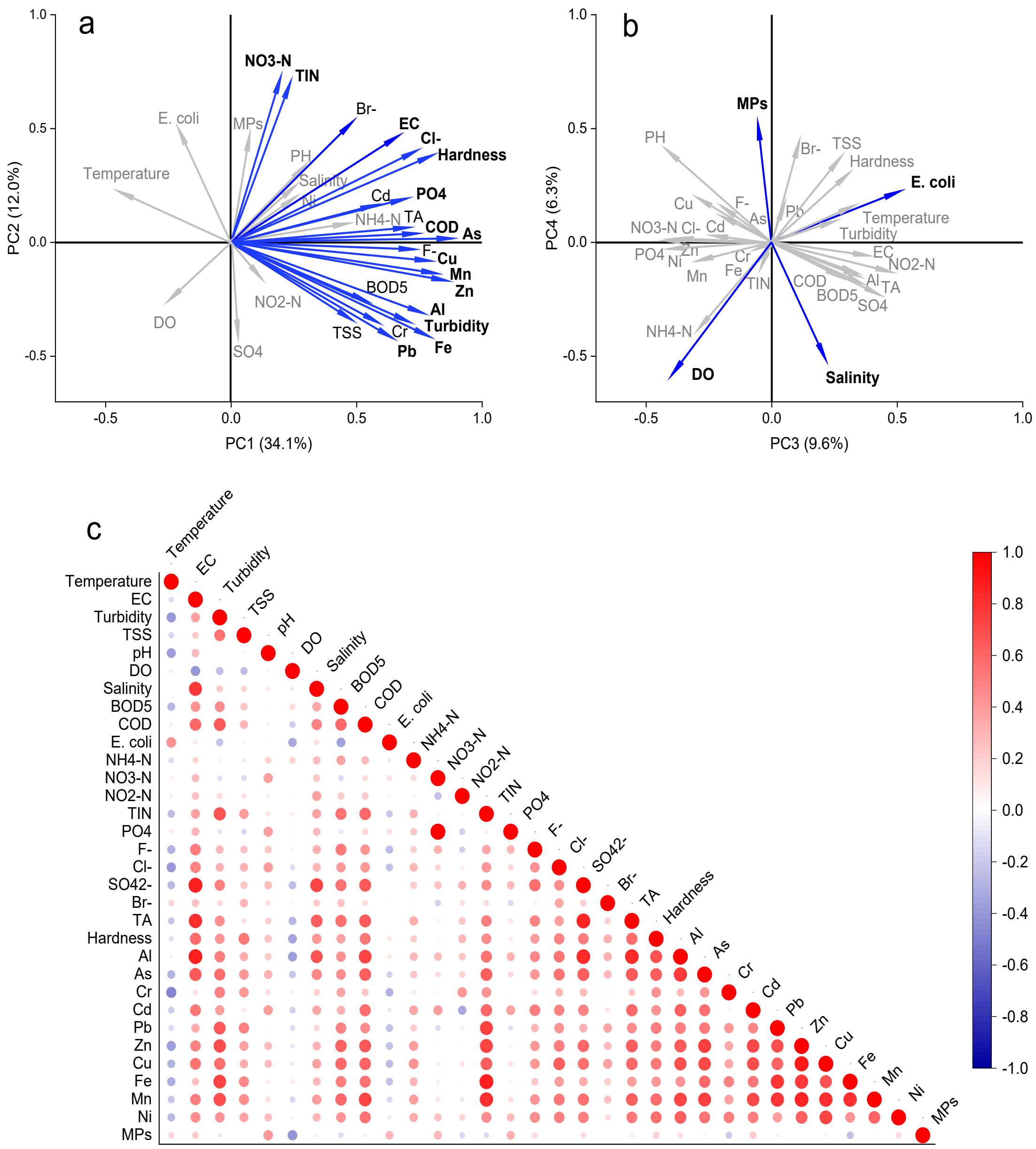

Figure 5.2. Principal component analysis (PCA) and Spearman correlation of 32 stormwater quality parameters in road runoff across 11 rainfall events. (a) Loading plot for PC1 (34.1%) and PC2 (12.0%), and (b) loading plot for PC3 (9.6%) and PC4 (6.3%): blue vectors (|loadings| ≥ 0.5) and grey vectors (|loadings| < 0.5) indicate the strength of contributions. (c) Spearman correlation matrix: colours from blue (-1.0) to red (1.0) indicate correlation strength.

5.3.3 First flush effects of stormwater parameters throughout rainfall

Seven representative parameters (COD, *E. coli*, PO_4^{3-}, TIN, Zn, Fe, TSS) that exceeded urban water quality objectives, together with one emerging pollutant (MPs), were evaluated to characterize their temporal dynamics and first-flush behaviour in road runoff.

Figure 5.3a and 5.3b show the dimensionless M(V) curves for the monitored rainfall events, providing a visual indication of pollutant transport patterns. For COD, TSS, Zn, and MPs, the M(V) curves consistently lie above the 45° bisector line, consistent with previous studies (Chaudhary, Chua, & Kansal, 2022; Do et al., 2023). In contrast, PO_4^{3-}, TIN, *E. coli*, and Fe exhibited M(V) curves fluctuating around the bisector, indicating more variable transport patterns influenced by rainfall intensity, surface mixing, and heterogeneous pollutant sources. Temporal concentration patterns further support these observations (Figure A-2).

To quantitatively characterize the first-flush effect, the first-flush coefficients MFF_{20} and MFF_{30} were calculated (Figures 5.3c and 5.3d). The mean MFF_{20} and MFF_{30} values for COD, TSS, Zn, and Fe exceeded 2.0 in both events, suggesting that these pollutants were predominantly mobilized during the initial runoff. MPs and *E. coli* also showed strong first-flush behaviours, with MFF values above 1.5. By contrast, PO_4^{3-} and TIN had MFF values close to 1.0, reflecting relatively variable first-flush effects.

The proportion of pollutant load transported during the early runoff stage further highlights the significance of the first flush. Across the monitored events, over 80% of the total mass of TSS, MPs, and Fe was carried within the first 60–70% of runoff volume, corresponding to the initial 20 minutes (Figures 5.3a, 5.3b; 4.3). Similarly, more than 40% of the total mass of COD, *E. coli*, TSS, and Zn was delivered within the first 20–35% of runoff volume, occurring within the first 10 minutes. An extreme early-flush phenomenon was observed in rainfall event 11, where 37–42% of COD, Zn, and TSS were transported by the first 17% of runoff volume, within only the first 5 minutes (Figures 5.3b; 4.3).

Overall, these findings provide quantitative evidence that the initial runoff phase carries a disproportionately large fraction of total pollutant loads, particularly for TSS, MPs, COD, and metals. These findings offer concrete parameters for designing early-stage stormwater control measures to maximize pollutant removal efficiency.

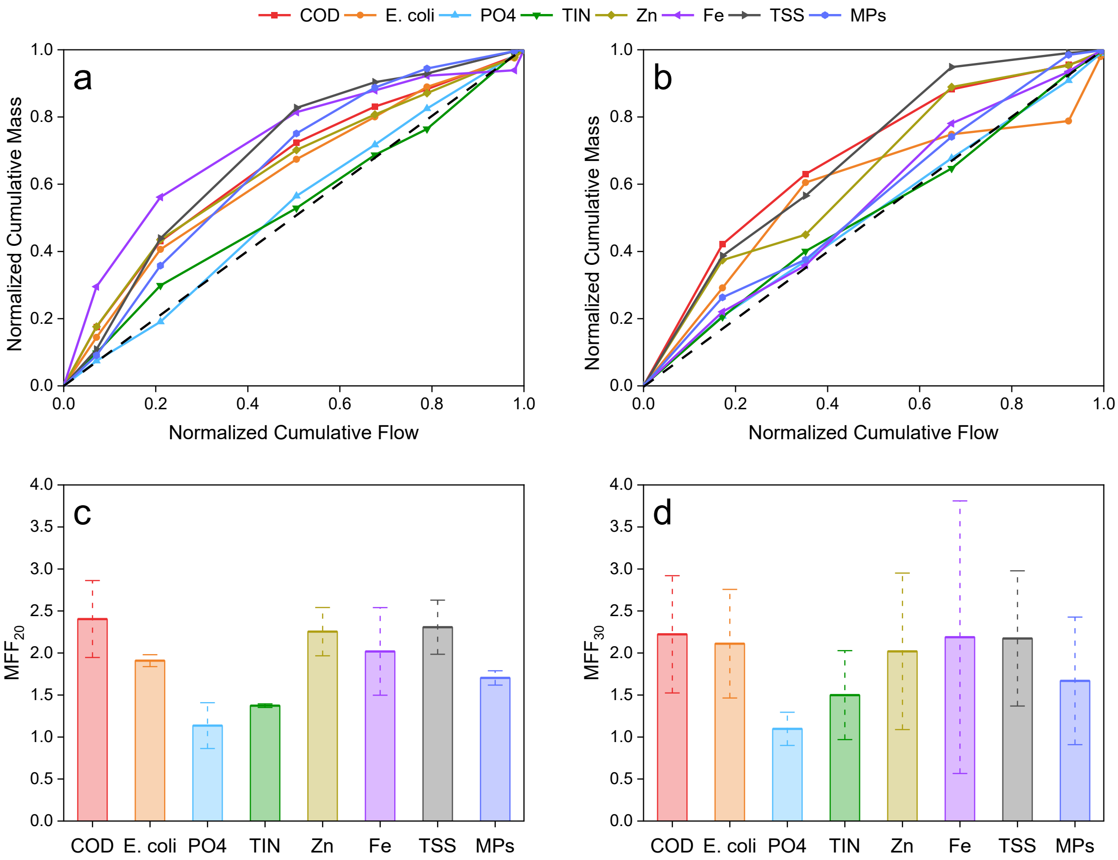

Figure 5.3. Dimensionless M(V) curves and first-flush coefficients (MFF_{20} and MFF_{30}) for eight stormwater parameters (COD, *E. coli*, PO_4^{3-}, TIN, Zn, Fe, TSS, and MPs) across two rainfall events: (a) M(V) curves at Site A during Event 10; (b) M(V) curves at Site C during Event 11; (c) MFF_{20} for all parameters across both events; and (d) MFF_{30} for all parameters across both events. Bars show the mean values, and whiskers represent the range from minimum to maximum.

5.3.4 Influencing factors of parameter concentrations in urban road runoff

Based on the analysis of stormwater characteristics and PCA, we selected eight representative parameters, COD, *E. coli*, Cl^-, TIN, Zn, Fe, TSS, and MPs, which encompass organic matter, pathogens, ions, nutrients, metals, and solids in urban road runoff. These parameters were used to analyse their distribution across different land uses and the influence of seasonal variations.

5.3.4.1 Land use

Figure 5.4 presents the distribution of eight representative parameters (COD, *E. coli*, Cl^-, TIN, Zn, Fe, TSS, and MPs) in road runoff across six land-use types, alongside NR. All parameters in NR exhibited the lowest concentrations, confirming that pollutant enrichment in road runoff primarily arises from road-related urban activities rather than atmospheric deposition.

Significant land-use differences were observed for COD and Cl^- (Kruskal–Wallis H test, $p < 0.05$). COD levels in RR (median 274 mg/L) were approximately twice those in CR (median 138 mg/L) and IR (median 135 mg/L) (Figure 5.4a). Likewise, Cl^- concentrations in C-RR (median 1,198 mg/L) were substantially higher than in CR and IR (Figure 5.4c). These elevated levels indicate more intensive inputs of organic matter and chlorine-based chemicals in residential districts, consistent with observations from other Hong Kong studies (Liu et al., 2022). *E. coli* and TIN were also higher in RR than in CR and IR (Figure 5.4b, 5.4d, 5.4g, and 5.4h). The increased microbial and nutrient loads are likely driven by residential activities—pet waste, litter accumulation, detergent-rich wash water from open street markets, and improper disposal of food residues associated with restaurant clusters in mixed-use buildings. Leakage from aging sewage infrastructure in older residential neighbourhoods can further amplify these signals (Abdelkhalek & Zayed, 2023). These patterns may be reinforced by the morphological characteristics of Hong Kong's residential areas: extremely high pedestrian densities (which can exceed 0.2 persons/m^2 during peak periods) and very high residential population densities (up to 110,000 persons/km^2), together with frequent street washing and prevalence of ground-floor markets and shops (Sarkar et al., 2021; Tan et al., 2024; Zacharias, 2021).

In contrast, TSS concentrations in A-CR (median 188 mg/L) were higher than those in RR and IR (Figure 5.4g). Site A is located alongside a major arterial road in a high-density commercial district, where heavy traffic flow and frequent braking and acceleration likely enhance particulate emissions. Fe and Zn concentrations were also higher in CR than in RR and IR (Figure 5.4e and 5.4f), most likely linked to non-exhaust traffic emissions such as brake wear and tyre abrasion (Wiseman, Levesque, & Rasmussen, 2021). These emissions are strongly influenced by traffic volume, speed, and fleet composition. Notably, Hong Kong has one of the highest traffic loads per unit road length globally due to its dense vehicle fleet operating on a highly constrained road network (HKHD, 2024). Reported brake-wear and tyre-wear emission factors can reach 18.5 and 7.4 mg/km/vehicle, respectively (Piscitello et al., 2021), which can substantially exacerbate metal pollution in road runoff.

Furthermore, higher MP abundance was observed in F-IR (median 280 particles/L) compared with CR and RR, likely attributable to intensified mechanical activities and material-handling processes, including goods transportation, packaging operations, plastic cutting, machining, and abrasion of polymer-based components (Karakurt et al., 2025)—which are typical of Hong Kong's light-industrial facilities.

Overall, the spatial contrasts among land-use types indicate that pollutant concentrations in road runoff are shaped by the combined influence of anthropogenic activity intensity, emission profiles, and infrastructural characteristics typical of compact, high-density urban environments. These findings highlight the importance of incorporating functional-area characteristics into future stormwater treatment and management strategies.

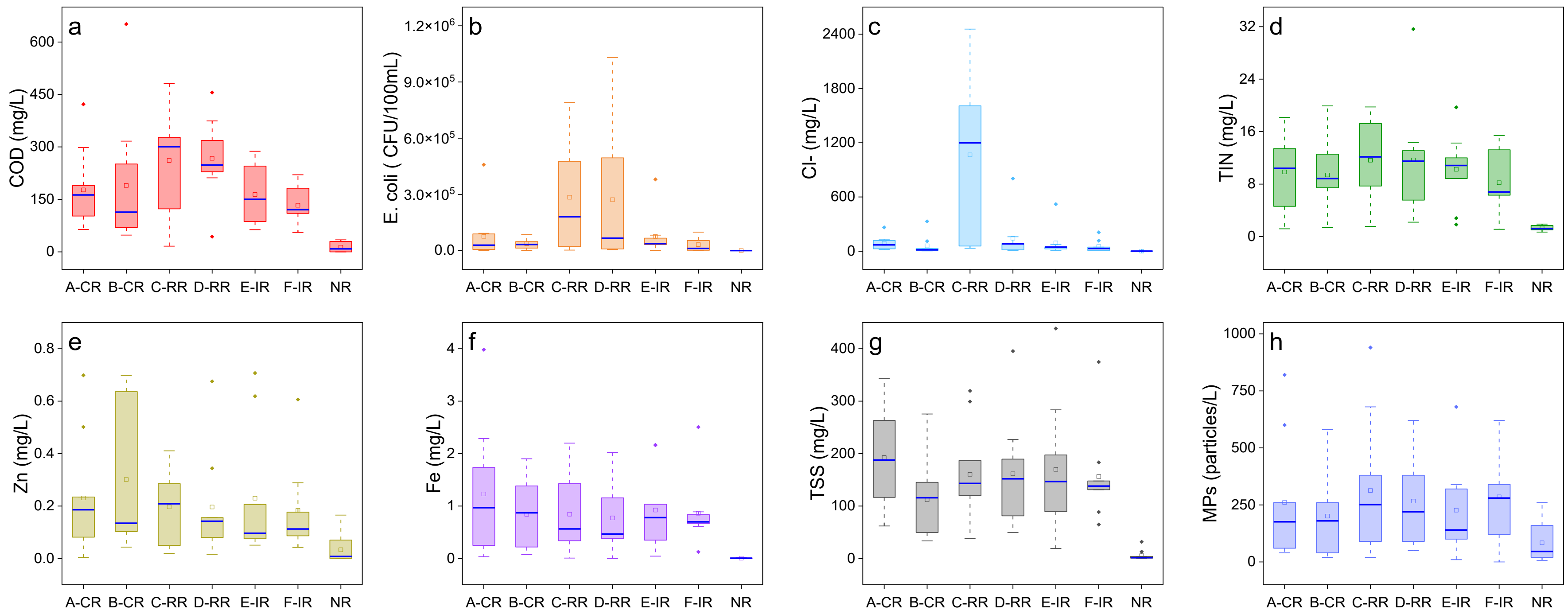

Figure 5.4. Box-and-whisker plots of eight representative parameters in road runoff at six sites with different land uses—(a) COD, (b) *E. coli*, (c) Cl^-, (d) TIN, (e) Zn, (f) Fe, (g) TSS, and (h) MPs—as well as in natural rainwater (NR) across 11 rainfall events. The road sites are classified as A-CR, B-CR, C-RR, D-RR, E-IR, and F-IR, where CR = Commercial Roads, RR = Residential Roads, and IR = Industrial Roads. The box represents the interquartile range (25%–75% of the data), the whiskers indicate the range within 1.5 times the interquartile range (IQR). The blue line denotes the median, the rectangle indicates the mean, and points outside the box represent outliers.

5.3.4.2 Seasonal variations

We analysed 56 samples collected during 11 rainfall events across four seasons (spring: n=6, summer: n=25, autumn: n=13, winter: n=12). Although sample sizes varied among seasons, eight representative parameters (COD, *E. coli*, Cl^-, TIN, Zn, Fe, TSS, and MPs) showed statistically significant seasonal differences in road runoff (Kruskal–Wallis H test, $p < 0.05$; Figure 5.5).

Median concentrations of COD, Cl^-, Zn, Fe, and TSS peaked in winter (Figure 5.5a, 5.5c, 5.5e, 5.5f, and 5.5g), likely reflecting accumulation of sediments and chemical residues during prolonged dry periods and increased surface pollution loads. TIN and MPs showed similar seasonal patterns, peaking in autumn (Figure 5.5d and 5.5h), suggesting that nutrients may adsorb onto MP surfaces, leading to concurrent accumulation trends. Higher concentrations of TIN and MPs may be due to high-intensity autumn storms, such as typhoons, which mobilize sediments and surface debris. In addition, the median *E. coli* concentration peaked in summer (Figure 5.5b), indicating that elevated temperatures promote microbial growth. These seasonal patterns likely arise from a combination of factors, including variations in rainfall intensity, changes in surface conditions, pollutant mobility, and the physicochemical behaviour of individual contaminants (Helmreich et al., 2010; Xue, Zhao, & Liu, 2020).

Although clear seasonal patterns were observed for these representative parameters, it should be noted that the number of monitored storm events varied among seasons due to the episodic nature of rainfall in Hong Kong (e.g., relatively few samples in spring). Consequently, the seasonal comparisons presented here should be interpreted as indicative tendencies rather than strictly generalizable statistical contrasts. Nevertheless, similar seasonal differences have been consistently reported in subtropical urban watersheds, and the trends observed across our multi-site dataset suggest underlying climatic controls rather than artifacts of sampling imbalance. Therefore, while caution is warranted in interpreting the magnitude of seasonal differences, the consistent signals across multiple parameters highlight that seasonal dynamics are a non-negligible driver of road-runoff pollution, underscoring the importance of season-responsive stormwater management strategies.

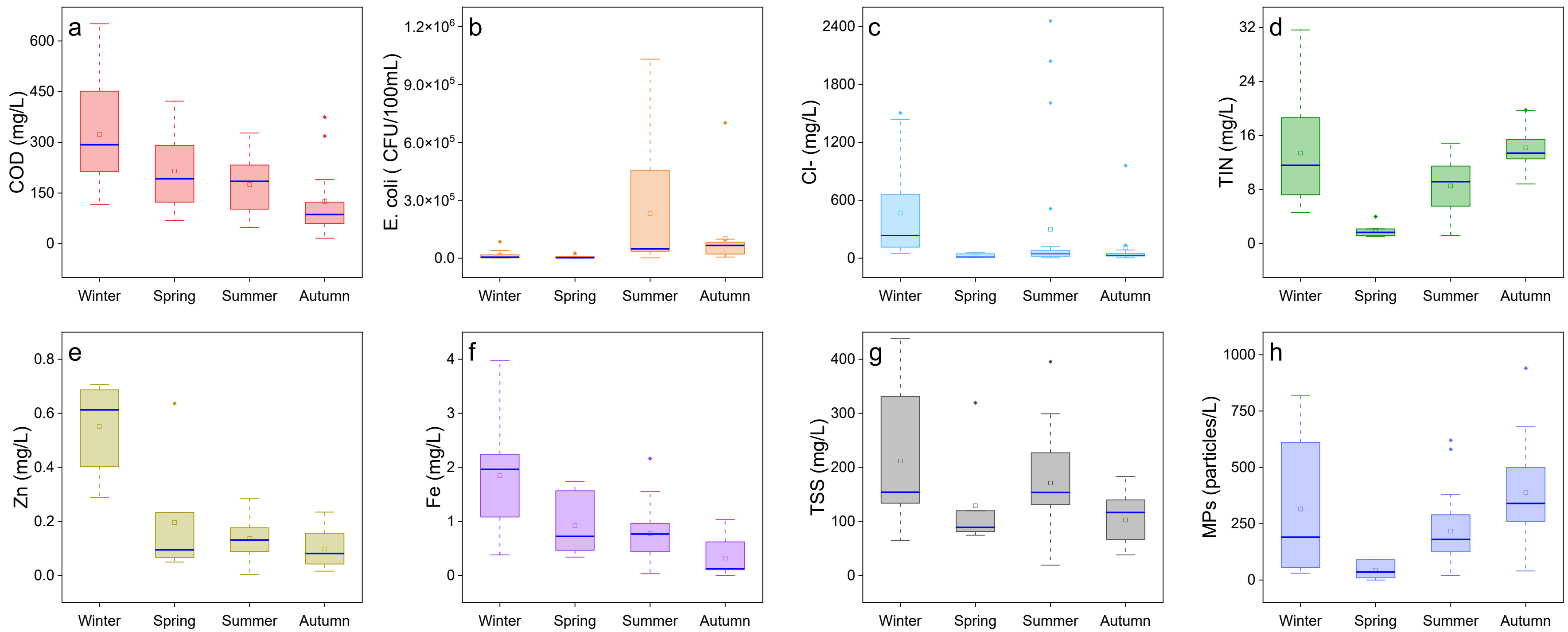

Figure 5.5. Box-and-whisker plots of eight representative parameters—(a) COD, (b) *E. coli*, (c) Cl^-, (d) TIN, (e) Zn, (f) Fe, (g) TSS, and (h) MPs—in road runoff across four seasons (winter, spring, summer, and autumn) over 11 rainfall events. The box represents the interquartile range (25%–75% of the data), the whiskers indicate 1.5 × IQR. The blue line denotes the median, the rectangle indicates the mean, and points outside the whiskers represent outliers.

5.3.5 Ecological risk and pollution load in urban road runoff

We assessed the ecological risks and pollution loads of metals (As, Cr, Pb, Zn, Cu, and Ni) and MPs across six road sites (A–F) during 11 rainfall events, incorporating seasonal variations and land-use specific differences to elucidate spatio-temporal patterns of risk (Figure 5.6).

The metal *RI* ranged from 652 to 970 across sites, consistently exceeding the very high-risk threshold (*RI* > 600). Clear spatial differentiation was observed across land uses, with IR showing the highest mean *RI* values (857), followed by CR (747), and RR (660) (Figure 5.6e). Pb was the dominant contributor to metal risk at site F (an industrial catchment, IR), exhibiting the highest *RI* (mean 820.5, Figure 5.6a). This spatial pattern highlights the influence of intense traffic, industrial activities, and construction operations on metal accumulation in urban road runoff. Additionally, the metal *PLI* varied seasonally from 6.8 to 26.5, consistently exceeding the threshold for very high pollution loads (*PLI* > 5). Peaks in winter suggest that prolonged dry periods facilitate metal accumulation on road surfaces, which is then rapidly mobilized during intermittent rainfall events.

For MPs, *PRI* ranged from 7.3 to 138.0 across the six road sites, with most sites falling within moderate to high-risk categories (PRI category II–III: $10 < H < 1000$). Spatially, *PRI* values in CR (mean 72.7) and IR (mean 65.9) were much higher than those in RR (mean 18.9) (Figure 5.6f). High-risk polymers, including polyvinyl chloride (PVC) and polymethyl methacrylate (PMMA), were particularly enriched at sites F and A (Figure 5.6b), corresponding to industrial and commercial catchments (IR, CR). This distribution reflects their widespread use in construction materials, vehicle components, and piping (Kabir et al., 2024). Furthermore, the MP *PLI* ranged from 2.1 to 6.0 across all seasons, peaking in autumn (Figure 5.6d). In Hong Kong, autumn is characterized by episodic high-intensity tropical storms, such as typhoons, which can resuspend accumulated plastic debris and enhance MP mobilization, thereby amplifying pollution loads.

Overall, the convergence of high-risk land-use zones and critical seasons drives superimposed ecological risks: metals peak in industrial areas during winter, while MPs peak in industrial and commercial areas during autumn. These spatio-temporal “hot regions” and “hot periods” highlight priority targets for stormwater management and urban runoff mitigation in densely urbanized megacities.

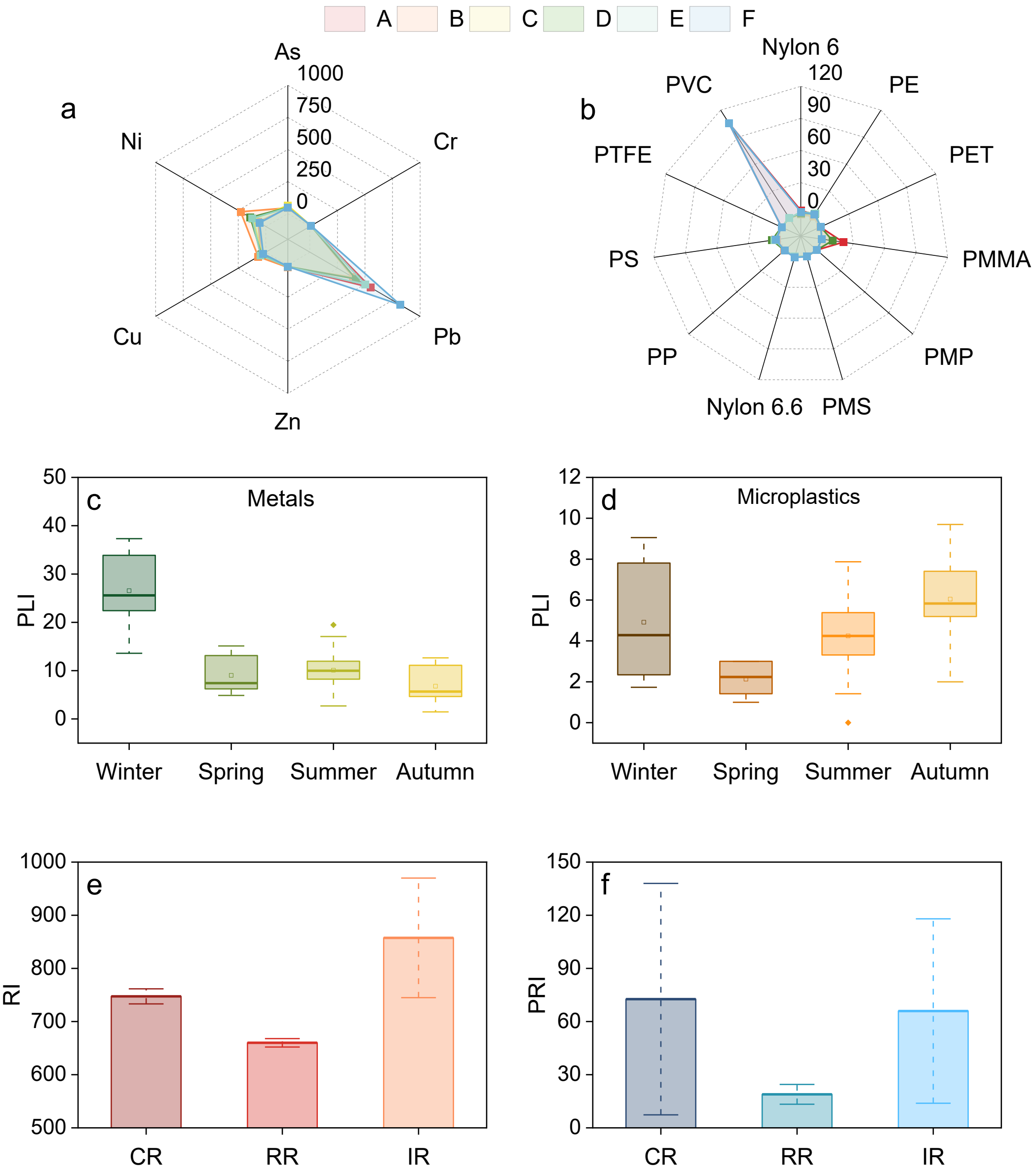

Figure 5.6. Ecological risks and pollution loads of metals and MPs in road runoff. (a) Radar chart of metal ecological risk factor (*Er*) at six road sites (A–F); (b) Radar chart of microplastic risk factor (*H*) of at six road sites (A–F); (c) Seasonal pollution load index (*PLI*) of metals; (d) Seasonal pollution load index (*PLI*) of MPs; (e) Mean ecological risk index (*RI*) of metals across land uses (CR = Commercial Roads, RR = Residential Roads, and IR = Industrial Roads); (f) Mean polymer risk index (*PRI*) of MPs across land uses. For (c)–(d): Boxes show the interquartile range (IQR), whiskers extend to 1.5 × IQR, lines indicate

medians, rectangles indicate means, and points outside whiskers represent outliers. For (e)–(f): Bars show mean values, with whiskers indicating minimum–maximum ranges.

5.3.6 Comparison with other compact cities or high-density urban areas

Compared with road runoff studies from other compact or high-density cities, the pollutant levels observed in Hong Kong fall within the upper range for several key parameters (Table B-9). Mean organic matter and nutrient concentrations in this study (e.g., COD 200 mg/L, NO_3^-–N 9.02 mg/L, and PO_4^{3-} 2 mg/L) exceed those reported for dense urban roads in Singapore and major Chinese megacities such as Beijing and Shenzhen (e.g., COD 45–114 mg/L, NO_3^-–N 0.3–4 mg/L, and PO_4^{3-} 0.2–1.2 mg/L; population densities 8,000–9,000 people/km^2) (Liu et al., 2019; Song et al., 2019; W. Zhang et al., 2021). Similarly, traffic-related metals, including Cu, Pb, and Zn, across different land uses in Hong Kong (56–93 μg/L, 9.6–15 μg/L, and 205–271 μg/L, respectively) occur at higher concentrations than those documented in Singapore and in moderate-to-low-density cities such as Munich, Germany (20–83 μg/L, 5.8 μg/L, and 130–261 μg/L, respectively) (Rommel, Stinshoff, & Helmreich, 2021; Song et al., 2019), potentially leading to higher ecological risks. These differences may be consistent with Hong Kong's exceptionally intense residential activity, extremely high traffic volumes, and the predominance of heavy buses and minibuses within its public transport system.

MP abundance in Hong Kong (mean 185 particles/L) is also comparable to or substantially higher than values reported for dense urban roads in Tijuana, Mexico (88–289 particles/L), Beijing (1.6–29.6 particles/L), and the San Francisco Bay Area (1.1–24.6 particles/L), as well as moderate-to-low-density cities such as Melbourne (24–35 particles/L) (Kabir et al., 2024; Piñon-Colin et al., 2020; Werbowski et al., 2021; J. Zhang et al., 2023). Such elevated MP load likely reflects severe tyre wear, widespread plastic usage, and high pedestrian and commercial turnover within Hong Kong's narrow street canyons.

In contrast, certain parameters (e.g., TSS, Cr, Ni, Mn, and Fe) remain broadly comparable to those in other compact cities, suggesting that not all pollutant groups are equally amplified by Hong Kong's urban configuration.

These comparisons are indicative rather than strictly quantitative, as reported concentrations are affected by rainfall characteristics, urban morphology, and methodological differences such as sampling protocols and MP filter mesh sizes. Overall, the cross-city comparisons indicate that while Hong Kong shares many features of composite road-runoff contamination with other compact or high-density cities, its unique combination of steep road gradients, mixed commercial–residential land use, and extremely dense traffic contributes to particularly pronounced risks for traffic-related metals and MPs. This highlights the need for tailored stormwater control strategies in compact coastal megacities.

5.4 Chapter Summary

This study systematically characterized 32 stormwater quality parameters in urban road runoff from six road sites during 11 rainfall events covering 17 months in Hong Kong. The main findings are:

(1) Contaminant levels in initial road runoff—including microbial (E. coli), particulate (TSS), metals (e.g., Cu, Zn, Fe, Pb), nutrients (TIN, PO_4^{3-}), organic matter (COD), and MPs—were markedly higher than those in natural rainwater and exceeded urban water pollution control standards by several to dozens of times. These elevated loadings contribute substantially to the deterioration of urban water quality in Hong Kong and can severely compromise downstream water quality if discharged untreated.

(2) A pronounced first-flush effect was observed for COD, TSS, Zn, and MPs (MFF > 1.5), indicating that initial runoff transported a disproportionately large fraction of these pollutants. COD correlated with metals (Cu, Zn, Mn) and turbidity, suggesting particulate-associated processes such as surface adsorption and aggregation. The co-occurrence of MPs with *E. coli*, PO_4^{3-}, and NO_3^-–N indicates that MPs may act as vectors for both nutrients and pathogens in urban road runoff.

(3) Land use and seasonal variations exert significant influences on pollutant concentrations in urban road runoff. Levels of COD, Cl^-, *E. coli*, TIN, TSS, and MPs were higher in residential roads than in commercial and industrial roads. Seasonally, COD, Cl^-, Zn, Fe, and TSS peaked in winter; TIN and MPs peaked in autumn; and *E. coli* peaked in summer. These spatial-

temporal differences may be shaped by the combined effects of anthropogenic activity intensity, rainfall characteristics, and infrastructural features typical of compact, high-density urban environments. Collectively, these findings underscore the importance of considering functional area characteristics and seasonal dynamics in stormwater treatment planning.

(4) Ecological risk assessment indicated that metals (*RI* 652–970), dominated by Pb and Ni, consistently exceeded very high-risk thresholds, while MPs (*PRI* 7.3–138), driven by polymers such as PVC and PMMA, posed moderate-to-high risks. The spatio-temporal superposition of risks—metals peaking in industrial areas during winter and MPs in industrial and commercial areas during autumn—identifies critical hotspots and periods for targeted stormwater management in densely urbanized megacities.

Overall, these findings demonstrate that urban road runoff significantly degrades water quality in compact cities like Hong Kong. They highlight the critical importance of managing first-flush discharges and implementing integrated stormwater mitigation strategies that combine land-use–specific controls, seasonal scheduling of street cleaning, and targeted removal of high-risk contaminants to reduce ecological impacts and enhance the sustainability of urban stormwater systems.

Specifically, measures should target traffic-related road wear, street litter, and cleaning-related discharges from wet markets. Actions include adopting low-copper brake pads (Sriwiboon et al., 2021) and wear-resistant pavement materials (Si et al., 2024; Zhai et al., 2021) to reduce road wear, replacing conventional cleaners with eco-friendly formulations for wet-market street washing (e.g., alkyl polyglucosides [APG], enzyme-based cleaners), and strengthening solid-waste management in wet markets to curb litter inputs. Seasonal patterns should guide the scheduling of interventions: increase street sweeping or vacuum cleaning during winter to mitigate metal loads, enhance litter and leaf collection during autumn to reduce MPs and nutrient inputs, and intensify disinfection during summer storms to minimize *E. coli* surges.

In compact cities, limited open space constrains the use of large stormwater facilities such as constructed wetlands and retention tanks. Instead, small-scale bioretention systems (e.g., tree boxes, bioswales) can be deployed to remove metals, nutrients, and suspended solids, with functional media (e.g., sand, biochar, and granular activated carbon) to enhance MP capture (Almenar et al., 2021; Biswal et al., 2022; Dierkes, Lucke, & Helmreich, 2015; Stinshoff et al., 2025). High-risk polymers (e.g., PVC, PMMA) in industrial and commercial zones should be prioritized for advanced treatment using high-surface-area filter media. For example, runoff diverters and interceptors can be strategically installed along urban roads to prevent first-flush discharges from entering drainage systems and to route them to advanced treatment facilities.

CHAPTER 6. TREE-BASED REMEDIATION METHODS FOR STORMWATER POLLUTION

6.1 Introduction

Urban road runoff represents one of the dominant pathways of stormwater pollution in contemporary cities. During precipitation events, runoff generated from impervious urban surfaces mobilizes a wide spectrum of pollutants, which are subsequently conveyed through urban drainage networks and discharged directly into receiving waters, often without any form of pretreatment. This unregulated discharge has been widely recognized as a major driver of urban water quality degradation. Previous studies have consistently identified nutrients—particularly nitrogen (N) and phosphorus (P)—and heavy metals, including lead (Pb), chromium (Cr), arsenic (As), zinc (Zn), cadmium (Cd), copper (Cu), and nickel (Ni), as two principal classes of contaminants in urban road runoff. These pollutants pose significant threats to aquatic ecosystems and public health, contributing to eutrophication, toxic bioaccumulation, carcinogenic risks, and neurodegenerative effects.

The occurrence and concentration of nutrients and heavy metals in road runoff are strongly linked to traffic-related activities, such as vehicle exhaust emissions, tire and brake wear, and lubricant leakage (Da Silva et al., 2023). In particular, road runoff has been identified as a dominant source of nitrate and particulate organic nitrogen in urban environments (Ma et al., 2021). Meanwhile, heavy metals in stormwater are largely associated with road-deposited sediments (RDS), which accumulate over time as a result of vehicular activity and are readily mobilized during rainfall events (Faisal et al., 2022; Gao et al., 2022). Together, these characteristics make road runoff a critical yet challenging target for urban stormwater pollution control.

To mitigate pollutant loads in urban stormwater, a wide range of management frameworks have been implemented globally, including Low Impact Development (LID), Best Management Practices (BMPs), Water Sensitive Urban Design (WSUD), Sustainable Urban Drainage Systems (SUDS), and the Sponge City concept. Within these frameworks, source control has emerged as an especially effective strategy, as it aims to intercept and treat pollutants close to their point of generation (Fletcher et al., 2015; Hamel, Daly, & Fletcher, 2013; Liao et al., 2013; Liu, Jia, & Niu, 2017; Pratt, 1995). Permeable pavements are among the most commonly adopted source control measures and have demonstrated effectiveness in reducing runoff volumes and retaining nutrients and heavy metals through infiltration and filtration processes (Brown & Borst, 2015; Z. Zhang et al., 2023). However, their long-term performance is often compromised by clogging caused by fine particulates, sediments, and debris, leading to reduced hydraulic conductivity and increased maintenance demands (Zhang et al., 2018).

In response to these limitations, green infrastructure (GI) has become a central component of contemporary urban stormwater management. GI encompasses a network of natural and semi-natural systems designed to intercept, retain, and treat stormwater through physical, chemical, and biological processes (Grabowski et al., 2022; Ying et al., 2022). Common GI practices—such as green roofs, rain gardens, vegetated buffer strips, retention ponds, and constructed wetlands—have demonstrated substantial potential for removing nutrients and heavy metals via plant uptake, soil filtration, and sedimentation (Sharma & Malaviya, 2021; Wróblewska & Jeong, 2021). Nevertheless, the widespread implementation of these systems is often constrained by their relatively large spatial footprint and associated costs, posing significant challenges in high-density urban environments where land availability is limited.

Against this backdrop, the concept of Nature-Based Solutions (NBS) has gained increasing attention in recent years. Building upon the principles of GI, NBS emphasizes the strategic use of ecosystem processes to address interconnected societal challenges, including climate adaptation, water security, biodiversity conservation, and public health improvement (Almenar et al., 2021). When integrated with conventional grey infrastructure, NBS can offer flexible, cost-effective, and multifunctional approaches to urban sustainability (Kabisch, Frantzeskaki, & Hansen, 2022). However, despite the growing recognition of NBS, the role of urban trees as active treatment components for road runoff pollution remains insufficiently explored.

Urban trees are widely valued for their aesthetic contributions and ecosystem services, such as air pollution mitigation, carbon sequestration, microclimate regulation, and thermal comfort (Adegun et al., 2021). However, their potential capacity to intercept, retain, and remediate nutrients and heavy metals from road runoff has received comparatively limited attention. Existing studies on tree-based stormwater treatment remain fragmented, and systematic evaluations of pollutant removal performance—particularly under space-constrained urban conditions—are scarce. This knowledge gap underscores the need to investigate urban trees not merely as passive landscape elements, but as functional and engineered components of stormwater management systems. Moreover, there is still limited understanding of how tree-based stormwater systems perform in managing multi-contaminant road runoff in high-density cities, as well as insufficient evidence regarding scalable tree-box designs and the underlying roles of trees—especially root and rhizosphere processes—in pollutant removal.

Accordingly, guided by the NBS framework, this study aims to develop and field-evaluate tree-box systems incorporating different filter media to quantify their long-term effectiveness in removing multiple pollutants from urban road runoff. In particular, the study investigates the role of trees and key environmental drivers, such as seasonality and pH, in regulating pollutant removal performance, with the goal of informing the optimization of tree-based stormwater solutions for compact urban environments. These tree–media–based bioretention systems are designed to provide a space-efficient and controllable approach for pollutant interception, while simultaneously delivering co-benefits such as first-flush capture, urban heat mitigation, and enhanced environmental sustainability.

The study was conducted in Hong Kong, a representative high-density metropolis characterized by limited urban space and a subtropical monsoon climate with high annual rainfall. Frequent intense rainfall events in this region exacerbate stormwater runoff and associated pollutant loads, making effective source control particularly critical. By evaluating tree-based biofiltration systems under real urban conditions, this research seeks to advance the understanding of urban trees as cost-effective and space-efficient NBS for road runoff pollution control, with broader implications for sustainable stormwater management in compact cities worldwide.

6.2 Materials and Methods

6.2.1. Design of the tree boxes and filter columns

The experiment was conducted in the outdoor garden of Block Z at The Hong Kong Polytechnic University. A total of 24 banyan trees with comparable height and trunk diameter were individually planted in square tree boxes (40 cm × 40 cm × 60 cm). Each planting box was filled with a designated filter medium, as summarized in Figure 6.1 and Table 6.1a. Sand was selected as the base material for all filter media instead of conventional soil in order to enhance hydraulic conductivity, facilitate rapid drainage of stormwater runoff, and reduce the risk of surface ponding and localized flooding. This design choice reflects practical considerations for stormwater control in compact urban environments.

Among the 24 tree box systems, 16 were irrigated with synthetic stormwater runoff, while the remaining 8 were irrigated with tap water to serve as controls for comparative assessment of pollutant removal performance under different influent water types (Table 6.1a and Table 6.2). The 16 tree boxes receiving synthetic stormwater runoff were divided into four filter media groups:

(a) Sand only;

(b) Sand mixed with forest soil (soil-to-sand volume ratio= 6.0%);

(c) Sand mixed with granular activated carbon (GAC-to-sand volume ratio= 30%);

(d) Sand mixed with wood biochar (biochar-to-sand volume ratio = 6.0%).

The remaining 8 tree boxes irrigated with tap water were assigned as controls, including four boxes filled with media group (a) and four with media group (b). All tree boxes were constructed with a consistent filter media depth of 30 cm (Figure 6.1). Each filter media group included four replicates to reduce experimental variability and improve statistical robustness. The particle size ranges of the filter materials were 0.5–6.0 mm for sand, 2.0–4.0 mm for GAC, and 2.0–4.0 mm for wood biochar.

In addition to the tree-based systems, six filter columns without trees were established to isolate and evaluate the contribution of tree roots to pollutant uptake and removal (Figure 6.1; Table 6.1b and Table 6.2). These cylindrical columns (diameter × height = 10 cm × 50 cm) were filled with filter media groups (a), (c), and (d), with each group tested in duplicate. Similar to the tree boxes, each column contained a 30 cm layer of filter media.

Prior to installation, all filter media (sand, GAC, and biochar) were rinsed three times with tap water and air-dried to remove residual fines and potential contaminants. The roots of the banyan trees were also thoroughly washed to eliminate adhering soil, pre-existing microorganisms, and residual nutrients that could confound experimental outcomes. Following preparation, the trees were transplanted into the designated planting boxes and cultivated for one month under outdoor conditions to ensure stable establishment and healthy growth prior to the start of the monitoring period.

Due to limitations in the available experimental space at the time of system installation, it was not feasible to construct tree boxes for all possible media combinations. Therefore, representative media groups were selected as controls. For each selected media type, multiple replicate units were established to minimize experimental uncertainty and ensure data reliability.

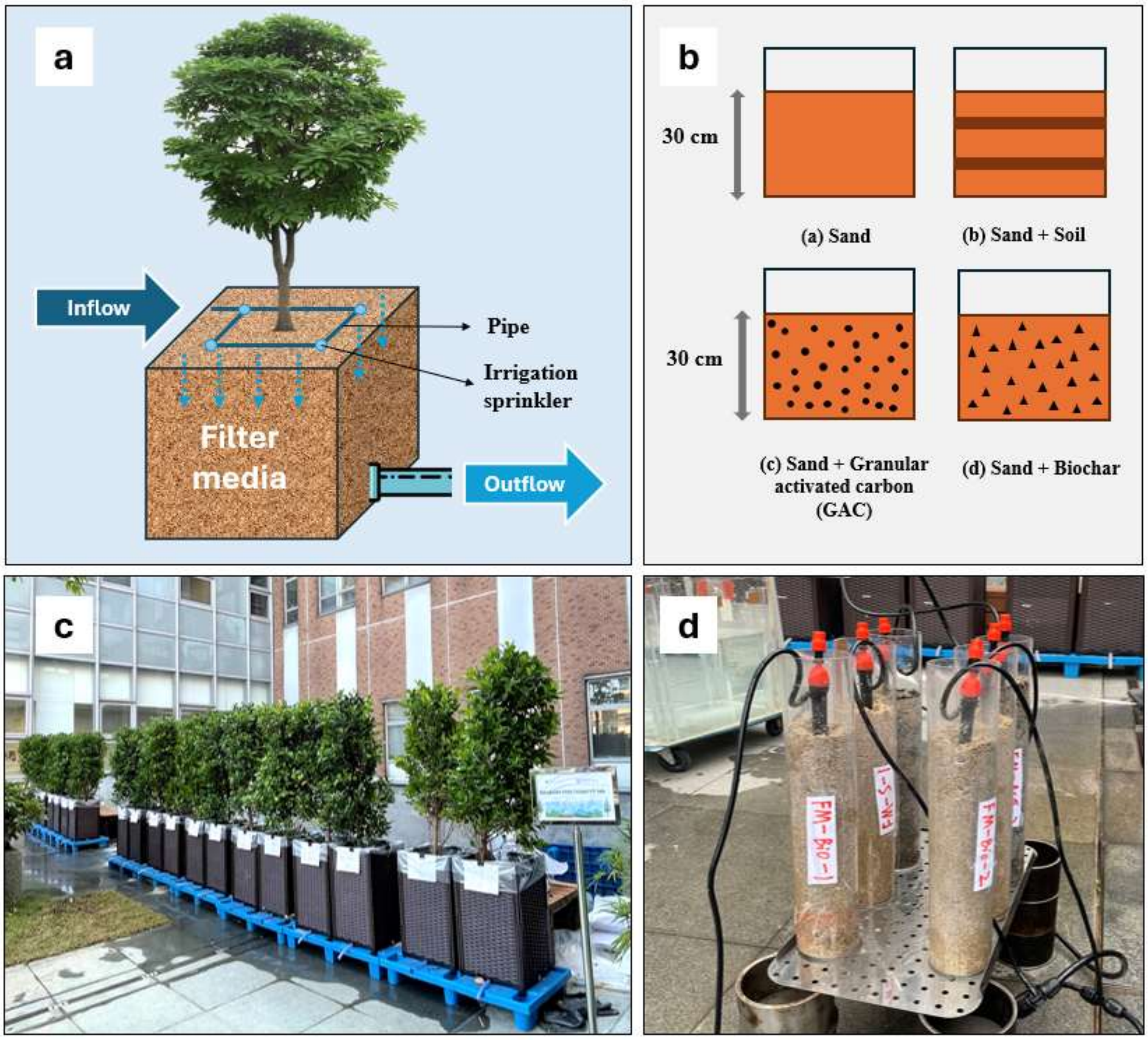

Figure 6.1. (a) Schematic diagram of the tree box filter system; (b) structural composition of the four different filter media groups (a–d); (c) field photograph of the 24 tree boxes; and (d) field photograph of the 6 filter columns installed in the outdoor garden at The Hong Kong Polytechnic University.

Table 6.1a. Information on the 24 tree box filters used in this experiment, including box number, abbreviation, and corresponding filter media group.

Tree box number	Tree box abbreviation	Filter media groups
1	SW-S-1	Sand
2	SW-SS-1	Sand + Soil
3	SW-SG-1	Sand + Granular Activated Carbon (GAC)
4	SW-SG-2	Sand + Granular Activated Carbon (GAC)
5	SW-S-2	Sand
6	SW-SS-2	Sand + Soil
7	SW-S-3	Sand
8	SW-SS-3	Sand + Soil
9	SW-SG-3	Sand + Granular Activated Carbon (GAC)
10	SW-SG-4	Sand + Granular Activated Carbon (GAC)
11	SW-SS-4	Sand + Soil
12	SW-S-4	Sand
13	TW-S-1	Sand
14	TW-SS-1	Sand + Soil
15	TW-S-2	Sand
16	TW-SS-2	Sand + Soil
17	TW-S-3	Sand
18	TW-SS-3	Sand + Soil
19	TW-S-4	Sand
20	TW-SS-4	Sand + Soil

21	SW-SB-1	Sand + Biochar
22	SW-SB-2	Sand + Biochar
23	SW-SB-3	Sand + Biochar
24	SW-SB-4	Sand + Biochar

Table 6.1b. Information on the 6 filter columns without trees used in this experiment, including column number, abbreviation, and corresponding filter media group.

Filter column number	**Filter column abbreviation**	**Filter media groups**
1	FM-S-1	Sand
2	FM-S-2	Sand
3	FM-SG-1	Sand + Granular Activated Carbon (GAC)
4	FM-SG-2	Sand + Granular Activated Carbon (GAC)
5	FM-SB-1	Sand + Biochar
6	FM-SB-2	Sand + Biochar

Table 6.2. Overview of tree boxes and filter columns, including filter media groups and irrigation water types used in the experiment.

Filter media system	Filter media groups	Types of watering							
		Tap water				Synthetic stormwater			
Tree boxes	Sand	TW-S-1	TW-S-2	TW-S-3	TW-S-4	SW-S-1	SW-S-2	SW-S-3	SW-S-4
Tree boxes	Sand + Soil	TW-SS-1	TW-SS-2	TW-SS-3	TW-SS-4	SW-SS-1	SW-SS-2	SW-SS-3	SW-SS-4
Tree boxes	Sand + GAC					SW-SG-1	SW-SG-2	SW-SG-3	SW-SG-4
Tree boxes	Sand + Biochar					SW-SB-1	SW-SB-2	SW-SB-3	SW-SB-4
Filter columns	Sand					FM-S-1	FM-S-2		
Filter columns	Sand + GAC					FM-SG-1	FM-SG-2		
Filter columns	Sand + Biochar					FM-SB-1	FM-SB-2		

6.2.2 Synthetic rainwater preparation

Due to limitations in replicating real climatic conditions and conducting consistent field sampling, synthetic stormwater was used for all experiments (Ekanayake et al., 2021). Given the significant regional variability in stormwater runoff characteristics, the pollutant concentrations in the synthetic stormwater were selected based on the 75% range of concentrations of various water quality parameters observed in urban road runoff samples collected in Hong Kong (see Chapter 5.3.1). This approach aimed to simulate the elevated pollutant concentrations typically found during the initial stage of runoff. The concentrations of key constituents were adjusted to reflect typical values reported in the Hong Kong context. The composition and target concentrations of the synthetic stormwater are detailed in Table 6.3. Tap water served as the base and was left to stand overnight to allow chlorine to dissipate before use. All components were precisely weighed, added to the tap water, and thoroughly mixed to ensure homogeneity. Due to minor laboratory variations, the actual concentrations of the synthesized stormwater were within ±10% of the intended target values.

Table 6.3. Characteristics of synthetic stormwater representing urban road runoff used in this experiment.

Compound	**Pollutant**	**Concentration**
KNO_3	NO_3^{-}-N	12.50 mg/L
$NaNO_2$	NO_2^{-}-N	0.44 mg/L
NH_4Cl	NH_4^+-N	1.04 mg/L
Na_2HPO_4	PO_4^{3-}	2.50 mg/L
$CuCl_2$	Cu	87.75 μg/L
$PbCl_2$	Pb	16.37μg/L
$ZnCl_2$	Zn	272.57 μg/L
$Cr(NO_3)_3 \cdot 9H_2O$	Cr	16.67 μg/L
$FeCl_3$	Fe	1399.24 μg/L
$Mn(NO_3)_2$	Mn	46.25 μg/L
$Ni(NO_3)_2$	Ni	6.72 μg/L

6.2.3 Sampling method

Stormwater samples were collected from the outflow of each tree box during 12 simulated rainfall events conducted between December 2023 and April 2025. The detailed information of 12 simulated rainfall events was recorded in Table 6.4. In each event, 16 tree boxes were irrigated evenly with synthetic stormwater at a constant flow rate of 0.680 L/min for approximately 40 minutes. During the irrigation, four grab samples (250 mL each) were collected at the 0^{th}, 5^{th}, 15^{th}, and 25^{th} minutes, starting when filtered runoff began to discharge from the tree boxes. The collected samples were then combined into a 1-liter bottle for further analysis. Similarly, the remaining 8 tree boxes were irrigated with tap water using the same procedure to obtain comparative water samples. Meanwhile, to ensure a consistent flow rate per unit volume, the 6 filter media columns without trees were evenly irrigated with synthetic stormwater at a constant flow rate of 0.034 L/min for approximately 40 minutes. A similar sampling method was applied to the filter columns: four grab water samples (250 mL each) were collected at 0^{th}, 5^{th}, 15^{th}, and 25^{th} minutes after the onset of outflow. These samples were then combined into a 1-liter composite sample for further analysis.

All samples were then transported to the laboratory for water quality testing. 12 typical stormwater quality items were measured in the laboratory, including pH, NH_4^+-N, NO_3^--N, NO_2^--N, PO_4^{3-}, Cr, Cu, Fe, Mn, Ni, Pb, and Zn. All experiments were conducted on sunny days to minimize the impact of extreme weather conditions. Additionally, the event mean concentration (EMC) was used in this study to represent the average concentration in the filtered samples, enabling a more comprehensive evaluation of the pollutant removal performance of both the tree boxes and filter columns. EMC is defined as the average concentration of a specific pollutant or contaminant in the runoff over the entire duration of the rainfall event (Behrouz et al., 2022; Kong et al., 2021). In this study, the sampling strategy allowed for the calculation of EMC by compositing the concentrations measured at multiple time intervals, providing a more representative assessment of the overall stormwater quality after filtration through the tree box systems (Behrouz et al., 2022; Kong et al., 2021).

Table 6.4. Summary of the 12 simulated rainfall events conducted between December 2023 and April 2025.

Simulated rainfall events	Sampling date	Meteorological seasons	Monitoring points
1	2023/12/13	Winter	Tree boxes No.1-20
2	2024/3/4-2024/3/12	Spring	Tree boxes No.1-24, Filter columns No.1-6
3	2024/5/9-2024/5/14	Spring	Tree boxes No.1-24, Filter columns No.1-6
4	2024/6/18-2024/6/21	Summer	Tree boxes No.1-24, Filter columns No.1-6
5	2024/7/10-2024/7/17	Summer	Tree boxes No.1-24, Filter columns No.1-6
6	2024/8/22-2024/8/27	Summer	Tree boxes No.1-24, Filter columns No.1-6
7	2024/9/25-2024/9/30	Autumn	Tree boxes No.1-24, Filter columns No.1-6
8	2024/10/21-2024/10/25	Autumn	Tree boxes No.1-24, Filter columns No.1-6
9	2024/11/20-2024/11/27	Autumn	Tree boxes No.1-24, Filter columns No.1-6
10	2024/12/12-2024/12/17	Winter	Tree boxes No.1-24, Filter columns No.1-6
11	2025/1/14-2025/1/17	Winter	Tree boxes No.1-24, Filter columns No.1-6
12	2025/4/8-2025/4/11	Spring	Tree boxes No.1-24, Filter columns No.1-6

6.2.4 Tree growth assessment

The growth conditions of the 24 banyan trees were monitored monthly from December 2023 to April 2025 through standardized morphological measures. Tree height was measured vertically from the surface of the filter media to the apex of the crown using a telescopic altimeter pole. Trunk circumference was measured at a fixed reference point on the main trunk, approximately 1.0 m above the surface of the filter media, using a flexible measuring tape.

Measurement uncertainty was minimized by employing consistent tools and trained personnel throughout the study. The estimated measurement error was ±1 cm for tree height (due to the resolution of the telescopic pole) and ±2 mm for trunk circumference (attributable to tape resolution and human handling variation). In cases where tree trunks exhibited irregular morphology, circumference was measured in two orthogonal directions, and the average value was used to reduce geometric bias. In addition, all measurements were recorded along with the corresponding dates to allow for growth trend analysis over time.

6.2.5 Data analysis

In this study, the removal efficiency of various stormwater pollutants was used to assess the filtration performance through different tree boxes and filter columns across 12 simulated rainfall events. The removal efficiency was calculated using the following equation:

$$E(\%) = \frac{C_{in} - C_{out}}{C_{in}} \times 100$$

Where E is the removal efficiency of the stormwater pollutant through the tree boxes for each rainfall event; C_{in} is the concentration of the inflow of synthetic stormwater to the tree boxes for each rainfall event; C_{out} is the even mean concentration of the outflow through the tree boxes for each rainfall event.

The removal efficiency data from the tree boxes and filter columns exhibited a non-normal distribution over the 12 rainfall events. Differences in removal efficiency among tree box filter media groups, filter column groups, and seasonal conditions were analyzed using the Kruskal–Wallis test. A Spearman correlation analysis was performed to examine the relationship between Ph variation and the removal efficiency of heavy metals. A significance threshold of $p < 0.05$ was applied for all statistical tests.

6.3 Results and Discussion

6.3.1 Removal efficiency of nutrients in tree boxes and filter columns

Figure 6.2 illustrates the removal efficiencies of NH_4^+-N, NO_3^--N, NO_2^--N, and PO_4^{3-} from stormwater treated using different filter media groups within tree boxes and filter columns across 12 simulated rainfall events.

Both tree boxes and filter columns effectively removed nutrients from stormwater, particularly NH_4^+-N and PO_4^{3-}, with tree boxes demonstrating superior overall performance. Specifically, tree boxes exhibited the highest mean removal efficiency for NH_4^+-N (95.05%, ranging from 93.18% to 97.24%), followed by PO_4^{3-} (92.49%, ranging from 89.56% to 94.11%), NO_2^--N (59.46%; ranging from 46.85% to 73.74%), and NO_3^--N (55.10%; ranging from 46.85% to 59.09%) (Figure 6.2a). Similarly, in filter columns without trees, the removal efficiencies for NH_4^+-N and PO_4^{3-} (mean ranges of 84.84%–94.36% and 74.17%–90.47%, respectively) were higher than those for NO_2^--N and NO_3^--N (mean ranges of 10.19%–12.13% and 10.23%–20.17%, respectively) (Figure 6.2b). Compared to tree boxes, the nutrient removal efficiencies in filter columns without trees were notably lower, with overall mean values of 89.53% for NH_4^+-N, 82.26% for PO_4^{3-}, 11.19% for NO_2^--N, and 14.83% for NO_3^--N. On average, the removal efficiencies of NO_2^--N and NO_3^--N in tree boxes were 5.3 and 3.7 times higher, respectively, than in the filter columns. These findings strongly suggest that tree roots play a significant role in enhancing nutrient removal from stormwater runoff.

Nutrient removal efficiencies varied significantly across different filter media within tree boxes. The Kruskal–Wallis test showed statistically significant differences ($P < 0.05$) among the four media types for all nutrient pollutants. In particular, the sand-biochar mixture exhibited the highest removal efficiencies for NH_4^+-N (mean = 97.24%) and PO_4^{3-} (mean = 94.11%). This high efficiency may be attributed to reduced porosity of the mixture after the addition of biochar, which enhanced the retention of NH_4^+-N and PO_4^{3-} in the tree boxes. In contrast, the groups of sand-GAC mixture demonstrated the highest removal efficiency for NO_2^--N and NO_3^--N, with mean values of 73.74% and 59.09%, respectively. This may be attributed to the strong adsorption capacity of granular activated carbon (Yuan, Passeport, & Hofmann, 2022).

However, this group showed the lowest removal efficiency for PO_4^{3-}, with a mean value of 89.56%. The increased porosity of this mixture may have reduced PO_4^{3-} retention during filtration. Furthermore, the groups of sand-soil mixture exhibited relatively low removal efficiencies for NH_4^+-N, NO_2^--N, and NO_3^--N. The leaching of nitrogenous compounds from the soil may be an important cause. These findings indicate that the groups of sand-biochar mixture and sand-GAC mixture in tree boxes performed better in nutrient removal than the groups of pure sand and sand-soil mixture.

Similarly, significant differences were observed among the three filter media types in filter columns concerning the removal efficiencies for NH_4^+-N and PO_4^{3-} (Kruskal-Wallis test, $P < 0.05$). Within filter columns, the sand-biochar mixture also exhibited the highest mean removal efficiencies for NH_4^+-N (94.36%) and PO_4^{3-} (90.47%), though slightly lower than the performance observed in tree boxes. Additionally, the sand-GAC mixture in filter columns achieved the highest removal efficiencies for NO_2^--N (mean = 12.13%) and NO_3^--N (mean = 20.17%), although these values were significantly lower than those observed in tree boxes. The mean removal efficiencies of NO_2^--N and NO_3^--N in tree boxes filled with the sand-GAC mixture were 6.1 and 2.9 times higher, respectively, than in comparable filter columns. These results underscore the critical role of tree roots in nitrogen retention and uptake, particularly for nitrate, within tree-box systems. Consistent with findings from the tree boxes, the sand-biochar and sand-GAC mixtures demonstrated better nutrient removal than pure sand and sand-soil mixtures in filter columns.

Additionally, the outflow concentrations from the other 8 tree boxes irrigated with tap water showed relatively low nutrient levels (Appendix B, Table B-6), indicating minimal influence from the filter media itself. These results suggest that the filter media did not serve as a significant source of pollution, thereby validating the pollutant removal performance of the tree boxes.

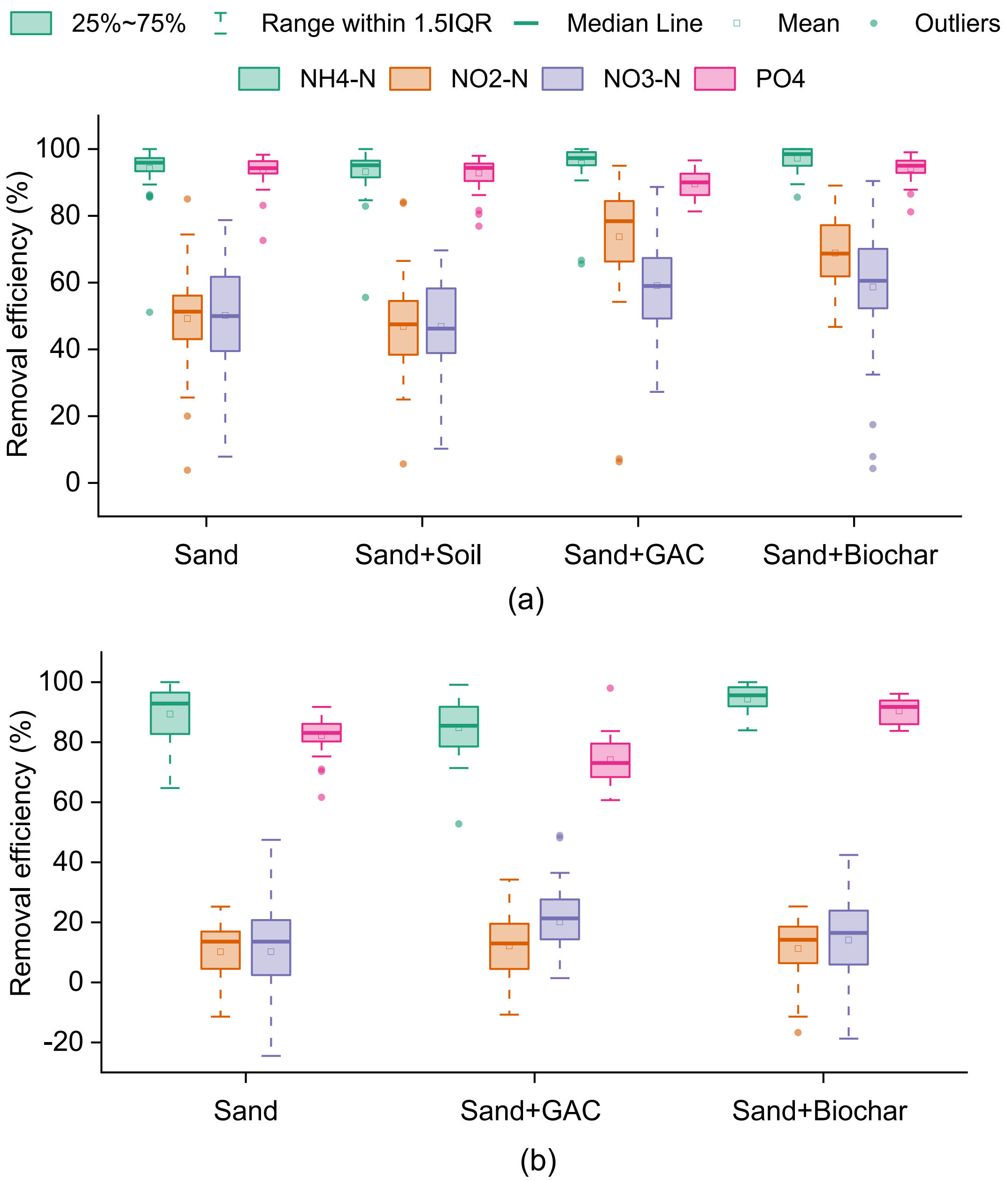

Figure 6.2. Removal efficiency of nutrients (NH_4^+-N, NO_3^-—N, NO_2^-—N, and PO_4^{3-}) from stormwater through (a) tree boxes with four different filter media groups (Sand, Sand-Soil, Sand-GAC, and Sand-Biochar), and (b) filter columns with three different filter media groups (Sand, Sand-GAC, and Sand-Biochar) during 12 simulated rainfall events.

6.3.2 Removal efficiency of heavy metals in tree boxes and filter columns

Removal efficiencies of heavy metals (Cr, Cu, Fe, Pb, Zn, Mn, and Ni) in stormwater treated by different filter media within tree boxes and filter columns during 12 simulated rainfall events were analysed as shown in Figure 6.3.

Both tree boxes and filter columns demonstrated excellent removal performance for Cr, Cu, Zn, and Fe, with mean removal efficiencies exceeding 80% across media types. Specifically, in tree boxes (Figure 6.3a), the highest mean removal efficiency was observed for Cu (92.69%), followed by Cr (89.94%), Zn (84.94%), Fe (80.46%), Pb (77.41%), and Ni (54.16%). Similarly, filter columns (Figure 6.3b) exhibited mean removal efficiencies above 86% for Cr, Cu, Zn, and Fe. The highest performance was noted for Fe (93.92%), followed by Cu (92.02%), Cr (92.01%), Zn (86.80%), Pb (82.32%), and Ni (48.19%). However, a notable difference was observed in Mn removal between the two systems. Filter columns achieved a mean Mn removal efficiency of 84.15%, while tree boxes showed unsatisfactory performance, with evidence of Mn leaching. This discrepancy may be attributed to differences in flow rates and manganese sand application. The lower filtration rates in filter columns may promote Mn sedimentation, whereas the use of larger quantities of manganese sand in tree boxes may introduce variability or leaching during the cleaning process. Elevated concentrations of Mn were also detected in the outflows from the eight additional tree boxes irrigated with tap water, further supporting the leaching hypothesis (Appendix B, Table B-7). In contrast, the outflow concentrations of other heavy metals remained relatively low, suggesting minimal leaching and limited influence from the filter media itself.

Heavy metal removal efficiencies varied significantly across different filter media within the tree boxes (Figure 6.3a). A statistically significant difference was observed among the four media groups regarding the removal efficiencies of Fe and Mn (Kruskal–Wallis test, $P < 0.05$). Specifically, the median removal efficiencies of Fe in the sand–GAC and sand–biochar groups (93.33% and 90.10%, respectively) were significantly higher than those in the pure sand and sand–soil groups (78.36% and 80.28%, respectively). Overall, all four filter media groups in the tree boxes exhibited excellent performance for Cr and Cu removal, with removal efficiencies exceeding 90%. Among them, the sand–GAC mixture achieved the highest mean removal efficiencies for Cu (93.29%) and Fe (87.15%). The sand–biochar group demonstrated superior removal of Pb and Zn, with mean efficiencies of 82.25% and 86.94%, respectively. In contrast, the sand–soil group achieved the best performance for Cr and Ni removal. These findings suggest that functionalized media mixtures—such as those incorporating GAC, biochar, or soil—are more effective than pure sand in enhancing the removal of heavy metals from stormwater when used in tree-based filtration systems.

Similarly, significant differences were observed among the three filter media types in filter columns. Filter columns containing pure sand exhibited higher mean removal efficiencies for Cr (92.56%), Fe (97.59%), Ni (50.42%), Pb (85.30%), and Zn (87.57%) compared to the other two media groups. Additionally, filter columns with the sand–biochar mixture achieved the highest mean removal efficiencies for Cu (92.75%) and Mn (86.41%). The filter columns containing sand–GAC mixtures showed relatively poor performance in retaining heavy metals. This reduced efficiency may be attributed to increased porosity, which could reduce contact time and retention capacity.

Overall, the filter columns exhibited relatively higher mean removal efficiencies for heavy metals in stormwater compared to the tree boxes. This difference may be closely associated with the pH variance between the two systems. As trees grow, their root systems can release organic acids, leading to a more acidic environment within the tree boxes. In contrast, the filter columns, which lack vegetation, tend to maintain a more alkaline pH. According to the principle of charge conservation, alkaline conditions promote the precipitation of metal ions, thereby enhancing the removal efficiency of heavy metals in the filter columns.

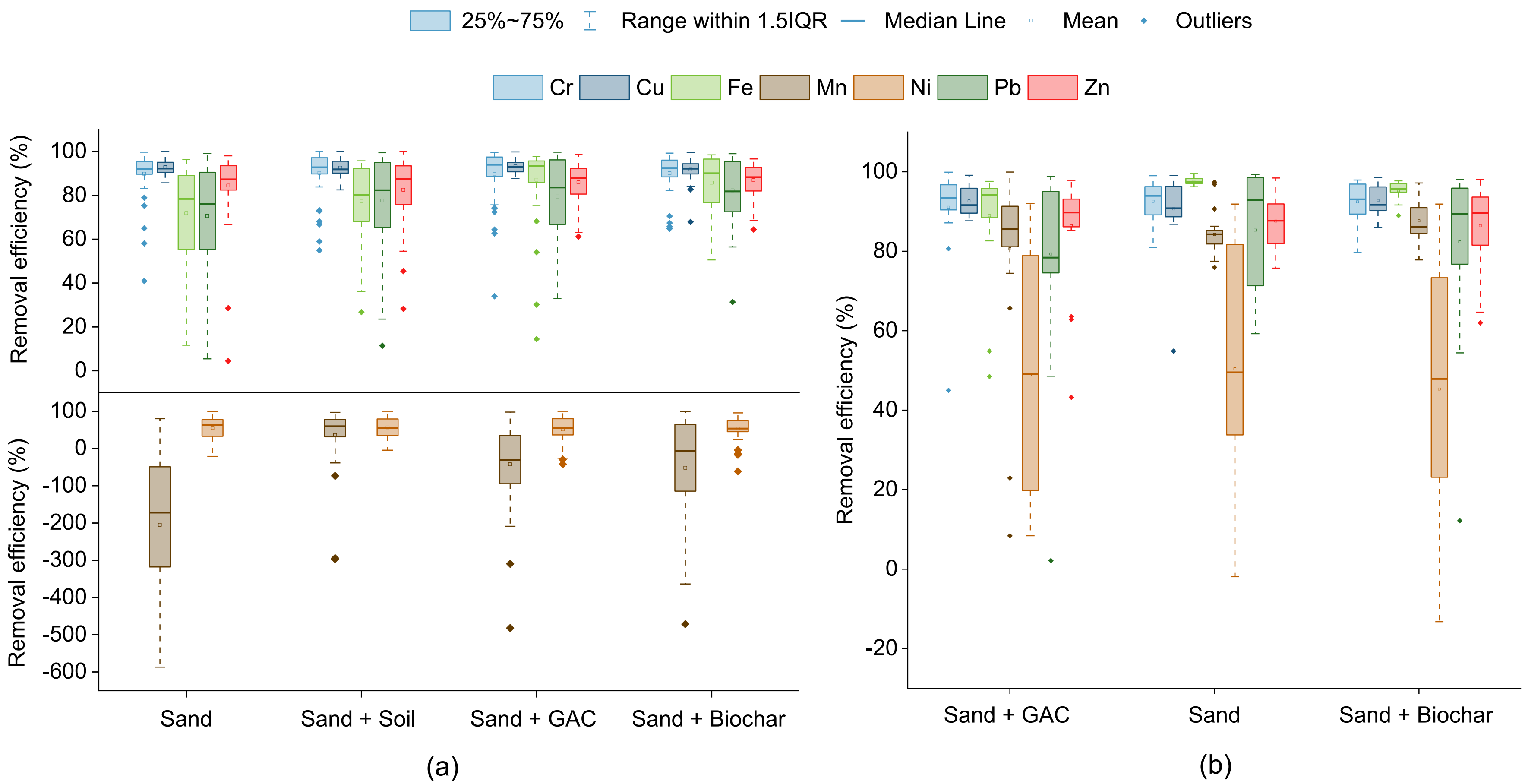

Figure 6.3. Removal efficiencies of heavy metals (Cr, Cu, Fe, Pb, Zn, Mn, and Ni) from stormwater through (a) tree boxes with four different filter media groups (Sand, Sand-Soil, Sand-GAC, and Sand-Biochar), and (b) filter columns with three different filter media groups (Sand, Sand-GAC, and Sand-Biochar) during 12 simulated rainfall events.

6.3.3 The influence of pH on heavy metal removal efficiency

We analyzed pH variation and its correlation with the removal efficiency of heavy metals in tree boxes and filter columns across 12 simulated rainfall events (Figure 6.4). The outflow pH from filter columns was consistently higher than that from tree boxes, with a mean range of 7.36 to 8.07 (Figure 6.4a). This alkalinity may be attributed to the basic nature of the filter media (e.g., sand and GAC) and the generation of alkaline byproducts from microbial degradation of organic matter. In contrast, the outflow pH from tree boxes was lower, ranging from 5.58 to 6.87, and gradually decreased over time (Figure 6.4a). This trend confirmed that root exudates from growing trees release acidic compounds, thereby lowering the system pH. Such pH differences between systems may significantly influence the removal efficiency of heavy metals in stormwater.

In tree boxes, a positive correlation was observed between pH and the removal efficiencies of Mn, Zn, and Pb, with a particularly strong correlation for Mn (Figure 6.4b1; Spearman correlation, $P \leq 0.05$). In contrast, Fe exhibited a negative correlation with pH in the tree boxes. These results suggest that as pH increases, Mn, Zn, and Pb are more likely to form insoluble precipitates or be adsorbed onto the filter media, thereby enhancing their removal. By comparison, Fe removal primarily depends on oxidation followed by precipitation. Under more alkaline conditions, incomplete oxidation or the formation of colloidal ferric hydroxides may reduce Fe removal efficiency. In addition, organic acids released by plant roots may form soluble complexes with Fe, further inhibiting its precipitation and retention within the system.

In filter columns without trees, a positive correlation was found between pH and Fe removal (Figure 6.4 b2), likely due to the absence of root exudates and the enhanced oxidation and precipitation of Fe at higher pH. A positive correlation was also observed for Cr, while negative correlations were found for Cu and Zn. The reduced removal of Cu and Zn at higher pH may be attributed to their increased solubility in the form of carbonate or organic complexes, as well as decreased electrostatic attraction to the filter media under alkaline conditions. These trends reflect the distinct chemical behaviors of different metal ions in response to pH, which influence their removal through precipitation and adsorption mechanisms. This also suggests that tree roots have an important influence in pH regulation and heavy metal removal.

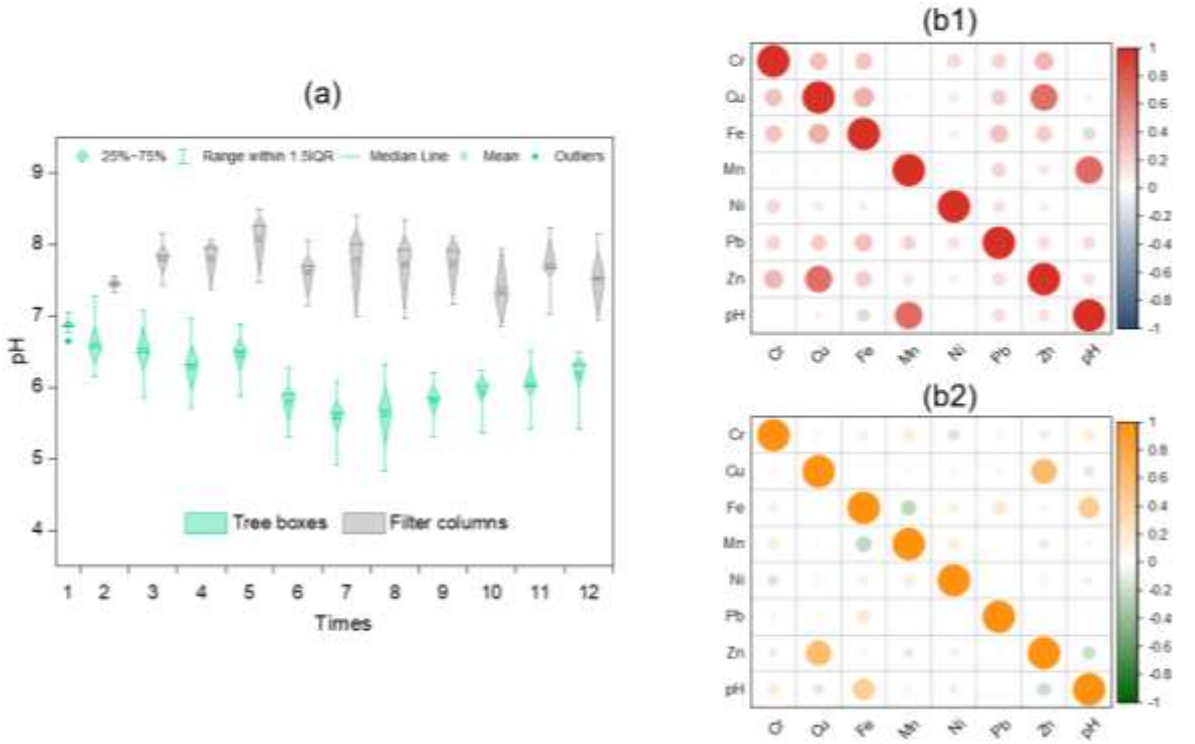

Figure 6.4. pH variation and its correlation with the removal efficiency of heavy metals. (a) Outflow pH values from tree boxes and filter columns across 12 simulated rainfall events. (b1) Spearman correlations between pH and the removal efficiency of different heavy metals in tree boxes. (b2) Spearman correlations between pH and the removal efficiency of different heavy metals in filter columns.

6.3.4 Factors affecting the performance of tree boxes for treating stormwater pollutants

6.3.4.1 Temporal variability

We analyzed the temporal impacts of average removal performance of nutrients and heavy metals by different filter media systems (tree boxes vs. filter columns) and by various media combinations within tree boxes across 12 simulated rainfall events conducted between December 2023 and April 2025 (Figure 6.5).

Tree boxes demonstrated superior nutrient removal efficiency compared to filter columns (Figure 6.5a). In contrast, filter columns outperformed tree boxes in the removal of heavy metals. This difference may be attributed to pH variations influenced by root exudates and plant–microbe interactions, which alter the acid–base environment in the media systems. While both systems showed temporal fluctuations in removal efficiency, a divergent trend emerged over time. The nutrient removal efficiency of filter columns gradually declined, whereas that of tree boxes continued to improve during later stages. This indicates that tree-based systems offer enhanced durability and long-term resilience for nutrient removal in stormwater treatment.

Further analysis was conducted on the performance of tree boxes containing four different filter media combinations (Figure 6.5b). For nutrient removal, tree boxes filled with sand–GAC and sand–biochar mixtures showed markedly higher performance than those with pure sand or sand–soil mixtures. Notably, the sand–biochar group exhibited greater fluctuations but also showed a distinct upward trend in later stages. This suggests that biochar-based media may enhance long-term nutrient removal through improved sorption capacity and biological activity.

Regarding heavy metal removal, all three functional media mixtures (sand–GAC, sand–biochar, and sand–soil) performed better than pure sand, with a gradual increase in efficiency observed over time. This highlights the importance of incorporating functional materials to enhance metal adsorption and retention. Temporal variability in removal performance may also be influenced by seasonal changes in temperature and climate, which can affect microbial communities, root activity, and the overall dynamics of pollutant removal within vegetated systems.

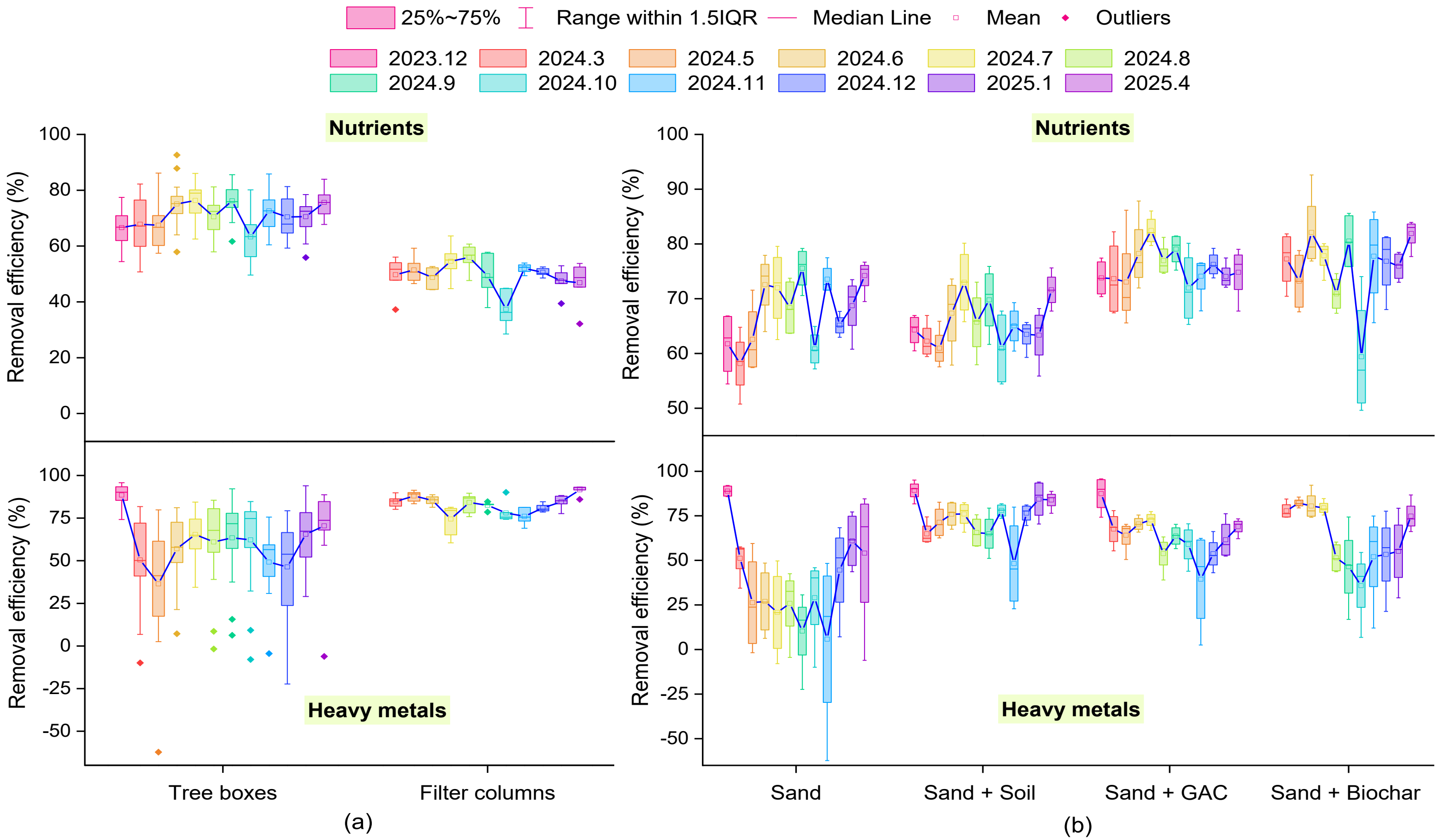

Figure 6.5. Trends of average removal efficiency of nutrients and heavy metals by different filter media systems (tree boxes vs. filter columns) and by various media groups in tree boxes across 12 simulated rainfall events from December 2023 to April 2025. (a) Mean removal efficiency trends of nutrients and heavy metals by tree boxes and filter columns. (b) Mean removal efficiency trends of nutrients and heavy metals by four different filter media groups (Sand, Sand-Soil, Sand-GAC, and Sand-Biochar) in tree boxes.

6.3.4.2 Seasonal variation

Seasonal variations significantly influenced the pollutant removal efficiency of both the tree box systems and the filter column systems (Figure 6.6). In the tree boxes, a significant seasonal difference was observed in the removal efficiency of NH_4^+-N and NO_2^--N between spring and autumn (Figure 6.6a; Kruskal–Wallis test, $P \leq 0.05$). For heavy metals, significant differences were detected across all four seasons (Figure 6.6b; Kruskal–Wallis test, $P \leq 0.05$). These seasonal patterns are likely associated with variations in plant activity, microbial metabolism, temperature-dependent reaction kinetics, and hydrological dynamics. Together, these factors modulate the biological and physicochemical processes underlying stormwater treatment.

Compared to tree boxes, filter columns are less sensitive to seasonal fluctuations. Nevertheless, a significant difference in NO_2^--N removal efficiency was observed between winter and summer (Figure 6.6a; Kruskal–Wallis test, $P \leq 0.05$). Additionally, for both tree boxes and filter columns, the removal efficiencies of Cu, Ni, Pb, and Zn varied significantly across seasons (Figure 6.6b; Kruskal–Wallis test, $P \leq 0.05$). These findings suggest that microbial activity, hydrological conditions, and the physicochemical properties of filter media are also influenced by temperature and seasonal changes, even in non-vegetated systems.

Overall, these results indicate that tree boxes maintained higher nutrient removal and stable metal removal (>70%) across seasons, demonstrating stronger resilience compared with filter columns.

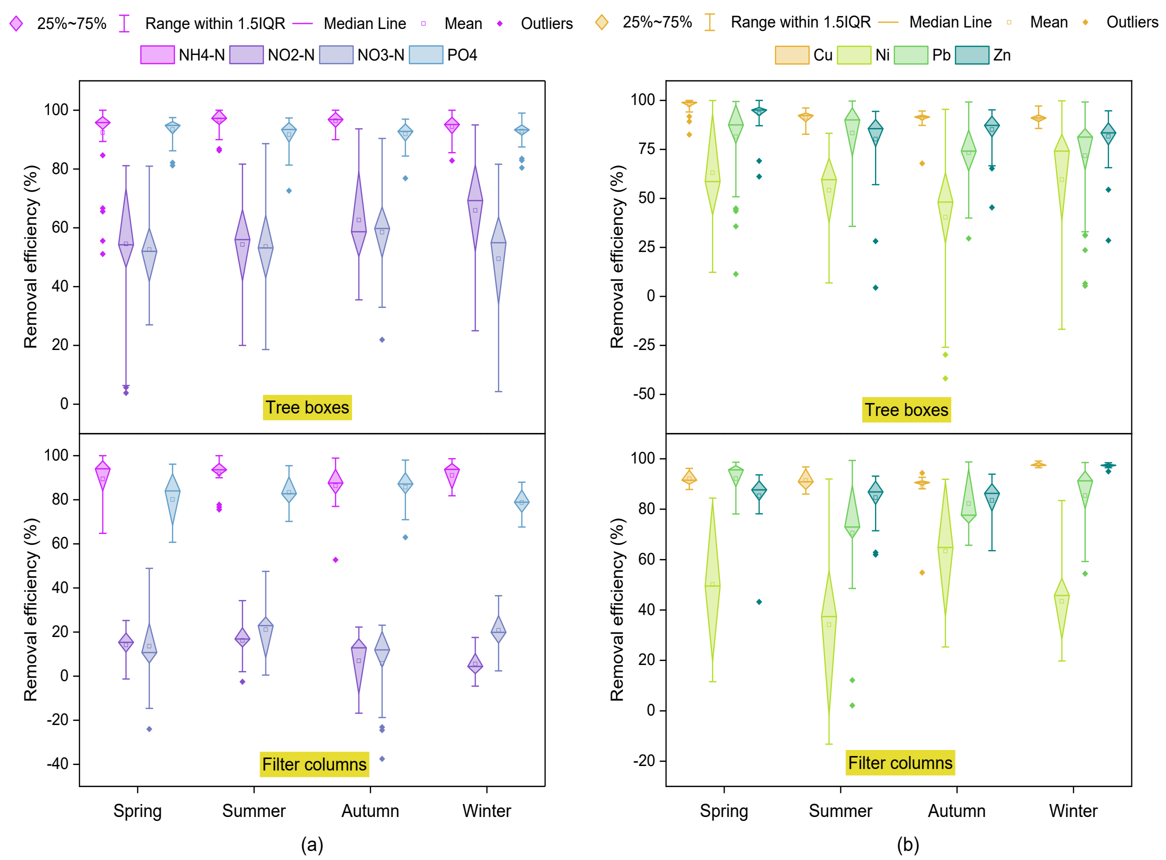

Figure 6.6. Seasonal removal efficiency of nutrients and typical heavy metals in stormwater by tree boxes and filter columns. (a) Removal efficiency of NH_4^+-N, NO_3^--N, NO_2^--N, and PO_4^{3-} by tree boxes and filter columns, (b) Removal efficiency of Cu, Ni, Pb, and Zn by tree boxes and filter columns.

6.3.5 Tree growth performance in tree box systems

The growth trends of tree roots, height, and trunk circumference of banyan trees planted in 24 tree boxes were monitored from December 2023 to April 2025, as shown in Figure 6.7. Over the 16-month monitoring period, average tree height increased by 10.08 cm (ranging from 7 to 15 cm), corresponding to a mean growth rate of 7.02%. Similarly, the average trunk circumference increased by 1.35 cm (ranging from 0.9 to 1.7 cm), representing a mean growth rate of 18.89%. In addition, root systems expanded markedly, with the development of denser and longer aerial roots, indicating active belowground growth.

Tree height exhibited a fluctuating temporal pattern, with slight declines observed during autumn and winter, followed by pronounced increases in spring and summer. This variability is likely associated with seasonal changes in temperature and foliage dynamics, particularly leaf senescence and regrowth, which may influence measurements of the crown apex. In contrast, trunk circumference growth remained comparatively stable throughout the year. Reduced growth rates were observed during colder months, while substantial increases occurred in spring and summer, likely supported by higher temperatures, increased solar radiation, and favorable moisture conditions within the filter media.

Overall, the observed vitality and sustained growth of the banyan trees suggest that the integrated tree–media–microbe system within the tree boxes creates a supportive root-zone environment capable of sustaining long-term vegetative development while simultaneously treating stormwater runoff. As such, tree boxes function as multifunctional green infrastructure, delivering both effective stormwater treatment and valuable ecosystem services, in alignment with the core principles of nature-based solutions and urban sustainability.

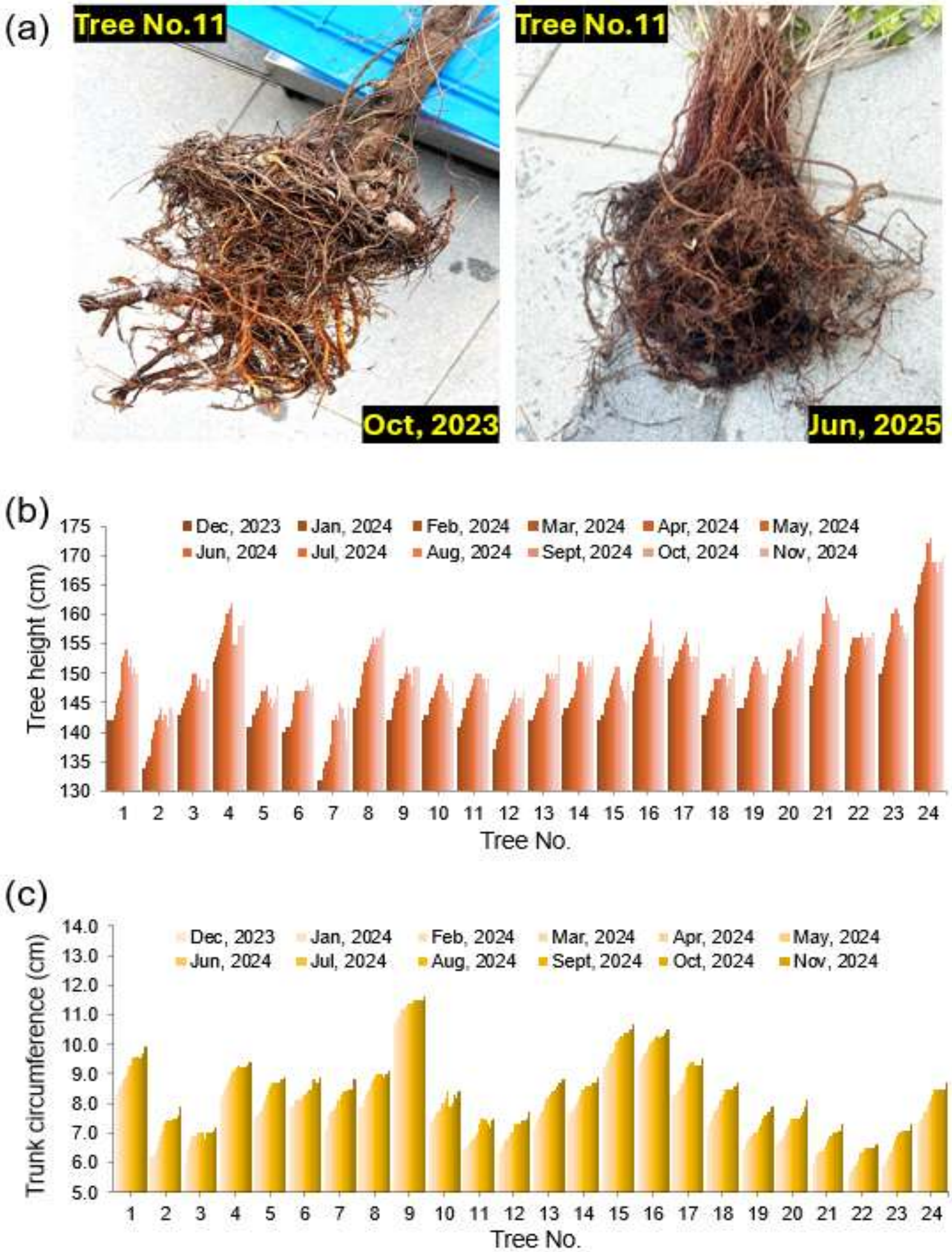

Figure 6.7. Growth trends of (a) roots, (b) height, and (c) trunk circumference of banyan trees in 24 tree boxes over 16 months.

6.4 Chapter Summary

By examining the pollutant removal performance of tree boxes across 12 simulated rainfall events over more than one year, this comprehensive study offers valuable insights into the capacity and resilience of tree boxes in treating stormwater pollutants, as well as the critical role of tree roots in pollutant retention and transformation.

Overall, the tree boxes demonstrated a strong ability to remove nutrients and most heavy metals from stormwater runoff. The average removal efficiencies of NH_4^+-N, PO_4^{3-}, and Cu exceeded 90% across all filter media during the 12 rainfall events. Meanwhile, the mean removal efficiencies of Cr, Zn, and Fe were above 80%. Notably, the average removal efficiencies of NO_2^--N and NO_3^--N in tree boxes were 6.1 and 2.9 times higher, respectively, than those observed in filter columns (which lacked trees), suggesting that tree roots may play a crucial role in nitrate retention and uptake. Additionally, pH variations were found to significantly affect the removal efficiency of heavy metals. A positive correlation was observed between pH and the removal of Mn, Zn, and Pb, with Mn showing the strongest correlation. These findings imply that tree roots have an important influence on pH regulation and heavy metal removal.

The removal efficiencies of nutrients and heavy metals varied significantly across different filter media within the tree boxes. Tree boxes filled with sand–GAC and sand–biochar mixtures demonstrated significantly improved removal performance for nutrients and several heavy metals compared to other media combinations. The sand-biochar mixture exhibited the highest removal efficiencies for NH_{4+}-N (mean= 97.24%), PO_4^{3-} (mean= 94.11%), Pb (mean= 82.25%), and Zn (mean= 86.94%). The sand–GAC mixture achieved the highest mean removal efficiencies for NO_2^-–N (73.74%), NO_3^-–N (59.09%), Cu (93.29%), and Fe (87.15%). Additionally, the median removal efficiencies of Fe in the sand–GAC and sand–biochar groups (93.33% and 90.10%, respectively) were significantly higher than those in the pure sand and sand–soil groups (78.36% and 80.28%, respectively). These results indicate that functional media mixtures (e.g., sand–GAC and sand–biochar) outperform pure sand, highlighting the importance of incorporating functional materials to enhance nutrient and heavy metal adsorption and retention in tree-based stormwater treatment systems.

Long-term monitoring further revealed that tree boxes possess strong resilience and durability. While pollutant removal in filter columns gradually declined over time, tree boxes maintained or even improved nutrient removal performance during later stages of operation. In parallel, sustained and healthy tree growth was observed throughout the monitoring period, confirming the compatibility of sand-based filter media with long-term vegetation development. Pollutant removal in tree boxes was also significantly influenced by pH dynamics and seasonal variability, suggesting that the integrated tree–media–microbe system responds adaptively to changing environmental conditions.

Collectively, these findings demonstrate that tree box systems offer a multifunctional and resilient approach to urban stormwater management, delivering high pollutant removal efficiency, long-term stability, and ecological co-benefits. Future research will focus on elucidating the underlying mechanisms governing microbial processes and root-induced pH regulation to further optimize the design and performance of tree-based stormwater treatment systems.

CHAPTER 7. CONCLUSIONS AND FUTURE WORK

This chapter summarizes the key findings and major conclusions of the study. It also outlines the study's limitations and provides recommendations for future research.

7.1 Conclusions

We investigated 32 stormwater quality parameters from six urban road sites across 11 rainfall events over one year in Hong Kong. This comprehensive study provides important insights into the characteristics, ecological risks, environmental impacts, and interrelationships of multi-pollutants—including nutrients, heavy metals, conventional indicators, and microplastics (MPs). These findings enhance our understanding of pollution sources, transport mechanisms, and environmental impacts of road runoff, particularly in high-density urban environments. The results provide important implications for improving urban stormwater management strategies.

Building upon the pollutant characterization work, we designed and implemented tree-box filters—a tree–media–microbe system—as a NBS to mitigate key road runoff pollutants. Field-scale experiments were conducted using 24 bayan tree boxes with different filter media compositions over 12 simulated rainfall events across one year. The results demonstrated the effectiveness of this tree-based system in removing multiple runoff pollutants and provided new insights into the performance of NBS in real-world urban settings.

Together, these findings support the development of sustainable, nature-based urban stormwater pollution solutions and contribute to the broader goals of ecological resilience and sustainable urban development.

The major findings and conclusions for this research can be summarized in Chapter 7.1.1 and 7.1.2.

7.1.1 Characterization and dynamics of urban road runoff pollutants

Based on over one year of field investigations into stormwater quality across various urban roads in Hong Kong, this study has yielded several important insights into the characteristics, dynamics, and ecological risks of urban road runoff pollutants.

The key findings and conclusions are summarized as follows:

1. Microplastic contamination was an important contributor to urban road runoff pollution. The median MP abundance in the initial road runoff (185 particles/L) was approximately 4.6 times higher than that observed in natural rainwater (40 particles/L).
2. MPs of various types, shapes, and sizes were identified in the road runoff samples. A total of eleven polymer types were detected, including polypropylene (PP), polyethylene (PE), polystyrene (PS), polyethylene terephthalate (PET), polycaprolactam (Nylon 6), poly (hexamethylene adipamide) (Nylon 6,6), poly (methyl methacrylate) (PMMA), poly(tetrafluoroethylene) (PTFE), poly (vinyl chloride) (PVC), poly(4-methyl-pentene) (PMP), and poly(alpha-methyl styrene) (PMS). PP, PE, and PS were dominant, accounting for 39.0%, 36.0%, and 17.0% of all MPs, respectively. Fragments were the most common shape, and over 60% of MPs measured less than 300 μm.
3. Contaminant levels in initial road runoff—including microbial (E. coli), particulate (TSS), metals (e.g., Cu, Zn, Fe, Pb), nutrients (TIN, PO_4^{3-}), organic matter (COD), and MPs—were markedly higher than those in natural rainwater and exceeded urban water pollution control standards by several to dozens of times. These elevated loadings contribute substantially to the deterioration of urban water quality in Hong Kong and can severely compromise downstream water quality if discharged untreated.
4. Principal component analysis (PCA) on 32 stormwater quality indicators revealed four principal components that collectively explained 75.7% of the total variance. The principal components in urban road runoff identified included metals, particles, and organic matter (Zn, Cu, Mn, Fe, Pb, As, Al, turbidity, and COD; 34.1%); ions and nutrient compounds (EC, Cl-, PO_4^{3-}, NO_3^-–N, TIN, and hardness; 12%); fecal contamination (*E. coli*; 9.6%); and microplastics (MPs; 6.3%). These pollutants were linked to various anthropogenic sources, including road dust, vehicular emissions, atmospheric deposition, road cleaning, urban functional activities, and drainage infrastructure.
5. A pronounced first-flush effect was observed for COD, TSS, Zn, and MPs (MFF > 1.5), indicating that initial runoff transported a disproportionately large fraction of these pollutants. COD correlated with metals (Cu, Zn, Mn) and turbidity, suggesting

particulate-associated processes such as surface adsorption and aggregation. The co-occurrence of MPs with *E. coli*, PO_4^{3-}, and NO_3^-–N indicates that MPs may act as vectors for both nutrients and pathogens in urban road runoff.

6. Land use and seasonal variations exert significant influences on pollutant concentrations in urban road runoff. Levels of COD, Cl^-, *E. coli*, TIN, TSS, and MPs were higher in residential roads than in commercial and industrial roads. Seasonally, COD, Cl^-, Zn, Fe, and TSS peaked in winter; TIN and MPs peaked in autumn; and *E. coli* peaked in summer. These spatial-temporal differences may be shaped by the combined effects of anthropogenic activity intensity, rainfall characteristics, and infrastructural features typical of compact, high-density urban environments. Collectively, these findings underscore the importance of considering functional area characteristics and seasonal dynamics in stormwater treatment planning.
7. Ecological risk assessment indicated that metals (*RI* 652–970), dominated by Pb and Ni, consistently exceeded very high-risk thresholds, while MPs (*PRI* 7.3–138), driven by polymers such as PVC and PMMA, posed moderate-to-high risks. The spatio-temporal superposition of risks—metals peaking in industrial areas during winter and MPs in industrial and commercial areas during autumn—identifies critical hotspots and periods for targeted stormwater management in densely urbanized megacities.

This part concludes the analysis of the characteristics, interrelationships, and ecological risks of various stormwater pollutants in urban road runoff in Hong Kong. The findings collectively underscore the urgent need for targeted stormwater management strategies that should consider land use patterns, seasonal variability, and multi-pollutant risk assessments. Particular attention should be given to heavy metals and microplastics, which pose significant ecological risks in urban road runoff. Moreover, the results highlight the pivotal role of hydrological dynamics, especially during the initial stages of rainfall, in shaping pollutant loading behaviours. This reinforces the importance of managing the first flush in urban stormwater control. Accordingly, effective mitigation strategies should prioritize the early runoff phase through approaches such as source control, flow buffering, or early-stage capture systems to substantially reduce pollutant loads from impervious urban surfaces.

7.1.2 Mitigation strategies for urban road runoff pollution

Based on an integrated field investigation of urban road runoff pollutants, this study designed and evaluated a tree-based NBS consisting of 24 banyan tree box filters and 6 independent filter columns without trees. System performance was assessed over one year through 12 simulated rainfall events, enabling a comprehensive evaluation of pollutant removal efficiency, long-term resilience, and ecological co-benefits.

The main conclusions are summarized as follows:

1. Tree box systems demonstrated a strong and consistent capacity to remove nutrients and heavy metals from urban road runoff. High removal efficiencies were achieved across multiple filter media configurations, with NH_4^+–N, PO_4^{3-}, and Cu showing particularly robust removal, and most monitored metals (including Cr, Zn, and Fe) consistently exceeding high removal thresholds. These results confirm that tree boxes are effective treatment units for diverse urban runoff pollutants.
2. Tree roots played a critical role in enhancing nitrogen removal. Compared with filter columns lacking vegetation, tree boxes exhibited substantially higher removal of NO_2^-–N and NO_3^-–N, highlighting the importance of root-mediated retention and uptake processes. This finding emphasizes that vegetation is not merely a structural component, but a key functional driver in nutrient transformation within tree-based stormwater systems.
3. Pollutant removal—particularly for heavy metals—was strongly influenced by pH dynamics. Tree boxes generally exhibited lower outflow pH, likely associated with root exudation and biogeochemical interactions within the root zone. The observed relationships between pH and metal removal indicate that tree roots contribute to regulating local chemical conditions, thereby indirectly controlling metal speciation and retention.
4. Filter media composition significantly affected system performance. Tree boxes incorporating functional materials, especially sand–GAC and sand–biochar mixtures, consistently outperformed conventional sand or sand–soil media in removing nutrients and most heavy metals. These results demonstrate the added value of functional media in enhancing adsorption capacity and sustaining pollutant retention in tree-based stormwater treatment systems.

5. Seasonal variability influenced pollutant removal in both tree boxes and filter columns. However, tree boxes exhibited greater sensitivity and adaptive response to seasonal changes, suggesting that the integrated tree–media–microbe system responds dynamically to environmental variability. This adaptability underlines the suitability of tree box systems for long-term stormwater management under changing climatic conditions.
6. Sustained tree growth was observed throughout the monitoring period, with measurable increases in both tree height and trunk circumference. These results confirm that the sand-based filter media provided a favorable growth environment for vegetation, while simultaneously delivering effective stormwater treatment. The coexistence of pollutant removal and healthy tree development highlights the broader ecological and urban co-benefits of tree box systems.

In summary, this study demonstrates that tree box systems represent a sustainable, resilient, and multifunctional mitigation strategy for urban road runoff pollution. By combining effective pollutant removal, long-term system stability, and ecological enhancement, tree-based NBS offer a promising pathway for integrated and space-efficient stormwater management in high-density urban environments.

7.2 Limitations

Despite the valuable insights generated from this study, several limitations should be acknowledged:

1. The study was conducted at a limited number of urban road sites and during a constrained number of rainfall events in Hong Kong. As such, the findings may not be fully generalized to other cities with different climates, land use patterns, or urban infrastructure.
2. The temporal resolution and number of sampling sites for analyzing pollutant loading dynamics were restricted due to limited experimental manpower, potentially affecting the comprehensiveness of the observed first flush behavior and pollutant transport trends.
3. The detection of MPs was limited to particles larger than 20 μm due to the resolution

constraints of the available instrumentation. This may underestimate the presence and impact of smaller-sized MPs, which can also pose significant environmental risks.

4. Due to constraints in experimental materials, space, and resources, the pollutant removal performance of the tree box systems was primarily evaluated for nutrients and heavy metals. Key contaminants such as MPs, as well as broader ecological indicators, including microbial diversity, soil health, and carbon sequestration, were not assessed in this study.
5. The study utilized 12 simulated rainfall events to evaluate the pollutant removal performance of the tree box systems. While this approach ensured controlled conditions, it may not accurately replicate the variability of flow rates, pollutant loads, and hydrological patterns encountered under real rainfall events. As such, the environmental impacts and system performance under natural stormwater conditions may not be fully captured, limiting the generalizability of the results.
6. The research primarily focused on pollutant removal efficiency and tree growth performance. However, key hydraulic aspects—such as infiltration rates, long-term hydraulic conductivity, and potential clogging of the filter media—were not comprehensively assessed. These factors are critical for evaluating the long-term functionality and maintenance requirements of tree box systems in real-world applications.

7.3 Recommendations for Future Work

Building on the findings and limitations of this study, the following recommendations are proposed for future research:

1. Future studies should extend field investigations to a broader range of urban contexts, encompassing different climatic conditions, land-use patterns, and infrastructure configurations. Expanding beyond the subtropical setting of Hong Kong will enhance the generalizability of the findings and support the transferability of tree box systems to cities with contrasting hydrological and environmental conditions.
2. Monitoring strategies should be refined by increasing the number of sampling locations and the temporal resolution of sampling during rainfall events. High-frequency measurements are particularly important for capturing pollutant dynamics associated

with first-flush effects. The deployment of automated samplers and real-time monitoring technologies would help overcome manpower constraints and substantially improve data resolution and reliability.

3. Future research should prioritize mechanistic investigations into the key processes governing pollutant removal in tree box systems. In particular, the roles of microbial community composition, microbial activity, and root–pH interactions in controlling nutrient transformation and heavy metal immobilization warrant systematic examination. Integrating molecular biological tools and geochemical analyses will provide deeper insight into the coupled biological and physicochemical mechanisms underpinning system performance.
4. The scope of target pollutants should be expanded to include emerging contaminants such as microplastics, hydrocarbons, and per- and polyfluoroalkyl substances (PFAS). Advanced analytical techniques, including micro-FTIR and Raman spectroscopy, should be employed to detect smaller microplastic particles (<20 μm). Targeted mechanistic experiments will be essential to elucidate removal pathways and assess the effectiveness of tree-based systems in mitigating these emerging urban runoff pollutants.
5. Future studies should incorporate long-term monitoring under natural storm conditions in addition to controlled or simulated rainfall events. Continuous field observations across different storm types and seasons will enable more realistic assessments of system resilience, hydrological performance, and pollutant removal efficiency under real-world variability.
6. Future work should place greater emphasis on quantifying the ecological and urban co-benefits of tree box systems. Assessments of biodiversity enhancement, soil microbial function, carbon sequestration, urban heat mitigation, and overall ecosystem services will help establish the multifunctionality of tree-based bioretention systems. Such evidence is essential for supporting large-scale implementation and policy adoption of tree boxes as space-efficient stormwater solutions in compact cities.

By addressing these research gaps, future studies can significantly advance the design, implementation, and long-term evaluation of nature-based solutions for urban stormwater management.

APPENDIX A

Figure A-1. Photographs of the 6 sampling sites of the stormwater sampling survey (Note: red lines are the sampling area).

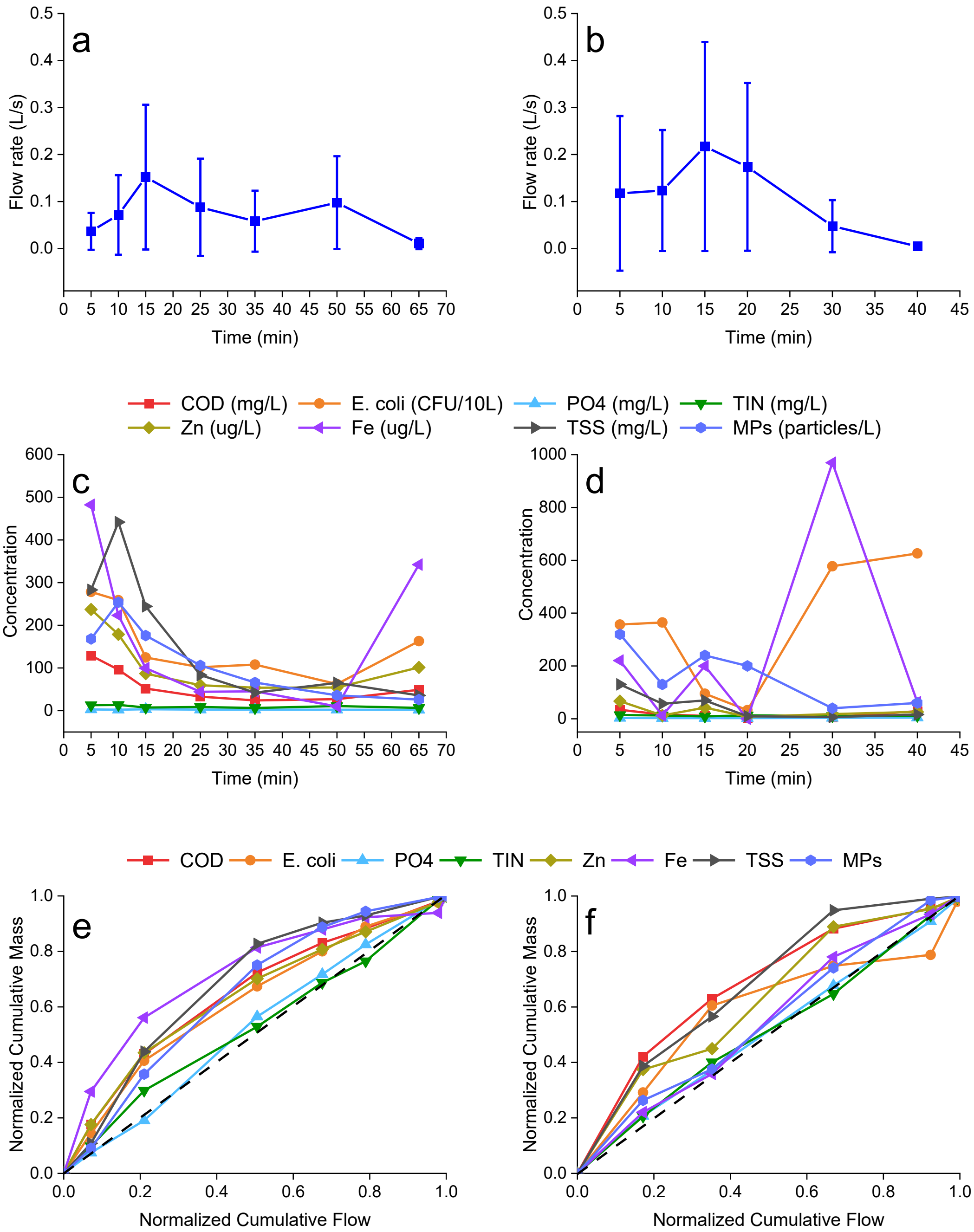

Figure A-2. Temporal changes of flow rates, concentrations, and the dimensionless M(V) curves of eight representative parameters (COD, *E. coli*, PO_4^{3-}, TIN, Zn, Fe, TSS, and MPs): (a, c, e) Data from site A during the 10th rainfall event; (b, d, f) Data from site C during the 11th rainfall event. Each set includes flow rates (a, b), concentrations (c, d), and M(V) curves (e, f) for stormwater on road surfaces.

APPENDIX B

Table B-1. Microplastic abundance is found in plastic categories (particles/L).

Sampling location	Nylon 6	Nylon 6,6	PE	PET	PMMA	PMP	PMS	PP	PS	PTFE	PVC
A	80	10	910	60	50	20	0	800	210	20	10
B	0	0	350	40	0	0	0	1150	270	0	0
C	20	0	1010	190	0	0	0	990	690	0	0
D	20	0	980	200	10	0	0	640	550	0	0
E	40	0	970	120	0	0	0	580	330	0	0
F	20	30	850	230	0	0	10	1070	300	0	10
NR	10	0	480	20	0	0	0	320	30	0	0

Table B-2. Microplastic abundance is found in different shapes (particles/L).

Polymer	Fiber	Film	Fragment	Pellet
Nylon 6	10	0	120	60
Nylon 6,6	0	0	40	0
PE	410	340	4800	0
PET	510	0	350	0
PMMA	0	30	30	0
PMP	0	0	20	0
PMS	0	0	0	10
PP	710	200	4640	0
PS	160	220	1980	20
PTFE	0	0	20	0
PVC	0	0	10	10

Table B-3. Microplastic abundance in particle size range (particles/L).

Sampling sites	20-100 μm	100-200 μm	200-300 μm	300-500 μm	500-1000 μm	1000-5000 μm
A	750	900	200	290	30	0
B	470	860	140	210	70	60
C	320	890	590	610	360	130
D	400	840	290	240	400	230
E	600	740	290	290	70	50
F	650	1000	330	310	160	70
NR	170	280	130	200	60	20

Table B-4. The data of the smallest reporting size of MPs, and mean abundance of MPs found in urban stormwater drains, outfalls, and adjunct harbors in various studies, including the current results (Mak et al., 2020; Piñon-Colin et al., 2020; Tsang et al., 2017; Zhang et al., 2022).

No	Location		Sampling Site	Reporting the smallest MP size (μm)	Average Abundance (particles/L)	References
1	Hong Kong	SD	Hong Kong, Fo Tan Nullah	20	1.9	Zhang et al., 2022
2	Hong Kong	SD	Hong Kong, Ng Tung River	20	1.9	
3	Hong Kong	SD	Hong Kong, Tin Shui Wai Nullah	20	20	
4	Hong Kong	SD	Hong Kong, Tuen Mun River	20	1.7	
5	Hong Kong	SD	Hong Kong, Shau Kei Wan	20	3.3	
6	Hong Kong	SD	Hong Kong, Kwai Chung	20	7.4	
7	Hong Kong	SWO	Hong Kong, Kwun Tong SWO	54	4.1	Mak et al., 2020
8	Hong Kong	SWO	Hong Kong, Yau Ma Tei SWO	54	5.1	
9	Hong Kong	AH	Hong Kong, Victoria Harbour	30	14	Tsang et al., 2017
10	Hong Kong	AH	Hong Kong, Tolo Harbour	30	0.7	
11	Hong Kong	AH	Hong Kong, Tsing Yi North	30	3.2	
12	Hong Kong	AH	Hong Kong, Deep Bay	30	5.6	
13	Mexico, Tijuana	RR	Mexico, Tijuana Altabrisa	25	289	Piñon-Colin et al., 2020
14	Mexico, Tijuana	RR	Mexico, Tijuana Parte Baja	25	128	
15	Mexico, Tijuana	RR	Mexico, Tijuana Buena Vista	25	187	

16	Mexico, Tijuana	RR	Mexico, Tijuana 20 de Noviembre	25	88	
17	Mexico, Tijuana	RR	Mexico, Tijuana Industrial Otay	25	180	
18	Hong Kong	IRR	Hong Kong, Chatham Road South	20	140	This study
19	Hong Kong	IRR	Hong Kong, Baker Street	20	157	
20	Hong Kong	IRR	Hong Kong, Station Lane	20	190	
21	Hong Kong	IRR	Hong Kong, Ming On Street	20	166	
22	Hong Kong	IRR	Hong Kong, Wong Chuk Yeung Street	20	131	
23	Hong Kong	IRR	Hong Kong, Au Pui Wan Street	20	170	
24	Hong Kong	NR	Hong Kong, HK PolyU	20	83.6	

Table B-5. Summarized concentrations of 32 stormwater quality parameters in the natural rainwater during 11 rainfall events.

No.	Indicators	Unit	n	Minimum	Maximum	Mean	Median
1	Temperature	℃	11	16.3	25.9	21.2	20.5
2	Electrical conductivity (EC)	mS/cm	11	0.01	0.59	0.12	0.02
3	Turbidity	NTU	11	0.27	2.25	1.05	0.72
4	Total suspended solids (TSS)	mg/L	11	0.00	31.80	5.45	1.70
5	pH	–	11	4.43	6.88	6.05	6.15
6	Dissolved oxygen (DO)	mg/L	11	3.56	10.21	6.64	6.56
7	Salinity	–	11	0.01	0.35	0.07	0.02
8	Biochemical oxygen demand (BOD_5)	mg/L	11	0.29	2.45	1.16	1.15
9	Chemical oxygen demand (COD)	mg/L	11	0.00	34.38	13.31	8.59
10	*Escherichia coli* (*E. coli*)	CFU/100mL	11	0	47	10	0
11	Ammonia nitrogen (NH_4^+-N)	mg/L	11	0.01	0.44	0.18	0.15
12	Nitrate nitrogen (NO_3^--N)	mg/L	11	0.60	1.65	1.10	1.05
13	Nitrite nitrogen (NO_2^--N)	mg/L	11	0.00	0.06	0.01	0.01
14	Total inorganic nitrogen (TIN)	mg/L	11	0.68	1.90	1.30	1.19
15	Phosphate (PO_4^{3-})	mg/L	11	0.04	0.28	0.14	0.13
16	Fluoride (F^-)	mg/L	11	0.00	0.21	0.05	0.04
17	Chloride (Cl^-)	mg/L	11	0.26	3.49	1.32	1.23
18	Sulfate (SO_4^{2-})	mg/L	11	0.33	2.96	1.08	0.94

19	Bromide (Br^-)	mg/L	11	0.00	0.26	0.02	0.00
20	Total alkalinity (TA)	mg/L	11	10.00	25.00	15.68	15.00
21	Hardness	mg/L	11	0.00	28.33	12.88	11.67
22	Aluminum (Al)	µg/L	11	0.0042	0.101	0.024	0.019
23	Arsenic (As)	µg/L	11	0.00	0.0002	0.0001	0.0001
24	Chromium (Cr)	µg/L	11	0.0001	0.014	0.007	0.005
25	Cadmium (Cd)	µg/L	11	0.0000	0.0002	0.0000	0.0000
26	Lead (Pb)	µg/L	11	0.0000	0.0012	0.0004	0.0003
27	Zinc (Zn)	µg/L	11	0.0000	0.166	0.033	0.008
28	Copper (Cu)	µg/L	11	0.0006	0.039	0.007	0.004
29	Iron (Fe)	µg/L	11	0.0000	0.0175	0.0066	0.0059
30	Manganese (Mn)	µg/L	11	0.0007	0.025	0.007	0.004
31	Nickel (Ni)	µg/L	11	0.0003	0.003	0.001	0.001
32	Microplastics (MPs)	Particles/L	11	7.0	260.0	83.9	46.0

Note: n= number of samples

Table B-6. Outflow concentrations of nutrients from tree boxes with different filter media, irrigated with either tap water or synthetic stormwater during 12 simulated rainfall events from December 2023 to April 2025.

Rainfall events	Tree boxes No.	Filter media	Watering types	NH_4^+-N (mg/L)	NO_2^--N (mg/L)	NO_3^--N (mg/L)	PO_4^{3-} (mg/L)
1	13	Sand	Tap water	0.03	0.00	4.64	0.07
1	14	Sand+Soil	Tap water	0.13	0.00	16.50	0.25
1	15	Sand	Tap water	0.14	0.01	37.00	0.30
1	16	Sand+Soil	Tap water	0.22	0.01	11.00	0.41
1	17	Sand	Tap water	0.22	0.01	32.00	0.31
1	18	Sand+Soil	Tap water	0.17	0.01	12.58	0.14
1	19	Sand	Tap water	0.02	0.01	10.00	0.10
1	20	Sand+Soil	Tap water	0.17	0.01	12.00	0.21
2	13	Sand	Tap water	0.03	0.00	2.90	0.29
2	14	Sand+Soil	Tap water	0.02	0.00	5.80	0.24
2	15	Sand	Tap water	0.05	0.00	3.80	0.32
2	16	Sand+Soil	Tap water	0.02	0.00	8.20	0.13
2	17	Sand	Tap water	0.03	0.01	5.00	0.29
2	18	Sand+Soil	Tap water	0.01	0.00	7.50	0.25
2	19	Sand	Tap water	0.01	0.00	7.45	0.20
2	20	Sand+Soil	Tap water	0.04	0.00	5.40	0.15
3	13	Sand	Tap water	0.08	0.01	0.00	0.22
3	14	Sand+Soil	Tap water	0.07	0.00	1.40	0.14
3	15	Sand	Tap water	0.05	0.00	7.25	0.25
3	16	Sand+Soil	Tap water	0.12	0.00	0.00	0.27
3	17	Sand	Tap water	0.05	0.01	3.60	0.15
3	18	Sand+Soil	Tap water	0.06	0.00	4.20	0.21
3	19	Sand	Tap water	0.03	0.00	2.50	0.05
3	20	Sand+Soil	Tap water	0.05	0.00	0.00	0.21
4	13	Sand	Tap water	0.06	0.01	2.70	0.13
4	14	Sand+Soil	Tap water	0.01	0.00	4.85	0.13

4	15	Sand	Tap water	0.05	0.00	8.50	0.16
4	16	Sand+Soil	Tap water	0.04	0.00	6.75	0.16
4	17	Sand	Tap water	0.04	0.00	10.80	0.11
4	18	Sand+Soil	Tap water	0.05	0.00	5.25	0.13
4	19	Sand	Tap water	0.04	0.00	3.70	0.09
4	20	Sand+Soil	Tap water	0.04	0.00	0.00	0.15
5	13	Sand	Tap water	0.08	0.01	0.00	0.13
5	14	Sand+Soil	Tap water	0.02	0.00	6.95	0.05
5	15	Sand	Tap water	0.07	0.00	4.75	0.10
5	16	Sand+Soil	Tap water	0.03	0.00	5.65	0.05
5	17	Sand	Tap water	0.05	0.01	6.00	0.13
5	18	Sand+Soil	Tap water	0.04	0.01	5.85	0.12
5	19	Sand	Tap water	0.02	0.00	4.25	0.11
5	20	Sand+Soil	Tap water	0.04	0.00	4.40	0.14
6	13	Sand	Tap water	0.02	0.00	7.50	0.06
6	14	Sand+Soil	Tap water	0.03	0.00	3.90	0.06
6	15	Sand	Tap water	0.08	0.01	9.55	0.07
6	16	Sand+Soil	Tap water	0.09	0.00	8.20	0.05
6	17	Sand	Tap water	0.06	0.01	7.30	0.05
6	18	Sand+Soil	Tap water	0.03	0.01	0.30	0.04
6	19	Sand	Tap water	0.05	0.01	7.15	0.05
6	20	Sand+Soil	Tap water	0.02	0.01	5.80	0.06
7	13	Sand	Tap water	0.04	0.01	2.55	0.06
7	14	Sand+Soil	Tap water	0.02	0.00	8.95	0.03
7	15	Sand	Tap water	0.09	0.01	8.55	0.06
7	16	Sand+Soil	Tap water	0.05	0.00	11.45	0.05
7	17	Sand	Tap water	0.04	0.00	9.90	0.08
7	18	Sand+Soil	Tap water	0.06	0.00	9.70	0.05
7	19	Sand	Tap water	0.06	0.00	1.70	0.03
7	20	Sand+Soil	Tap water	0.02	0.00	5.50	0.05
8	13	Sand	Tap water	0.04	0.00	7.75	0.06
8	14	Sand+Soil	Tap water	0.03	0.00	7.25	0.04

8	15	Sand	Tap water	0.04	0.00	4.40	0.07
8	16	Sand+Soil	Tap water	0.03	0.00	7.15	0.09
8	17	Sand	Tap water	0.01	0.01	9.60	0.03
8	18	Sand+Soil	Tap water	0.01	0.00	5.05	0.08
8	19	Sand	Tap water	0.01	0.01	8.80	0.02
8	20	Sand+Soil	Tap water	0.01	0.00	9.00	0.04
9	13	Sand	Tap water	0.08	0.00	2.40	0.08
9	14	Sand+Soil	Tap water	0.01	0.00	6.95	0.07
9	15	Sand	Tap water	0.07	0.00	6.60	0.13
9	16	Sand+Soil	Tap water	0.07	0.00	3.20	0.17
9	17	Sand	Tap water	0.08	0.00	4.45	0.09
9	18	Sand+Soil	Tap water	0.04	0.00	5.40	0.07
9	19	Sand	Tap water	0.00	0.00	4.40	0.05
9	20	Sand+Soil	Tap water	0.01	0.00	5.70	0.09
10	13	Sand	Tap water	0.02	0.00	2.95	0.08
10	14	Sand+Soil	Tap water	0.04	0.01	6.85	0.11
10	15	Sand	Tap water	0.01	0.00	3.20	0.11
10	16	Sand+Soil	Tap water	0.02	0.01	6.90	0.10
10	17	Sand	Tap water	0.02	0.01	3.35	0.10
10	18	Sand+Soil	Tap water	0.01	0.00	4.55	0.07
10	19	Sand	Tap water	0.01	0.00	5.10	0.11
10	20	Sand+Soil	Tap water	0.02	0.00	4.50	0.10
11	13	Sand	Tap water	0.05	0.01	8.75	0.04
11	14	Sand+Soil	Tap water	0.01	0.01	7.30	0.02
11	15	Sand	Tap water	0.02	0.00	4.65	0.02
11	16	Sand+Soil	Tap water	0.00	0.00	7.80	0.01
11	17	Sand	Tap water	0.03	0.01	9.00	0.03
11	18	Sand+Soil	Tap water	0.01	0.00	8.95	0.03
11	19	Sand	Tap water	0.01	0.01	4.80	0.03
11	20	Sand+Soil	Tap water	0.00	0.00	5.10	0.03
12	13	Sand	Tap water	0.00	0.00	5.70	0.12
12	14	Sand+Soil	Tap water	0.08	0.01	1.95	0.18

12	15	Sand	Tap water	0.01	0.01	5.15	0.19
12	16	Sand+Soil	Tap water	0.03	0.00	6.40	0.13
12	17	Sand	Tap water	0.00	0.00	2.80	0.08
12	18	Sand+Soil	Tap water	0.00	0.00	7.30	0.03
12	19	Sand	Tap water	0.00	0.00	2.45	0.09
12	20	Sand+Soil	Tap water	0.00	0.00	7.15	0.19
1	1	Sand	Stormwater	0.04	0.07	12.05	0.04
1	2	Sand+Soil	Stormwater	0.04	0.06	9.64	0.06
1	5	Sand	Stormwater	0.03	0.08	10.70	0.02
1	6	Sand+Soil	Stormwater	0.04	0.06	11.95	0.05
1	7	Sand	Stormwater	0.01	0.07	11.50	0.02
1	8	Sand+Soil	Stormwater	0.05	0.09	9.36	0.05
1	11	Sand+Soil	Stormwater	0.02	0.04	11.85	0.21
1	12	Sand	Stormwater	0.04	0.05	14.00	0.32
2	1	Sand	Stormwater	0.04	0.07	15.40	0.28
2	2	Sand+Soil	Stormwater	0.06	0.06	13.90	0.61
2	5	Sand	Stormwater	0.03	0.06	12.15	0.50
2	6	Sand+Soil	Stormwater	0.04	0.07	13.05	0.40
2	7	Sand	Stormwater	0.04	0.08	13.50	0.63
2	8	Sand+Soil	Stormwater	0.06	0.06	9.95	0.53
2	11	Sand+Soil	Stormwater	0.06	0.07	13.60	0.94
2	12	Sand	Stormwater	0.05	0.09	18.80	0.38
3	1	Sand	Stormwater	0.02	0.05	14.05	0.73
3	2	Sand+Soil	Stormwater	0.08	0.06	14.65	0.11
3	5	Sand	Stormwater	0.04	0.05	12.30	0.12
3	6	Sand+Soil	Stormwater	0.09	0.04	16.35	0.13
3	7	Sand	Stormwater	0.13	0.07	16.50	0.38
3	8	Sand+Soil	Stormwater	0.13	0.05	17.90	0.21
3	11	Sand+Soil	Stormwater	0.02	0.05	13.40	0.18
3	12	Sand	Stormwater	0.00	0.05	11.25	0.20
4	1	Sand	Stormwater	0.09	0.04	7.90	0.27
4	2	Sand+Soil	Stormwater	0.08	0.04	9.75	0.15

4	5	Sand	Stormwater	0.10	0.05	5.45	0.09
4	6	Sand+Soil	Stormwater	0.12	0.04	8.95	0.14
4	7	Sand	Stormwater	0.12	0.05	11.60	0.12
4	8	Sand+Soil	Stormwater	0.12	0.05	14.60	0.11
4	11	Sand+Soil	Stormwater	0.04	0.04	12.20	0.27
4	12	Sand	Stormwater	0.07	0.04	8.70	0.11
5	1	Sand	Stormwater	0.01	0.04	15.95	0.12
5	2	Sand+Soil	Stormwater	0.01	0.03	14.60	0.07
5	5	Sand	Stormwater	0.02	0.04	14.10	0.07
5	6	Sand+Soil	Stormwater	0.04	0.04	9.45	0.12
5	7	Sand	Stormwater	0.04	0.04	7.20	0.07
5	8	Sand+Soil	Stormwater	0.03	0.03	8.45	0.06
5	11	Sand+Soil	Stormwater	0.08	0.05	12.95	0.19
5	12	Sand	Stormwater	0.01	0.04	12.75	0.06
6	1	Sand	Stormwater	0.04	0.04	13.65	0.06
6	2	Sand+Soil	Stormwater	0.03	0.03	12.40	0.19
6	5	Sand	Stormwater	0.07	0.04	10.70	0.05
6	6	Sand+Soil	Stormwater	0.08	0.05	12.25	0.10
6	7	Sand	Stormwater	0.07	0.06	8.55	0.07
6	8	Sand+Soil	Stormwater	0.06	0.05	9.70	0.03
6	11	Sand+Soil	Stormwater	0.11	0.06	12.20	0.07
6	12	Sand	Stormwater	0.08	0.04	11.60	0.05
7	1	Sand	Stormwater	0.02	0.04	12.10	0.06
7	2	Sand+Soil	Stormwater	0.03	0.04	10.15	0.05
7	5	Sand	Stormwater	0.03	0.04	6.10	0.08
7	6	Sand+Soil	Stormwater	0.03	0.04	8.05	0.23
7	7	Sand	Stormwater	0.03	0.04	6.10	0.08
7	8	Sand+Soil	Stormwater	0.04	0.04	11.50	0.09
7	11	Sand+Soil	Stormwater	0.07	0.03	14.75	0.06
7	12	Sand	Stormwater	0.06	0.02	12.45	0.05
8	1	Sand	Stormwater	0.02	0.01	21.60	0.04
8	2	Sand+Soil	Stormwater	0.00	0.01	17.50	0.05

8	5	Sand	Stormwater	0.00	0.01	20.10	0.04
8	6	Sand+Soil	Stormwater	0.04	0.01	15.15	0.04
8	7	Sand	Stormwater	0.03	0.01	15.60	0.06
8	8	Sand+Soil	Stormwater	0.02	0.02	19.65	0.06
8	11	Sand+Soil	Stormwater	0.08	0.04	18.35	0.07
8	12	Sand	Stormwater	0.03	0.04	15.55	0.09
9	1	Sand	Stormwater	0.10	0.05	9.75	0.14
9	2	Sand+Soil	Stormwater	0.12	0.05	19.00	0.20
9	5	Sand	Stormwater	0.05	0.03	11.95	0.17
9	6	Sand+Soil	Stormwater	0.05	0.04	14.55	0.17
9	7	Sand	Stormwater	0.07	0.03	6.65	0.13
9	8	Sand+Soil	Stormwater	0.03	0.05	11.95	0.10
9	11	Sand+Soil	Stormwater	0.13	0.04	12.60	0.19
9	12	Sand	Stormwater	0.13	0.04	9.30	0.13
10	1	Sand	Stormwater	0.04	0.05	10.40	0.28
10	2	Sand+Soil	Stormwater	0.04	0.05	12.80	0.23
10	5	Sand	Stormwater	0.04	0.03	11.85	0.15
10	6	Sand+Soil	Stormwater	0.05	0.03	11.15	0.17
10	7	Sand	Stormwater	0.06	0.03	12.00	0.10
10	8	Sand+Soil	Stormwater	0.05	0.03	12.50	0.09
10	11	Sand+Soil	Stormwater	0.09	0.06	13.05	0.26
10	12	Sand	Stormwater	0.09	0.05	12.65	0.16
11	1	Sand	Stormwater	0.10	0.04	15.00	0.09
11	2	Sand+Soil	Stormwater	0.05	0.05	16.40	0.15
11	5	Sand	Stormwater	0.02	0.03	13.35	0.08
11	6	Sand+Soil	Stormwater	0.05	0.04	17.90	0.09
11	7	Sand	Stormwater	0.05	0.04	15.00	0.14
11	8	Sand+Soil	Stormwater	0.06	0.04	18.80	0.12
11	11	Sand+Soil	Stormwater	0.12	0.06	15.90	0.04
11	12	Sand	Stormwater	0.02	0.05	16.35	0.04
12	1	Sand	Stormwater	0.00	0.04	16.60	0.17
12	2	Sand+Soil	Stormwater	0.03	0.06	11.90	0.20

12	5	Sand	Stormwater	0.03	0.04	11.70	0.09
12	6	Sand+Soil	Stormwater	0.01	0.04	11.20	0.09
12	7	Sand	Stormwater	0.04	0.04	11.35	0.07
12	8	Sand+Soil	Stormwater	0.05	0.04	16.35	0.08
12	11	Sand+Soil	Stormwater	0.01	0.05	12.45	0.17
12	12	Sand	Stormwater	0.00	0.04	10.15	0.15

Table B-7. Outflow concentrations of heavy metals from tree boxes with different filter media, irrigated with either tap water or synthetic stormwater during 12 simulated rainfall events from December 2023 to April 2025.

Rainfall events	Tree boxes No.	Filter media	Watering types	Cr (ug/L)	Cu (ug/L)	Fe (ug/L)	Mn (ug/L)	Ni (ug/L)	Pb (ug/L)	Zn (ug/L)
1	13	Sand	Tap water	0.28	7.86	500.37	8.03	1.69	4.54	50.30
1	14	Sand+Soil	Tap water	0.93	12.69	2096.40	53.30	0.04	1.40	43.78
1	15	Sand	Tap water	1.90	12.65	2491.33	50.24	0.61	8.74	20.09
1	16	Sand+Soil	Tap water	1.83	14.74	3408.18	98.89	1.61	13.23	36.31
1	17	Sand	Tap water	3.73	17.17	3925.01	92.06	5.34	14.38	40.05
1	18	Sand+Soil	Tap water	1.24	13.90	2802.79	63.47	1.46	13.57	60.48
1	19	Sand	Tap water	0.24	8.32	560.66	9.14	1.85	0.41	53.53
1	20	Sand+Soil	Tap water	1.66	11.85	2908.31	65.55	2.20	14.49	46.98
2	13	Sand	Tap water	7.01	12.16	774.22	38.05	14.83	4.26	31.08
2	14	Sand+Soil	Tap water	4.23	13.40	837.66	29.46	8.00	6.97	34.45
2	15	Sand	Tap water	1.31	16.48	1149.12	155.31	6.16	4.71	29.49
2	16	Sand+Soil	Tap water	0.95	13.52	285.08	10.56	5.89	11.13	82.61
2	17	Sand	Tap water	1.21	12.60	690.66	106.32	5.53	14.10	21.33
2	18	Sand+Soil	Tap water	1.18	13.68	537.31	19.54	5.30	3.55	78.50
2	19	Sand	Tap water	1.15	11.73	297.73	11.03	4.71	8.53	22.27
2	20	Sand+Soil	Tap water	1.29	12.88	421.71	6.52	5.56	5.41	36.84

3	13	Sand	Tap water	1.95	13.58	1005.05	57.63	2.78	11.92	42.05
3	14	Sand+Soil	Tap water	2.21	11.05	770.99	22.40	3.86	7.95	21.22
3	15	Sand	Tap water	0.91	16.28	657.31	260.37	5.75	10.40	41.70
3	16	Sand+Soil	Tap water	1.75	22.15	1359.80	33.78	3.78	9.66	58.41
3	17	Sand	Tap water	3.03	14.53	720.05	88.99	3.19	8.28	52.61
3	18	Sand+Soil	Tap water	1.37	16.79	708.98	20.17	4.57	13.62	44.85
3	19	Sand	Tap water	1.36	14.19	368.25	14.26	0.28	0.90	38.84
3	20	Sand+Soil	Tap water	1.83	14.56	1002.14	18.74	4.20	19.00	52.21
4	13	Sand	Tap water	2.65	12.01	858.82	58.01	6.41	2.33	32.62
4	14	Sand+Soil	Tap water	2.32	10.99	196.14	0.58	7.02	5.33	64.27
4	15	Sand	Tap water	4.09	13.70	627.34	103.27	7.64	2.74	59.29
4	16	Sand+Soil	Tap water	2.47	12.04	396.95	9.77	1.90	20.85	25.10
4	17	Sand	Tap water	4.31	14.47	1807.78	82.66	3.17	11.69	163.36
4	18	Sand+Soil	Tap water	2.22	13.51	565.67	20.32	5.67	3.16	49.43
4	19	Sand	Tap water	2.38	11.81	506.52	23.33	2.82	6.16	26.74
4	20	Sand+Soil	Tap water	3.28	11.33	935.14	22.91	4.18	9.16	23.92
5	13	Sand	Tap water	2.00	11.83	967.63	58.23	6.64	8.35	51.74
5	14	Sand+Soil	Tap water	0.95	9.77	196.98	5.63	1.38	9.94	15.71
5	15	Sand	Tap water	2.09	14.71	988.47	94.33	7.69	8.92	30.19
5	16	Sand+Soil	Tap water	1.74	8.98	322.35	25.73	2.69	0.34	44.38

5	17	Sand	Tap water	2.17	11.40	723.19	60.91	2.96	4.51	74.77
5	18	Sand+Soil	Tap water	1.88	9.45	350.26	21.62	2.09	2.45	41.37
5	19	Sand	Tap water	0.44	11.55	279.25	30.78	5.96	1.38	89.56
5	20	Sand+Soil	Tap water	1.13	12.56	445.63	11.96	6.38	13.07	45.40
6	13	Sand	Tap water	2.69	18.98	86.60	61.12	4.79	7.24	75.13
6	14	Sand+Soil	Tap water	2.26	11.84	328.27	11.05	3.96	6.20	35.33
6	15	Sand	Tap water	3.33	15.02	1224.07	143.41	2.78	17.75	105.77
6	16	Sand+Soil	Tap water	2.96	13.28	1068.03	65.15	6.63	13.86	30.79
6	17	Sand	Tap water	1.26	16.60	90.94	117.95	3.43	5.11	58.70
6	18	Sand+Soil	Tap water	1.78	17.37	209.40	23.29	3.04	11.55	56.67
6	19	Sand	Tap water	1.21	14.49	679.24	95.24	6.78	1.93	244.90
6	20	Sand+Soil	Tap water	2.89	14.63	1152.42	33.00	2.92	11.11	35.41
7	13	Sand	Tap water	1.41	10.53	585.54	78.56	5.88	7.52	60.63
7	14	Sand+Soil	Tap water	1.75	11.19	206.19	5.99	3.75	2.52	58.00
7	15	Sand	Tap water	1.99	14.50	1172.37	105.94	2.63	14.40	121.27
7	16	Sand+Soil	Tap water	0.15	13.02	446.13	35.05	3.16	5.46	42.93
7	17	Sand	Tap water	0.34	16.36	698.34	100.51	3.10	4.30	53.24
7	18	Sand+Soil	Tap water	0.69	3.42	652.76	31.10	5.84	1.52	9.73
7	19	Sand	Tap water	1.04	3.31	504.30	82.04	6.73	8.50	12.43
7	20	Sand+Soil	Tap water	0.38	5.48	363.88	7.86	6.35	0.41	20.42

8	13	Sand	Tap water	0.24	8.81	135.03	86.29	4.46	5.89	30.16
8	14	Sand+Soil	Tap water	0.58	11.29	120.39	2.28	5.35	0.10	46.03
8	15	Sand	Tap water	0.88	12.15	383.83	151.18	2.78	1.18	30.78
8	16	Sand+Soil	Tap water	0.05	12.69	152.29	25.05	4.27	1.01	38.67
8	17	Sand	Tap water	0.81	14.89	239.36	106.97	4.42	3.98	35.40
8	18	Sand+Soil	Tap water	0.73	11.95	180.22	11.15	4.87	1.80	51.74
8	19	Sand	Tap water	0.56	11.11	126.52	93.43	3.17	3.20	47.19
8	20	Sand+Soil	Tap water	0.48	12.15	167.09	2.17	1.71	1.26	33.65
9	13	Sand	Tap water	1.16	4.58	794.73	61.33	3.44	11.44	13.63
9	14	Sand+Soil	Tap water	2.30	2.93	258.72	4.20	6.33	7.68	8.10
9	15	Sand	Tap water	1.49	14.52	1047.58	64.24	7.69	9.27	38.89
9	16	Sand+Soil	Tap water	0.13	13.86	401.53	16.36	4.77	3.32	34.53
9	17	Sand	Tap water	1.02	17.15	944.68	51.82	3.21	0.90	30.19
9	18	Sand+Soil	Tap water	1.32	9.45	380.75	10.74	7.10	3.41	25.55
9	19	Sand	Tap water	1.04	14.84	274.73	26.48	5.58	8.86	77.75
9	20	Sand+Soil	Tap water	1.16	10.39	235.12	2.53	6.49	5.64	26.83
10	13	Sand	Tap water	0.67	1.43	255.78	74.31	6.15	4.26	10.11
10	14	Sand+Soil	Tap water	0.50	0.79	161.11	1.02	3.76	2.80	5.62
10	15	Sand	Tap water	0.14	5.45	461.93	62.40	3.21	2.12	11.44
10	16	Sand+Soil	Tap water	0.12	2.81	150.11	3.72	5.96	5.79	13.03

10	17	Sand	Tap water	0.23	3.10	215.26	33.18	7.17	4.37	11.11
10	18	Sand+Soil	Tap water	0.93	2.94	216.44	3.39	7.46	4.42	8.18
10	19	Sand	Tap water	0.44	174.57	124.59	2.88	6.56	5.08	8.25
10	20	Sand+Soil	Tap water	0.45	0.56	83.84	15.33	6.30	5.93	6.38
11	13	Sand	Tap water	7.01	2.45	415.20	12.48	14.83	9.32	200.40
11	14	Sand+Soil	Tap water	4.23	3.71	414.00	3.52	8.00	10.16	70.08
11	15	Sand	Tap water	1.31	4.74	548.40	120.00	6.16	10.00	5.82
11	16	Sand+Soil	Tap water	0.95	2.99	148.80	0.00	5.89	8.71	0.00
11	17	Sand	Tap water	1.21	2.62	348.00	73.92	5.53	9.48	1.55
11	18	Sand+Soil	Tap water	1.18	2.40	252.00	0.00	5.30	8.66	5.74
11	19	Sand	Tap water	1.15	0.73	148.80	0.00	4.71	8.04	0.00
11	20	Sand+Soil	Tap water	1.29	2.56	213.60	0.00	5.56	9.55	0.00
12	13	Sand	Tap water	0.65	20.24	120.82	24.51	1.23	1.60	72.52
12	14	Sand+Soil	Tap water	0.44	20.12	62.85	11.67	1.17	1.01	31.31
12	15	Sand	Tap water	0.59	19.61	218.31	49.64	1.30	2.23	19.33
12	16	Sand+Soil	Tap water	0.43	20.44	70.92	22.80	1.27	1.03	26.84
12	17	Sand	Tap water	0.46	18.78	120.37	94.22	1.37	1.39	15.23
12	18	Sand+Soil	Tap water	0.43	19.11	77.37	23.21	1.09	1.30	29.09
12	19	Sand	Tap water	0.38	18.60	66.39	44.14	1.14	1.12	22.80
12	20	Sand+Soil	Tap water	0.51	20.10	82.37	6.32	1.13	1.31	22.39

1	1	Sand	Stormwater	0.17	5.34	565.62	25.82	2.26	3.55	16.67
1	2	Sand+Soil	Stormwater	0.76	6.19	569.02	10.18	2.06	9.60	19.54
1	5	Sand	Stormwater	1.33	8.55	233.95	13.30	2.23	1.65	14.62
1	6	Sand+Soil	Stormwater	0.84	7.11	503.79	8.77	1.18	1.03	57.32
1	7	Sand	Stormwater	0.08	7.06	694.65	29.28	0.24	7.72	33.06
1	8	Sand+Soil	Stormwater	2.48	25.25	673.67	12.73	8.50	2.44	72.81
1	11	Sand+Soil	Stormwater	0.02	6.80	114.51	6.42	2.58	7.90	62.66
1	12	Sand	Stormwater	0.28	7.61	593.32	21.19	1.87	1.53	22.26
2	1	Sand	Stormwater	0.31	9.31	527.14	112.30	3.98	4.10	27.30
2	2	Sand+Soil	Stormwater	0.71	11.92	758.57	21.41	3.95	5.42	31.79
2	5	Sand	Stormwater	0.71	11.74	328.72	70.51	5.83	13.60	22.66
2	6	Sand+Soil	Stormwater	1.38	15.79	943.75	33.55	5.52	11.11	29.65
2	7	Sand	Stormwater	1.36	12.20	997.63	49.70	5.69	8.96	33.53
2	8	Sand+Soil	Stormwater	1.38	12.90	789.21	29.58	5.93	8.60	100.82
2	11	Sand+Soil	Stormwater	0.99	11.02	576.09	19.95	4.91	7.49	64.54
2	12	Sand	Stormwater	1.91	11.17	1051.82	93.51	5.40	9.79	23.16
3	1	Sand	Stormwater	5.72	13.28	475.11	296.86	3.36	5.57	50.40
3	2	Sand+Soil	Stormwater	7.40	12.28	355.09	9.80	2.80	1.83	27.89
3	5	Sand	Stormwater	8.28	10.91	387.06	231.29	3.41	4.69	43.91
3	6	Sand+Soil	Stormwater	8.10	12.27	1120.57	40.93	4.33	6.44	73.99

3	7	Sand	Stormwater	6.91	11.52	976.13	92.27	1.89	12.04	62.54
3	8	Sand+Soil	Stormwater	6.56	13.93	603.82	33.02	2.34	4.68	54.86
3	11	Sand+Soil	Stormwater	8.15	12.44	180.24	12.97	6.28	3.75	147.23
3	12	Sand	Stormwater	10.68	11.36	850.29	212.82	3.11	7.19	196.00
4	1	Sand	Stormwater	1.90	18.56	313.67	272.79	2.29	15.37	100.30
4	2	Sand+Soil	Stormwater	2.42	9.45	207.71	13.49	4.37	0.95	24.08
4	5	Sand	Stormwater	1.42	10.39	394.20	155.60	4.82	18.84	28.70
4	6	Sand+Soil	Stormwater	1.93	11.34	659.73	21.91	3.90	14.25	29.07
4	7	Sand	Stormwater	3.41	11.27	916.52	87.43	6.29	11.11	59.82
4	8	Sand+Soil	Stormwater	5.49	9.84	490.62	38.91	5.09	7.13	31.55
4	11	Sand+Soil	Stormwater	3.19	13.07	430.00	20.12	2.35	0.91	34.59
4	12	Sand	Stormwater	3.28	13.21	951.04	217.96	2.28	13.76	59.49
5	1	Sand	Stormwater	1.52	10.94	78.41	316.52	7.11	10.25	30.04
5	2	Sand+Soil	Stormwater	1.80	9.60	134.78	33.90	5.24	5.08	42.69
5	5	Sand	Stormwater	1.58	10.52	116.24	167.10	5.87	6.68	46.83
5	6	Sand+Soil	Stormwater	1.80	9.46	194.37	8.88	3.53	5.22	35.52
5	7	Sand	Stormwater	1.87	10.86	343.14	104.73	5.50	5.73	38.60
5	8	Sand+Soil	Stormwater	0.51	9.59	197.96	48.78	3.45	14.12	63.22
5	11	Sand+Soil	Stormwater	1.40	12.48	240.95	19.01	1.58	6.02	45.06
5	12	Sand	Stormwater	1.58	11.41	244.64	207.51	7.25	7.92	37.18

6	1	Sand	Stormwater	0.84	9.54	396.19	263.44	7.00	16.14	39.31
6	2	Sand+Soil	Stormwater	1.37	13.35	306.99	46.45	4.23	12.29	172.83
6	5	Sand	Stormwater	2.48	10.84	598.87	170.79	2.30	18.42	26.72
6	6	Sand+Soil	Stormwater	2.93	12.00	351.49	15.06	6.21	0.31	53.66
6	7	Sand	Stormwater	2.19	11.37	518.36	147.39	2.89	10.13	48.86
6	8	Sand+Soil	Stormwater	1.71	10.55	404.69	74.90	4.23	9.93	107.70
6	11	Sand+Soil	Stormwater	2.78	12.75	544.94	29.53	2.25	13.45	28.14
6	12	Sand	Stormwater	2.62	12.61	752.91	191.59	1.33	0.72	46.21
7	1	Sand	Stormwater	1.56	13.41	375.37	249.87	5.15	9.05	40.99
7	2	Sand+Soil	Stormwater	0.62	12.36	399.13	28.88	4.49	7.32	82.07
7	5	Sand	Stormwater	1.50	12.71	485.83	148.33	3.59	5.64	153.69
7	6	Sand+Soil	Stormwater	0.31	3.00	345.45	16.46	3.49	1.41	11.38
7	7	Sand	Stormwater	1.07	12.64	419.20	122.34	2.99	7.65	51.11
7	8	Sand+Soil	Stormwater	0.39	4.09	381.81	48.37	5.91	1.99	14.93
7	11	Sand+Soil	Stormwater	1.19	13.39	341.28	38.20	3.40	1.10	86.27
7	12	Sand	Stormwater	1.06	12.75	435.93	185.67	4.09	7.59	65.74
8	1	Sand	Stormwater	1.96	11.70	147.41	333.23	2.25	2.39	61.77
8	2	Sand+Soil	Stormwater	1.65	14.63	109.11	27.19	1.68	1.54	65.19
8	5	Sand	Stormwater	1.62	12.25	61.12	130.94	3.08	5.76	45.73
8	6	Sand+Soil	Stormwater	1.36	10.26	150.04	7.35	5.17	9.81	27.82

8	7	Sand	Stormwater	1.76	11.71	132.04	140.31	3.86	0.37	48.26
8	8	Sand+Soil	Stormwater	1.49	6.15	79.53	39.62	3.00	0.25	23.03
8	11	Sand+Soil	Stormwater	1.41	11.80	173.80	16.80	0.02	10.35	55.35
8	12	Sand	Stormwater	1.69	12.32	249.85	166.09	1.08	3.12	60.63
9	1	Sand	Stormwater	1.53	4.15	438.57	452.92	0.96	1.56	18.50
9	2	Sand+Soil	Stormwater	0.77	11.46	278.07	170.30	0.93	2.71	30.72
9	5	Sand	Stormwater	1.07	8.47	634.03	242.93	1.05	5.52	30.43
9	6	Sand+Soil	Stormwater	1.33	9.78	285.75	75.71	0.78	13.19	25.82
9	7	Sand	Stormwater	1.06	13.12	587.68	149.35	0.85	4.43	42.07
9	8	Sand+Soil	Stormwater	1.91	13.49	374.37	173.34	0.83	10.37	81.93
9	11	Sand+Soil	Stormwater	1.56	13.75	439.97	14.27	0.75	2.46	59.26
9	12	Sand	Stormwater	0.67	13.82	772.71	97.61	0.81	2.94	60.22
10	1	Sand	Stormwater	0.54	1.00	100.11	250.68	5.92	5.63	14.39
10	2	Sand+Soil	Stormwater	1.16	1.88	92.71	25.45	6.46	1.05	7.66
10	5	Sand	Stormwater	1.49	1.34	80.34	116.48	6.11	4.88	9.44
10	6	Sand+Soil	Stormwater	0.19	2.34	85.99	24.96	4.85	1.98	10.04
10	7	Sand	Stormwater	0.05	1.22	172.17	81.46	6.25	5.77	20.04
10	8	Sand+Soil	Stormwater	0.16	2.41	116.30	48.02	7.44	0.51	12.01
10	11	Sand+Soil	Stormwater	1.16	5.93	157.20	1.36	7.80	3.66	64.97
10	12	Sand	Stormwater	0.86	2.11	103.87	51.18	5.60	3.43	15.65

11	1	Sand	Stormwater	0.94	0.76	77.52	121.28	0.68	14.32	10.89
11	2	Sand+Soil	Stormwater	0.26	1.26	81.91	5.96	0.03	4.72	6.94
11	5	Sand	Stormwater	1.52	0.63	50.43	48.70	1.23	11.72	7.86
11	6	Sand+Soil	Stormwater	0.52	0.69	80.30	7.93	1.22	22.05	10.46
11	7	Sand	Stormwater	0.46	0.91	122.22	43.89	0.72	7.63	9.31
11	8	Sand+Soil	Stormwater	0.36	1.12	59.99	2.82	0.73	5.72	7.84
11	11	Sand+Soil	Stormwater	0.70	4.81	123.04	0.77	3.03	4.88	10.40
11	12	Sand	Stormwater	1.05	1.63	93.48	34.94	1.85	6.08	17.42
12	1	Sand	Stormwater	0.67	13.36	145.50	136.74	1.34	1.35	17.76
12	2	Sand+Soil	Stormwater	0.49	10.59	84.89	21.75	1.08	1.60	13.32
12	5	Sand	Stormwater	1.91	13.38	323.51	396.61	1.78	1.94	26.77
12	6	Sand+Soil	Stormwater	0.53	14.31	88.82	22.89	1.30	1.52	41.43
12	7	Sand	Stormwater	0.62	14.34	119.10	27.12	1.25	1.93	34.42
12	8	Sand+Soil	Stormwater	0.65	17.08	99.01	53.79	1.33	1.91	54.41
12	11	Sand+Soil	Stormwater	0.56	18.50	85.90	8.79	1.29	1.83	67.43
12	12	Sand	Stormwater	0.58	16.18	104.22	50.98	1.46	1.51	11.36

Table B-8. Eigenvalues of PCA for 32 stormwater quality parameters.

Principal Component Number	Eigenvalue	Percentage of Variance (%)	Cumulative (%)
1	**10.9**	**34.1**	**34.1**
2	**3.84**	**12.0**	**46.1**
3	**3.06**	**9.55**	**55.6**
4	**2.01**	**6.27**	**61.9**
5	**1.66**	**5.19**	**67.1**
6	**1.48**	**4.62**	**71.7**
7	**1.26**	**3.95**	**75.7**
8	0.96	3.00	78.7
9	0.926	2.89	81.6
10	0.699	2.18	83.7
11	0.645	2.02	85.8
12	0.634	1.98	87.7
13	0.550	1.72	89.5
14	0.530	1.66	91.1
15	0.383	1.19	92.3
16	0.371	1.16	93.5
17	0.324	1.01	94.5
18	0.305	0.954	95.4

19	0.260	0.812	96.3
20	0.226	0.705	96.9
21	0.192	0.600	97.6
22	0.165	0.516	98.1
23	0.133	0.417	98.5
24	0.108	0.336	98.8
25	0.0970	0.303	99.1
26	0.0753	0.235	99.4
27	0.0686	0.214	99.6
28	0.0518	0.162	99.7
29	0.0366	0.114	99.8
30	0.0309	0.096	99.9
31	0.0169	0.0527	100
32	0.00133	0.0042	100

Table B-9. Comparisons of stormwater quality parameters with road-runoff studies from cities worldwide, including urban density category, population density, and road type.

City	Density Category	Population density (people/km2)	Road Category	TSS (mg/L)	COD (mg/L)	NO3-N (mg/L)	NH4-N (mg/L)	TN (mg/L)	PO4 (mg/L)	Cr (µg/L)	Cu (µg/L)	Mn (µg/L)	Ni (µg/L)	Pb (µg/L)	Zn (µg/L)	Fe (µg/L)	MPs (particles/L)	Reference
Hong Kong (this study)	High	7044	Commercial roads	154.3	183.0	8.5	0.8	9.6	2.1	13.4	93.2	38.5	7.8	10.9	271.0	1092.5	230.1	
			Residential roads	160.9	264.1	10.4	0.9	11.7	2.6	14.1	60.8	39.6	7.0	9.6	205.6	849.7	291.2	
			Industrial roads	163.0	148.5	8.1	0.8	9.2	1.3	14.4	56.3	40.7	4.7	14.5	206.7	892.3	256	
Singapore	High	8387	Residential road	142.8	–	0.3	0.1	0.1	1.1	–	20.0	40.0	4.0	–	210.0	3000.0	–	(Song et al., 2019)
			Major road	23.8	–	0.5	0.2	0.1	1.1	–	20.0	20.0	7.0	–	130.0	680.0	–	
Beijing, China	High	8276	Asphalt road runoff	208.0	114.0	3.8	4.3	9.0	0.5	–	–	–	–	–	–	–	–	(W. Zhang et al., 2021)
Beijing, China	High	8276	General road	–	–	–	–	–	–	–	–	–	–	–	–	–	1.6-29.6	(J. Zhang et al., 2023)
Shenzhen, China	High	9054	Arterial road	148.7	45.4	–	–	–	0.4	–	–	–	–	–	–	–	–	(Liu et al., 2019)
			Residential area	208.9	110.4	–	–	–	0.6	–	–	–	–	–	–	–	–	
			Industrial area	56.6	61.1	–	–	–	0.2	–	–	–	–	–	–	–	–	
San Francisco Bay Area, California, USA	High	7194	General road	–	–	–	–	–	–	–	–	–	–	–	–	–	1.1-24.6	(Werbowski et al., 2021)
Munich, Germany	Moderate-low	4800	Highly trafficked road	85.1	–	–	–	–	–	13.3	82.8	–	6.4	5.8	261.0	–	–	(Rommel, Stinshoff, & Helmreich, 2021)
Tijuana, Mexico	High	6900	General road	–	–	–	–	–	–	–	–	–	–	–	–	–	88-289	(Piñon-Colin et al., 2020)

Melbourne, Australia	Moderate-low	5073	Industrial roads	–	–	–	–	–	–	–	–	–	–	–	–	–	35	(Kabir et al., 2024)
			Commercial roads	–	–	–	–	–	–	–	–	–	–	–	–	–	27	
			Residential roads	–	–	–	–	–	–	–	–	–	–	–	–	–	24	

REFERENCES

Abbasi, S. (2021). Microplastics washout from the atmosphere during a monsoon rain event. *Journal of Hazardous Materials Advances*, *4*, 100035.

Abdelkhalek, S., & Zayed, T. (2023). A multi-tier deterioration assessment models for sewer and stormwater pipelines in Hong Kong. *Journal of Environmental Management*, *345*, 118913. https://www.sciencedirect.com/science/article/abs/pii/S0301479723017012?via%3Dihub

Adegun, O. B., Ikudayisi, A. E., Morakinyo, T. E., & Olusoga, O. O. (2021). Urban green infrastructure in Nigeria: A review. *Scientific African*, *14*, e01044.

Ahiablame, L. M., Engel, B. A., & Chaubey, I. (2012). Effectiveness of low impact development practices: literature review and suggestions for future research. *Water, Air, & Soil Pollution*, *223*(7), 4253-4273.

Ahmad, T., Gul, S., Peng, L., Mehmood, T., Huang, Q., Ahmad, A., Ali, H., Ali, W., Souissi, S., & Zinck, P. (2025). Microplastic mitigation in urban stormwater using green infrastructure: a review. *Environmental chemistry letters*, 1-26.

Ahmed, F., & Borst, M. (2020). Tree box performance in exfiltrating stormwater runoff. *Water Environment Research*, *92*(1), 106-114.

Ahmed, S. F., Kumar, P. S., Rozbu, M. R., Chowdhury, A. T., Nuzhat, S., Rafa, N., Mahlia, T., Ong, H. C., & Mofijur, M. (2022). Heavy metal toxicity, sources, and remediation techniques for contaminated water and soil. *Environmental Technology & Innovation*, *25*, 102114.

Åkerlindh, G. (1950). Regnvädersavrinningens beskaffenhet. *The quality of storm water flow). Nord. Hyg. Tidskr*, *31*(1).

Almenar, J. B., Elliot, T., Rugani, B., Philippe, B., Gutierrez, T. N., Sonnemann, G., & Geneletti, D. (2021). Nexus between nature-based solutions, ecosystem services and urban challenges. *Land use policy*, *100*, 104898.

Andrady, A. L. (2011). Microplastics in the marine environment. *Marine pollution bulletin*, *62*(8), 1596-1605.

Aryal, R., Vigneswaran, S., Kandasamy, J., & Naidu, R. (2010). Urban stormwater quality and treatment. *Korean Journal of Chemical Engineering*, *27*, 1343-1359.

Ballo, S., Liu, M., Hou, L., & Chang, J. (2009). Pollutants in stormwater runoff in Shanghai (China): Implications for management of urban runoff pollution. *Progress in Natural Science*, *19*(7), 873-880.

Barbosa, A. E., Fernandes, J. N., & David, L. M. (2012). Key issues for sustainable urban stormwater management. *Water Research*, *46*(20), 6787-6798.

Behrouz, M. S., Yazdi, M. N., Sample, D. J., Scott, D., & Owen Jr, J. S. (2022). What are the relevant sources and factors affecting event mean concentrations (EMCs) of nutrients and sediment in stormwater? *Science of the Total Environment*, *828*, 154368.

Beom, J., Jeung, M., Choi, W., Her, Y., & Yoon, K. (2021). Characteristics of chloride loading from urban and agricultural watersheds during storm and non-storm periods. *Water Supply*, *21*(4), 1567-1579.

Berland, A., Shiflett, S. A., Shuster, W. D., Garmestani, A. S., Goddard, H. C., Herrmann, D. L., & Hopton, M. E. (2017). The role of trees in urban stormwater management. *Landscape and urban planning*, *162*, 167-177.

Besseling, E., Foekema, E. M., van den Heuvel-Greve, M. J., & Koelmans, A. A. (2017). The effect of microplastic on the uptake of chemicals by the lugworm Arenicola marina (L.) under environmentally relevant exposure conditions. *Environmental science & technology*, *51*(15), 8795-8804.

Biswal, B. K., Vijayaraghavan, K., Tsen-Tieng, D. L., & Balasubramanian, R. (2022). Biochar-based bioretention systems for removal of chemical and microbial pollutants from stormwater: A critical review. *Journal of Hazardous Materials*, *422*, 126886.

Björklund, K. (2011). *Sources and fluxes of organic contaminants in urban runoff*. Chalmers Tekniska Hogskola (Sweden).

Björklund, K., Bondelind, M., Karlsson, A., Karlsson, D., & Sokolova, E. (2018). Hydrodynamic modelling of the influence of stormwater and combined sewer overflows on receiving water quality: Benzo (a) pyrene and copper risks to recreational water. *Journal of Environmental Management*, *207*, 32-42.

Brezonik, P. L., & Stadelmann, T. H. (2002). Analysis and predictive models of stormwater runoff volumes, loads, and pollutant concentrations from watersheds in the Twin Cities metropolitan area, Minnesota, USA. *Water Research*, *36*(7), 1743-1757. https://doi.org/https://doi.org/10.1016/S0043-1354(01)00375-X

Briffa, J., Sinagra, E., & Blundell, R. (2020). Heavy metal pollution in the environment and their toxicological effects on humans. *Heliyon*, *6*(9).

Brown, R. A., & Borst, M. (2015). Nutrient infiltrate concentrations from three permeable pavement types. *Journal of Environmental Management*, *164*, 74-85.

Browne, M. A. (2015). Sources and pathways of microplastics to habitats. *Marine anthropogenic litter*, 229-244.

Campanale, C., Massarelli, C., Savino, I., Locaputo, V., & Uricchio, V. F. (2020). A detailed review study on potential effects of microplastics and additives of concern on human health. *International journal of environmental research and public health*, *17*(4), 1212.

Chaudhary, S., Chua, L. H., & Kansal, A. (2022). Event mean concentration and first flush from residential catchments in different climate zones. *Water Research*, *219*, 118594.

Chebbo, G. (1999). Characterisation of urban runoff pollution in Paris. *Wat Sci Tech*, *39*(2), 1-8.

Cheung, P. K., Hung, P. L., & Fok, L. (2019). River Microplastic Contamination and Dynamics upon a Rainfall Event in Hong Kong, China. *Environmental Processes*, *6*(1), 253-264. https://doi.org/10.1007/s40710-018-0345-0

Cho, Y., Shim, W. J., Ha, S. Y., Han, G. M., Jang, M., & Hong, S. H. (2023). Microplastic emission characteristics of stormwater runoff in an urban area: Intra-event variability and influencing factors. *Science of the Total Environment*, *866*, 161318.

Choi, J., Son, Y., Lee, S., Lee, Y., & Kim, L. H. (2013). Development of tree box filter LID system for treating road runoff. *Journal of wetlands research*, *15*(3), 407-412.

Chua, L. H., Lo, E. Y., Shuy, E., & Tan, S. B. (2009). Nutrients and suspended solids in dry weather and storm flows from a tropical catchment with various proportions of rural and urban land use. *Journal of Environmental Management*, *90*(11), 3635-3642.

Chui, T. W., Mar, B. W., & Horner, R. R. (1982). Pollutant loading model for highway runoff. *Journal of the Environmental Engineering Division*, *108*(6), 1193-1210.

Clapham, P. J., Young, S. B., & Brownell Jr, R. L. (1999). Baleen whales: conservation issues and the status of the most endangered populations. *Mammal review*, *29*(1), 37-62.

Codling, G., Yuan, H., Jones, P. D., Giesy, J. P., & Hecker, M. (2020). Metals and PFAS in stormwater and surface runoff in a semi-arid Canadian city subject to large variations in temperature among seasons. *Environmental Science and Pollution Research*, *27*(15), 18232-18241.

Cohen-Shacham, E., Walters, G., Janzen, C., & Maginnis, S. (2016). Nature-based solutions to address global societal challenges. *IUCN: Gland, Switzerland*, *97*(2016), 2036.

Da Silva, E. P., Filho, N. R. A., Pereira, J., & Martins Formiga, K. T. (2023). Temporal variation and risk assessment of heavy metals and nutrients from water and sediment in a stormwater pond, Brazil. *Water Supply*, *23*(1), 206-221.

Dannecker, W., Au, M., & Stechmann, H. (1990). Substance load in rainwater runoff from different streets in Hamburg. *Science of The Total Environment*, *93*, 385-392.

Davis, A. P., Shokouhian, M., & Ni, S. (2001). Loading estimates of lead, copper, cadmium, and zinc in urban runoff from specific sources. *Chemosphere*, *44*(5), 997-1009.

De Buyck, P.-J., Van Hulle, S. W., Dumoulin, A., & Rousseau, D. P. (2021). Roof runoff contamination: a review on pollutant nature, material leaching and deposition. *Reviews in Environmental Science and Bio/Technology*, *20*(2), 549-606.

Deletic, A. (1998). The first flush load of urban surface runoff. *Water Research*, *32*(8), 2462-2470.

Dierkes, C., Lucke, T., & Helmreich, B. (2015). General technical approvals for decentralised sustainable urban drainage systems (SUDS)—The current situation in Germany. *Sustainability*, *7*(3), 3031-3051.

Dietz, M. E. (2007). Low impact development practices: A review of current research and recommendations for future directions. *Water, air, and soil pollution*, *186*(1), 351-363.

Ding, T., Wei, L., Hou, Z., Li, J., Zhang, C., & Lin, D. (2022). Microplastics altered contaminant behavior and toxicity in natural waters. *Journal of Hazardous Materials*, *425*, 127908.

Division, U. S. E. P. A. W. P. (1982). *Results of the nationwide urban runoff program* (Vol. 1). Water planning division, US environmental protection Agency.

Do, T., Park, Y., Lim, B., Kim, S., Chae, M.-Y., & Chun, C.-H. (2023). Effect of the first-flush phenomenon on the quantification of microplastics in rainwater. *Marine pollution bulletin*, *187*, 114559.

Dong, J., Li, L., Liu, Q., Yang, M., Gao, Z., Qian, P., Gao, K., & Deng, X. (2022). Interactive effects of polymethyl methacrylate (PMMA) microplastics and salinity variation on a marine diatom Phaeodactylum tricornutum. *Chemosphere*, *289*, 133240.

Drapper, D., Tomlinson, R., & Williams, P. (2000). Pollutant concentrations in road runoff: Southeast Queensland case study. *Journal of Environmental Engineering*, *126*(4), 313-320.

Du, S., Zhu, R., Cai, Y., Xu, N., Yap, P.-S., Zhang, Y., He, Y., & Zhang, Y. (2021). Environmental fate and impacts of microplastics in aquatic ecosystems: a review. *RSC advances*, *11*(26), 15762-15784.

Du, X., Liang, H., Fang, X., Cui, S., & Li, J. (2021). Characteristics of colloids and their affinity for heavy metals in road runoff with different traffic in Beijing, China. *Environmental Science and Pollution Research*, *28*, 20082-20092.

Du, X., Zhu, Y., Han, Q., & Yu, Z. (2019). The influence of traffic density on heavy metals distribution in urban road runoff in Beijing, China. *Environmental Science and Pollution Research*, *26*, 886-895.

Eckart, K., McPhee, Z., & Bolisetti, T. (2017). Performance and implementation of low impact development–A review. *Science of The Total Environment*, *607*, 413-432.

Ekanayake, D., Loganathan, P., Johir, M. A. H., Kandasamy, J., & Vigneswaran, S. (2021). Enhanced removal of nutrients, heavy metals, and PAH from synthetic stormwater by incorporating different adsorbents into a filter media. *Water, Air, & Soil Pollution*, *232*, 1-12.

Elizalde-Velázquez, G. A., & Gómez-Oliván, L. M. (2021). Microplastics in aquatic environments: A review on occurrence, distribution, toxic effects, and implications for human health. *Science of the Total Environment*, *780*, 146551.

EPA, U. (2024). *Why Urban Waters?* https://www.epa.gov/urbanwaterspartners/why-urban-waters#:~:text=Urban%20waters%20take%20on%20large,stormwater%20runoff%20from%20urban%20landscapes.

EU. (2023). *Commission Regulation (EU) 2023/2055 of 25 September 2023 amending Annex XVII to Regulation (EC) No 1907/2006 of the European Parliament and of the Council concerning the Registration, Evaluation, Authorisation and Restriction of Chemicals (REACH) as regards synthetic polymer microparticles (Text with EEA relevance)*. https://eur-lex.europa.eu/legal-content/EN/TXT/?uri=uriserv%3AOJ.L_.2023.238.01.0067.01.ENG&toc=OJ%3AL%3A2023%3A238%3ATOC

Europe, P. (2023). Plastics – the fast Facts 2023. *PlasticEurope*, *1*. https://plasticseurope.org/knowledge-hub/plastics-the-fast-facts-2023/

Faisal, M., Wu, Z., Wang, H., Lin, X., Hussain, Z., & Azam, M. I. (2022). Potential heavy metals pollution contribution from wash-off of urban road-dust. *Toxics*, *10*(7), 397.

Farajollahi, M., Fahiminia, M., Fouladi-Fard, R., Rezaali, M., & Sorooshian, A. (2024). Human and ecological risk assessment, geo-accumulation, and source apportionment of road dust heavy metals in a semi-arid region of central Iran. *International Journal of Environmental Analytical Chemistry*, *104*(18), 6495-6518.

Färm, C. (2002). Metal sorption to natural filter substrates for storm water treatment—column studies. *Science of The Total Environment*, *298*(1-3), 17-24.

Fassman, E. A., & Blackbourn, S. (2010). Urban runoff mitigation by a permeable pavement system over impermeable soils. *Journal of Hydrologic Engineering*, *15*(6), 475-485.

Ferrans, P., Torres, M. N., Temprano, J., & Sánchez, J. P. R. (2022). Sustainable Urban Drainage System (SUDS) modeling supporting decision-making: A systematic quantitative review. *Science of The Total Environment*, *806*, 150447.

Fletcher, T. D., Shuster, W., Hunt, W. F., Ashley, R., Butler, D., Arthur, S., Trowsdale, S., Barraud, S., Semadeni-Davies, A., & Bertrand-Krajewski, J.-L. (2015). SUDS, LID, BMPs, WSUD and more–The evolution and application of terminology surrounding urban drainage. *Urban water journal*, *12*(7), 525-542.

Fok, L., & Cheung, P. K. (2015). Hong Kong at the Pearl River Estuary: A hotspot of microplastic pollution. *Marine pollution bulletin*, *99*(1-2), 112-118.

Gan, H., Zhuo, M., Li, D., & Zhou, Y. (2008). Quality characterization and impact assessment of highway runoff in urban and rural area of Guangzhou, China. *Environmental Monitoring and Assessment*, *140*(1), 147-159.

Gao, S., Wang, X., Li, H., Kong, Y., Chen, J., & Chen, Z. (2022). Heavy metals in road-deposited sediment and runoff in urban and intercity expressways. *Transportation Safety and Environment*, *4*(1), tdab030.

Gasperi, J., Sebastian, C., Ruban, V., Delamain, M., Percot, S., Wiest, L., Mirande, C., Caupos, E., Demare, D., & Kessoo, M. (2014). Micropollutants in urban stormwater: occurrence, concentrations, and atmospheric contributions for a wide range of contaminants in three French catchments. *Environmental Science and Pollution Research*, *21*(8), 5267-5281.

German, J., Vikstrom, M., Svensson, G., & Gustafsson, L. (2005). Integrated stormwater strategies to reduce impact on receiving waters. Proceedings of the 10th International Conference on Urban Drainage, Copenhagen/Denmark, 21th e26th August,

Geronimo, F. K. F., Maniquiz-Redillas, M. C., & Kim, L.-H. (2013). Treatment of parking lot runoff by a tree box filter. *Desalination and water treatment*, *51*(19-21), 4044-4049.

Ghofrani, Z., Sposito, V., & Faggian, R. (2017). A comprehensive review of blue-green infrastructure concepts. *International Journal of Environment and Sustainability*, *6*(1).

Gomes, P. I., & Wai, O. W. (2020). Investigation of Long-Term River Water Quality Trends in Hong Kong to Identify Role of Urbanization, Seasons and Pollution Sources. *Water, Air, & Soil Pollution*, *231*(7), 1-15.

Grabowski, Z. J., McPhearson, T., Matsler, A. M., Groffman, P., & Pickett, S. T. (2022). What is green infrastructure? A study of definitions in US city planning. *Frontiers in Ecology and the Environment*, *20*(3), 152-160.

Gronba-Chyła, A. (2022). Chloride content of street cleaning waste and its potential environmental impact. *Architecture Civil Engineering Environment*, *15*(1), 85--90.

Gupta, V. (2020). Vehicle-generated heavy metal pollution in an urban environment and its distribution into various environmental components. *Environmental Concerns and Sustainable Development: Volume 1: Air, Water and Energy Resources*, 113-127.

Hamel, P., Daly, E., & Fletcher, T. D. (2013). Source-control stormwater management for mitigating the impacts of urbanisation on baseflow: A review. *Journal of Hydrology*, *485*, 201-211.

Hathaway, J., Tucker, R., Spooner, J., & Hunt, W. (2012a). A traditional analysis of the first flush effect for nutrients in stormwater runoff from two small urban catchments. *Water, Air, & Soil Pollution*, *223*(9), 5903-5915.

Hathaway, J., Tucker, R., Spooner, J., & Hunt, W. (2012b). A traditional analysis of the first flush effect for nutrients in stormwater runoff from two small urban catchments. *Water, Air, & Soil Pollution*, *223*, 5903-5915.

Helmreich, B., Hilliges, R., Schriewer, A., & Horn, H. (2010). Runoff pollutants of a highly trafficked urban road–Correlation analysis and seasonal influences. *Chemosphere*, *80*(9), 991-997.

Hilliges, R., Schriewer, A., & Helmreich, B. (2013). A three-stage treatment system for highly polluted urban road runoff. *Journal of Environmental Management*, *128*, 306-312.

HKEPD. (2021). *Water Quality Impact-Enviromental Legislation, Standards and Guidelines*. Retrieved from https://www.epd.gov.hk/eia/register/report/eiareport/eia_2712021/DH_EIA/EIA/01%20HTML/DH_Chp05_v0.htm

HKHD. (2024). *Hong Kong: The Facts-Highways*. Retrieved from https://www.gov.hk/en/about/abouthk/factsheets/docs/highways.pdf#:~:text=Hong%20Kong's%20roads%20are%20among%20the%20most,a%20constant%20challenge%20to%20the%20highway%20engineers.

Ho, Y.-W., Lim, J. Y., Yeoh, Y. K., Chiou, J.-C., Zhu, Y., Lai, K. P., Li, L., Chan, P. K. S., & Fang, J. K.-H. (2022). Preliminary findings of the high quantity of microplastics in faeces of Hong Kong residents. *Toxics*, *10*(8), 414.

Hong Kong, O. (2021, 29 Nov 2023). *Climate of Hong Kong.* https://www.hko.gov.hk/en/cis/climahk.htm

Hong, N., Guan, Y., Yang, B., Zhong, J., Zhu, P., Ok, Y. S., Hou, D., Tsang, D. C., Guan, Y., & Liu, A. (2020). Quantitative source tracking of heavy metals contained in urban road deposited sediments. *Journal of Hazardous Materials*, *393*, 122362.

Hu, D., Zhang, C., Ma, B., Liu, Z., Yang, X., & Yang, L. (2020). The characteristics of rainfall runoff pollution and its driving factors in Northwest semiarid region of China-A case study of Xi'an. *Science of the Total Environment*, *726*, 138384.

Huang, C.-W., Li, Y.-L., Lin, C., Bui, X.-T., & Ngo, H. H. (2023). Seasonal influence on pollution index and risk of multiple compositions of microplastics in an urban river. *Science of the Total Environment*, *859*, 160021.

Huang, W., Song, B., Liang, J., Niu, Q., Zeng, G., Shen, M., Deng, J., Luo, Y., Wen, X., & Zhang, Y. (2021). Microplastics and associated contaminants in the aquatic environment: A review on their ecotoxicological effects, trophic transfer, and potential impacts to human health. *Journal of Hazardous Materials*, *405*, 124187.

Huang, Y., He, T., Yan, M., Yang, L., Gong, H., Wang, W., Qing, X., & Wang, J. (2021). Atmospheric transport and deposition of microplastics in a subtropical urban environment. *Journal of Hazardous Materials*, *416*, 126168.

Huber, M., Welker, A., & Helmreich, B. (2016). Critical review of heavy metal pollution of traffic area runoff: Occurrence, influencing factors, and partitioning. *Science of the Total Environment*, *541*, 895-919.

Hwang, H.-M., Fiala, M. J., Park, D., & Wade, T. L. (2016). Review of pollutants in urban road dust and stormwater runoff: part 1. Heavy metals released from vehicles. *International Journal of Urban Sciences*, *20*(3), 334-360.

Järlskog, I., Strömvall, A.-M., Magnusson, K., Galfi, H., Björklund, K., Polukarova, M., Garção, R., Markiewicz, A., Aronsson, M., & Gustafsson, M. (2021). Traffic-related microplastic particles, metals, and organic pollutants in an urban area under reconstruction. *Science of the Total Environment*, *774*, 145503.

Jayalakshmamma, M. P., Nagara, V. N., Borgaonkar, A., Sarkar, D., Sadik, O., & Boufadel, M. (2023). Characterizing microplastics in urban runoff: A multi-land use assessment with a focus on 1–125 µm size particles. *Science of the Total Environment*, *904*, 166685.

Jensen, D. M. R., Sandoval, S., Aubin, J.-B., Bertrand-Krajewski, J.-L., Xuyong, L., Mikkelsen, P. S., & Vezzaro, L. (2022). Classifying pollutant flush signals in stormwater using functional data analysis on TSS MV curves. *Water research*, *217*, 118394.

Jeong, H., Choi, J. Y., Lee, J., Lim, J., & Ra, K. (2020). Heavy metal pollution by road-deposited sediments and its contribution to total suspended solids in rainfall runoff from intensive industrial areas. *Environmental Pollution*, *265*, 115028. https://doi.org/https://doi.org/10.1016/j.envpol.2020.115028

Jeung, M., Baek, S., Beom, J., Cho, K. H., Her, Y., & Yoon, K. (2019). Evaluation of random forest and regression tree methods for estimation of mass first flush ratio in urban catchments. *Journal of Hydrology*, *575*, 1099-1110.

Kabir, A., Seking, M., Imai, T., & Yamamoto, K. (2020). Transportation pathways of land source based microplastics into the marine environments: The context of rivers. Proceedings of the 22nd IAHR-APD Congress,

Kabir, S. A., Bhuiyan, M. A., Zhang, G., & Pramanik, B. K. (2024). Microplastic distribution and ecological risks: investigating road dust and stormwater runoff across land uses. *Environmental Science: Advances*, *3*(1), 62-75.

Kabisch, N., Frantzeskaki, N., & Hansen, R. (2022). Principles for urban nature-based solutions. *Ambio*, *51*(6), 1388-1401.

Karakurt, O., Altuntaş, O., Şimşek, İ., Hatinoğlu, D., & Sanin, F. D. (2025). Microplastics from industrial sources: A known but overlooked problem. *Journal of Water Process Engineering*, *72*, 107487. https://doi.org/https://doi.org/10.1016/j.jwpe.2025.107487

Kayhanian, M., Fruchtman, B. D., Gulliver, J. S., Montanaro, C., Ranieri, E., & Wuertz, S. (2012). Review of highway runoff characteristics: Comparative analysis and universal implications. *Water Research*, *46*(20), 6609-6624.

Kayhanian, M., & Stenstrom, M. K. (2021). First flush phenomenon and its application for stormwater runoff management. 26-12), 6(*31* ,□□□□□□ □ □□ □□□□.

Kim, G., Yur, J., & Kim, J. (2007). Diffuse pollution loading from urban stormwater runoff in Daejeon city, Korea. *Journal of Environmental Management*, *85*(1), 9-16.

Koelmans, A. A., Bakir, A., Burton, G. A., & Janssen, C. R. (2016). Microplastic as a vector for chemicals in the aquatic environment: critical review and model-supported reinterpretation of empirical studies. *Environmental science & technology*, *50*(7), 3315-3326.

Kong, Z., Shao, Z., Shen, Y., Zhang, X., Chen, M., Yuan, Y., Li, G., Wei, Y., Hu, X., & Huang, Y. (2021). Comprehensive evaluation of stormwater pollutants characteristics, purification process and environmental impact after low impact development practices. *Journal of Cleaner Production*, *278*, 123509.

Kumar, R., Ivy, N., Bhattacharya, S., Dey, A., & Sharma, P. (2022). Coupled effects of microplastics and heavy metals on plants: Uptake, bioaccumulation, and environmental health perspectives. *Science of the Total Environment*, *836*, 155619.

Laist, D. W. (1997). Impacts of marine debris: entanglement of marine life in marine debris including a comprehensive list of species with entanglement and ingestion records. In *Marine debris* (pp. 99-139). Springer.

Lange, K., Österlund, H., Viklander, M., & Blecken, G.-T. (2022). Occurrence and concentration of 20–100 µm sized microplastic in highway runoff and its removal in a gross pollutant trap–Bioretention and sand filter stormwater treatment train. *Science of the Total Environment*, *809*, 151151.

Lee, H., Lau, S.-L., Kayhanian, M., & Stenstrom, M. K. (2004). Seasonal first flush phenomenon of urban stormwater discharges. *Water Research*, *38*(19), 4153-4163.

Lee, H., Swamikannu, X., Radulescu, D., Kim, S.-j., & Stenstrom, M. K. (2007). Design of stormwater monitoring programs. *Water Research*, *41*(18), 4186-4196.

Lee, J. H., & Bang, K. W. (2000). Characterization of urban stormwater runoff. *Water research*, *34*(6), 1773-1780.

Lee, S., Suits, M., Wituszynski, D., Winston, R., Martin, J., & Lee, J. (2020). Residential urban stormwater runoff: a comprehensive profile of microbiome and antibiotic resistance. *Science of the Total Environment*, *723*, 138033.

Leung, M. M.-L., Ho, Y.-W., Lee, C.-H., Wang, Y., Hu, M., Kwok, K. W. H., Chua, S.-L., & Fang, J. K.-H. (2021). Improved Raman spectroscopy-based approach to assess microplastics in seafood. *Environmental Pollution*, *289*, 117648.

Leung, M. M.-L., Ho, Y.-W., Maboloc, E. A., Lee, C.-H., Wang, Y., Hu, M., Cheung, S.-G., & Fang, J. K.-H. (2021). Determination of microplastics in the edible green-lipped mussel Perna viridis using an automated mapping technique of Raman microspectroscopy. *Journal of Hazardous Materials*, *420*, 126541.

Li, Q., Wang, F., Yu, Y., Huang, Z., Li, M., & Guan, Y. (2019). Comprehensive performance evaluation of LID practices for the sponge city construction: a case study in Guangxi, China. *Journal of Environmental Management*, *231*, 10-20.

Li, Y., Wei, M., Yu, B., Liu, L., & Xue, Q. (2022). Impact of simulating real microplastics on toluene removal from contaminated soil using thermally enhanced air injection. *Environmental Pollution*, *310*, 119895.

Liao, K.-H. (2019). The socio-ecological practice of building blue-green infrastructure in high-density cities: What does the ABC Waters Program in Singapore tell us? *Socio-Ecological Practice Research*, *1*(1), 67-81.

Liao, Z., He, Y., Huang, F., Wang, S., & Li, H. (2013). Analysis on LID for highly urbanized areas' waterlogging control: demonstrated on the example of Caohejing in Shanghai. *Water science and technology*, *68*(12), 2559-2567.

Lin, Y., Wang, Y., Ho, Y.-W., Fang, J. K.-H., & Li, Y. (2024). Characterization and ecological risks of microplastics in urban road runoff. *Science of the Total Environment*, *954*, 176590.

Lithner, D., Larsson, Å., & Dave, G. (2011). Environmental and health hazard ranking and assessment of plastic polymers based on chemical composition. *Science of the Total Environment*, *409*(18), 3309-3324.

Liu, H., Jia, Y., & Niu, C. (2017). "Sponge city" concept helps solve China's urban water problems. *Environmental Earth Sciences*, *76*(14), 1-5.

Liu, J., Hu, L. X., Deng, W. J., Ying, G. G., Hong, H., Tsang, E. P. K., & Barceló, D. (2022). Pilot Study of Pollution Characteristics and Ecological Risk of Disinfection Byproducts in Natural Waters in Hong Kong. *Environmental Toxicology and Chemistry*, *41*(10), 2613-2621. https://doi.org/10.1002/etc.5449

Liu, X., Liang, C., Zhou, M., Chang, Z., & Li, L. (2023). Exposure of Cyprinus carpio var. larvae to PVC microplastics reveals significant immunological alterations and irreversible histological organ damage. *Ecotoxicology and Environmental Safety*, *249*, 114377.

Liu, Y., Wang, C., Yu, Y., Chen, Y., Du, L., Qu, X., Peng, W., Zhang, M., & Gui, C. (2019). Effect of Urban Stormwater Road Runoff of Different Land Use Types on an Urban River in Shenzhen, China. *Water*, *11*(12), 2545. https://www.mdpi.com/2073-4441/11/12/2545

Lo, H. S., Po, B. H. K., Li, L., Wong, A. Y. M., Kong, R. Y. C., Li, L., Tse, W. K. F., Wong, C. K. C., Cheung, S. G., & Lai, K. P. (2021). Bisphenol A and its analogues in sedimentary microplastics of Hong Kong. *Marine pollution bulletin*, *164*, 112090.

Luo, Z., Su, X., Deng, Y., Deng, Z., Yang, S., Luo, X., Chen, J., Shi, L., & Chen, H. (2023). Insight into the pollution characteristics of road and roof runoff in Changsha, China. *Environmental Science and Pollution Research*, *30*(25), 67608-67620.

Lutz, N., Fogarty, J., & Rate, A. (2021). Accumulation and potential for transport of microplastics in stormwater drains into marine environments, Perth region, Western Australia. *Marine pollution bulletin*, *168*, 112362.

Ma, Y., Wang, S., Zhang, X., & Shen, Z. (2021). Transport process and source contribution of nitrogen in stormwater runoff from urban catchments. *Environmental Pollution*, *289*, 117824.

Maes, J., & Jacobs, S. (2017). Nature‐based solutions for Europe's sustainable development. *Conservation letters*, *10*(1), 121-124.

Mak, C. W., Tsang, Y. Y., Leung, M. M.-L., Fang, J. K.-H., & Chan, K. M. (2020). Microplastics from effluents of sewage treatment works and stormwater discharging into the Victoria Harbor, Hong Kong. *Marine pollution bulletin*, *157*, 111181.

Mamun, A. A., Shams, S., & Nuruzzaman, M. (2020). Review on uncertainty of the first-flush phenomenon in diffuse pollution control. *Applied Water Science*, *10*(1), 53.

Maniquiz-Redillas, M., Robles, M. E., Cruz, G., Reyes, N. J., & Kim, L.-H. (2022). First flush stormwater runoff in urban catchments: A bibliometric and comprehensive review. *Hydrology*, *9*(4), 63.

Mascarenhas, R., Santos, R., & Zeppelini, D. (2004). Plastic debris ingestion by sea turtle in Paraíba, Brazil. *Marine pollution bulletin*, *49*(4), 354-355.

McKee, A. M., & Cruz, M. A. (2021). Microbial and viral indicators of pathogens and human health risks from recreational exposure to waters impaired by fecal contamination. *Journal of Sustainable Water in the Built Environment*, *7*(2), 03121001.

Müller, A., Österlund, H., Marsalek, J., & Viklander, M. (2020). The pollution conveyed by urban runoff: A review of sources. *Science of The Total Environment*, *709*, 136125.

Müller, A., Österlund, H., Nordqvist, K., Marsalek, J., & Viklander, M. (2019). Building surface materials as sources of micropollutants in building runoff: A pilot study. *Science of The Total Environment*, *680*, 190-197.

Na, J., Song, J., Achar, J. C., & Jung, J. (2021). Synergistic effect of microplastic fragments and benzophenone-3 additives on lethal and sublethal Daphnia magna toxicity. *Journal of Hazardous Materials*, *402*, 123845.

Ngabe, B., Bidleman, T. F., & Scott, G. I. (2000). Polycyclic aromatic hydrocarbons in storm runoff from urban and coastal South Carolina. *Science of The Total Environment*, *255*(1-3), 1-9.

Niazkar, M., Evangelisti, M., Peruzzi, C., Galli, A., Maglionico, M., & Masseroni, D. (2024). Investigating first flush occurrence in agro-urban environments in Northern Italy. *Water*, *16*(6), 891.

Österlund, H., Blecken, G., Lange, K., Marsalek, J., Gopinath, K., & Viklander, M. (2023). Microplastics in urban catchments: Review of sources, pathways, and entry into stormwater. *Science of the Total Environment*, *858*, 159781.

Pan, Z., Liu, Q., Jiang, R., Li, W., Sun, X., Lin, H., Jiang, S., & Huang, H. (2021). Microplastic pollution and ecological risk assessment in an estuarine environment: The Dongshan Bay of China. *Chemosphere*, *262*, 127876.

Pannetier, P., Morin, B., Le Bihanic, F., Dubreil, L., Clérandeau, C., Chouvellon, F., Van Arkel, K., Danion, M., & Cachot, J. (2020). Environmental samples of microplastics induce significant toxic effects in fish larvae. *Environment international*, *134*, 105047.

Perera, T., McGree, J., Egodawatta, P., Jinadasa, K., & Goonetilleke, A. (2019). Taxonomy of influential factors for predicting pollutant first flush in urban stormwater runoff. *Water Research*, *166*, 115075.

Perera, T., McGree, J., Egodawatta, P., Jinadasa, K., & Goonetilleke, A. (2021). New conceptualisation of first flush phenomena in urban catchments. *Journal of Environmental Management*, *281*, 111820.

Peter, K. T., Hou, F., Tian, Z., Wu, C., Goehring, M., Liu, F., & Kolodziej, E. P. (2020). More than a first flush: Urban creek storm hydrographs demonstrate broad contaminant pollutographs. *Environmental science & technology*, *54*(10), 6152-6165.

Petrucci, G., Gromaire, M.-C., Shorshani, M. F., & Chebbo, G. (2014). Nonpoint source pollution of urban stormwater runoff: a methodology for source analysis. *Environmental Science and Pollution Research*, *21*(17), 10225-10242.

Piñon-Colin, T. d. J., Rodriguez-Jimenez, R., Rogel-Hernandez, E., Alvarez-Andrade, A., & Wakida, F. T. (2020). Microplastics in stormwater runoff in a semiarid region, Tijuana, Mexico. *Science of the Total Environment*, *704*, 135411. https://doi.org/https://doi.org/10.1016/j.scitotenv.2019.135411

Piscitello, A., Bianco, C., Casasso, A., & Sethi, R. (2021). Non-exhaust traffic emissions: Sources, characterization, and mitigation measures. *Science of the Total Environment*, *766*, 144440. https://doi.org/https://doi.org/10.1016/j.scitotenv.2020.144440

Pizzichetti, A. R. P., Pablos, C., Álvarez-Fernández, C., Reynolds, K., Stanley, S., & Marugán, J. (2023). Kinetic and mechanistic analysis of membrane fouling in microplastics removal from water by dead-end microfiltration. *Journal of Environmental Chemical Engineering*, *11*(2), 109338.

Pradhan, S., Ram, M. M., & Mishra, S. (2021). An overview on potential hydrometallurgical processes for separation and recovery of manganese. *Metallurgical and Materials Engineering*, *27*(2), 243-258.

Pratt, C. J. (1995). A Review of Source Control of Urban Stormwater Runoff 1. *Water and Environment Journal*, *9*(2), 132-139.

Qiao-ling, Q. About Concept, Idea and Practice of" Subsided Green Space.

Rakib, M. R. J., Sarker, A., Ram, K., Uddin, M. G., Walker, T. R., Chowdhury, T., Uddin, J., Khandaker, M. U., Rahman, M. M., & Idris, A. M. (2023). Microplastic toxicity in aquatic organisms and aquatic ecosystems: a review. *Water, Air, & Soil Pollution*, *234*(1), 52.

Raymond, C. M., Frantzeskaki, N., Kabisch, N., Berry, P., Breil, M., Nita, M. R., Geneletti, D., & Calfapietra, C. (2017). A framework for assessing and implementing the co-benefits of nature-based solutions in urban areas. *Environmental science & policy*, *77*, 15-24.

Rico, A., Redondo-Hasselerharm, P. E., Vighi, M., Waichman, A. V., de Souza Nunes, G. S., de Oliveira, R., Singdahl-Larsen, C., Hurley, R., Nizzetto, L., & Schell, T. (2023). Large-scale monitoring and risk assessment of microplastics in the Amazon River. *Water Research*, *232*, 119707.

Rochman, C. M., Tahir, A., Williams, S. L., Baxa, D. V., Lam, R., Miller, J. T., Teh, F.-C., Werorilangi, S., & Teh, S. J. (2015). Anthropogenic debris in seafood: Plastic debris and fibers from textiles in fish and bivalves sold for human consumption. *Scientific reports*, *5*(1), 1-10.

Rommel, S. H., Stinshoff, P., & Helmreich, B. (2021). Sequential extraction of heavy metals from sorptive filter media and sediments trapped in stormwater quality improvement devices for road runoff. *Science of The Total Environment*, *782*, 146875.

Roseen, R. M., Ballestero, T. P., Houle, J. J., Briggs, J. F., & Houle, K. M. (2012). Water Quality and Hydrologic Performance of a Porous Asphalt Pavement as a Storm-Water Treatment Strategy in a Cold Climate. *Journal of Environmental Engineering*, *138*(1), 81-89. https://doi.org/doi:10.1061/(ASCE)EE.1943-7870.0000459

Rosso, B., Bravo, B., Gregoris, E., Barbante, C., Gambaro, A., & Corami, F. (2023). Quantification and Chemical Characterization of Plastic Additives and Small Microplastics (< 100 μm) in Highway Road Dust. *Toxics*, *11*(11), 936.

Rosso, B., Corami, F., Vezzaro, L., Biondi, S., Bravo, B., Barbante, C., & Gambaro, A. (2022). Quantification and characterization of additives, plasticizers, and small microplastics (5–100 μm) in highway stormwater runoff. *Journal of Environmental Management*, *324*, 116348.

Roy, B. N., Roy, H., Rahman, K. S., Mahmud, F., Bhuiyan, M. M. K., Hasan, M., Bhuiyan, A.-A. K., Hasan, M., Mahbub, M. S., & Jahedi, R. M. (2024). Principal component analysis incorporated water quality index modeling for Dhaka-based rivers. *City and Environment interactions*, *23*, 100150.

Roy, S., Gupta, S. K., Prakash, J., Habib, G., & Kumar, P. (2022). A global perspective of the current state of heavy metal contamination in road dust. *Environmental Science and Pollution Research*, 1-22.

Saget, A., Chebbo, G., & Bertrand-Krajewski, J.-L. (1996). The first flush in sewer systems. *Water Science and Technology*, *33*(9), 101-108.

Salazar-Rojas, T., Cejudo-Ruiz, F. R., Gutiérrez-Soto, M. V., & Calvo-Brenes, G. (2023). Assessing heavy metal pollution load index (PLI) in biomonitors and road dust from vehicular emission by magnetic properties modeling. *Environmental Science and Pollution Research*, *30*(39), 91248-91261.

Sarkar, C., Lai, K. Y., Kumari, S., Leung, G. M., Webster, C., & Ni, M. Y. (2021). Characteristics of the residential environment and their association with depression in Hong Kong. *JAMA Network Open*, *4*(10), e2130777-e2130777.

Sartor, J. D., & Boyd, G. B. (1972). *Water pollution aspects of street surface contaminants* (Vol. 2). US Government Printing Office.

Senathirajah, K., Attwood, S., Bhagwat, G., Carbery, M., Wilson, S., & Palanisami, T. (2021). Estimation of the mass of microplastics ingested–A pivotal first step towards human health risk assessment. *Journal of Hazardous Materials*, *404*, 124004.

Shao, L., Li, Y., Jones, T., Santosh, M., Liu, P., Zhang, M., Xu, L., Li, W., Lu, J., & Yang, C.-X. (2022). Airborne microplastics: A review of current perspectives and environmental implications. *Journal of Cleaner Production*, *347*, 131048.

Sharma, R., & Malaviya, P. (2021). Management of stormwater pollution using green infrastructure: The role of rain gardens. *Wiley Interdisciplinary Reviews: Water*, *8*(2), e1507.

Shen, Z., Liu, J., Aini, G., & Gong, Y. (2016). A comparative study of the grain-size distribution of surface dust and stormwater runoff quality on typical urban roads and roofs in Beijing, China. *Environmental Science and Pollution Research*, *23*, 2693-2704.

Shi, M., Zhu, J., Hu, T., Xu, A., Mao, Y., Liu, L., Zhang, Y., She, Z., Li, P., & Qi, S. (2023). Occurrence, distribution and risk assessment of microplastics and polycyclic aromatic hydrocarbons in East lake, Hubei, China. *Chemosphere*, *316*, 137864.

Shoemaker, L., Lahlou, M., Doll, A., Cazenas, P., & Tech, T. (2000). Stormwater best management practices in an ultra-urban setting: selection and monitoring.

Shruti, V., & Kutralam-Muniasamy, G. (2023). Blanks and bias in microplastic research: Implications for future quality assurance. *Trends in Environmental Analytical Chemistry*, *38*, e00203.

Shruti, V., Pérez-Guevara, F., Elizalde-Martínez, I., & Kutralam-Muniasamy, G. (2021). Current trends and analytical methods for evaluation of microplastics in stormwater. *Trends in Environmental Analytical Chemistry*, *30*, e00123.

Shruti, V. C., Pérez-Guevara, F., Elizalde-Martínez, I., & Kutralam-Muniasamy, G. (2021). Current trends and analytical methods for evaluation of microplastics in stormwater. *Trends in Environmental Analytical Chemistry*, *30*, e00123. https://doi.org/https://doi.org/10.1016/j.teac.2021.e00123

Si, W., Gu, Q., Yin, Y., Luo, X., Xia, M., Li, X., Zhong, M., & Hu, Y. (2024). Performance optimization of novel wear-resistant reflective cooling coatings for asphalt pavement. *Construction and Building Materials*, *455*, 139207.

Silva, C. J., Silva, A. L. P., Gravato, C., & Pestana, J. L. (2019). Ingestion of small-sized and irregularly shaped polyethylene microplastics affect Chironomus riparius life-history traits. *Science of the Total Environment*, *672*, 862-868.

Smith, J. S., Winston, R. J., Tirpak, R. A., Wituszynski, D. M., Boening, K. M., & Martin, J. F. (2020). The seasonality of nutrients and sediment in residential stormwater runoff: Implications for nutrient-sensitive waters. *Journal of Environmental Management*, *276*, 111248.

Song, H., Qin, T., Wang, J., & Wong, T. H. F. (2019). Characteristics of Stormwater Quality in Singapore Catchments in 9 Different Types of Land Use. *Water*, *11*(5), 1089. https://www.mdpi.com/2073-4441/11/5/1089

Sriwiboon, M., Koetniyom, S., Rhee, S. K., Sukultanasorn, J., & Kaewlob, K. (2021). *An Investigation of Property Changes of Copper-Free Brake Pads During Wear Testing: Pressure and Temperature Dependence of Pad Modulus, and the Correlation Between Modulus and Friction Coefficient* (0148-7191).

Stang, C., Mohamed, B. A., & Li, L. Y. (2022). Microplastic removal from urban stormwater: Current treatments and research gaps. *Journal of Environmental Management*, *317*, 115510.

Stinshoff, P., Busse, L., Kick, D., & Helmreich, B. (2025). Stormwater treatment in infiltration swales with an engineered and planted soil media–Results of a pilot-scale approach. *Journal of Environmental Management*, *385*, 125693.

Strady, E., Kieu-Le, T.-C., Tran, Q.-V., & Thuong, Q.-T. (2021). Microplastic in atmospheric fallouts of a developing Southeast Asian megacity under tropical climate. *Chemosphere*, *272*, 129874.

Sugiura, M., Takada, H., Takada, N., Mizukawa, K., Tsuyuki, S., & Furumai, H. (2021). Microplastics in urban wastewater and estuarine water: Importance of street runoff. *Environmental Monitoring and Contaminants Research*, *1*, 54-65.

Sullivan, K., Thomas, S., & Rosano, M. (2018). Using industrial ecology and strategic management concepts to pursue the Sustainable Development Goals. *Journal of Cleaner Production*, *174*, 237-246. https://doi.org/https://doi.org/10.1016/j.jclepro.2017.10.201

Sun, X., Jia, Q., Ye, J., Zhu, Y., Song, Z., Guo, Y., & Chen, H. (2023). Real-time variabilities in microplastic abundance and characteristics of urban surface runoff and sewer overflow in wet weather as impacted by land use and storm factors. *Science of the Total Environment*, *859*, 160148.

Sun, Y., Deng, L., Pan, S.-Y., Chiang, P.-C., Sable, S. S., & Shah, K. J. (2020). Integration of green and gray infrastructures for sponge city: Water and energy nexus. *Water-Energy Nexus*, *3*, 29-40.

Taka, M., Sillanpää, N., Niemi, T., Warsta, L., Kokkonen, T., & Setälä, H. (2022). Heavy metals from heavy land use? Spatio-temporal patterns of urban runoff metal loads. *Science of the Total Environment*, *817*, 152855.

Tamis, J. E., Koelmans, A. A., Dröge, R., Kaag, N. H., Keur, M. C., Tromp, P. C., & Jongbloed, R. H. (2021). Environmental risks of car tire microplastic particles and other road runoff pollutants. *Microplastics and Nanoplastics*, *1*(1), 1-17.

Tan, Y., Song, J., Yu, L., Bai, Y., Zhang, J., Chan, M.-H., & van Ameijde, J. (2024). The mechanism of street markets fostering supportive communities in old urban districts: A case study of Sham Shui Po, Hong Kong. *Land*, *13*(3), 289.

Tanaka, K., & Takada, H. (2016). Microplastic fragments and microbeads in digestive tracts of planktivorous fish from urban coastal waters. *Scientific reports*, *6*(1), 1-8.

Tanaka, K., Takada, H., Yamashita, R., Mizukawa, K., Fukuwaka, M.-a., & Watanuki, Y. (2015). Facilitated leaching of additive-derived PBDEs from plastic by seabirds' stomach oil and accumulation in tissues. *Environmental science & technology*, *49*(19), 11799-11807.

Thompson, R. C., Olsen, Y., Mitchell, R. P., Davis, A., Rowland, S. J., John, A. W., McGonigle, D., & Russell, A. E. (2004). Lost at sea: where is all the plastic? *Science*, *304*(5672), 838-838.

Treilles, R., Gasperi, J., Gallard, A., Saad, M., Dris, R., Partibane, C., Breton, J., & Tassin, B. (2021). Microplastics and microfibers in urban runoff from a suburban catchment of Greater Paris. *Environmental Pollution*, *287*, 117352.

Tripathi, M., & Singal, S. K. (2019). Use of principal component analysis for parameter selection for development of a novel water quality index: a case study of river Ganga India. *Ecological indicators*, *96*, 430-436.

Tsang, Y., Mak, C., Liebich, C., Lam, S., Sze, E. T., & Chan, K. (2017). Microplastic pollution in the marine waters and sediments of Hong Kong. *Marine pollution bulletin*, *115*(1-2), 20-28.

Tsihrintzis, V. A., & Hamid, R. (1997). Modeling and management of urban stormwater runoff quality: a review. *Water resources management*, *11*(2), 136-164.

Tunali, M., Adam, V., & Nowack, B. (2023). Probabilistic environmental risk assessment of microplastics in soils. *Geoderma*, *430*, 116315.

Tuttolomondo, T., Virga, G., Licata, M., Leto, C., & La Bella, S. (2020). Constructed wetlands as sustainable technology for the treatment and reuse of the first-flush stormwater in agriculture—A case study in Sicily (Italy). *Water*, *12*(9), 2542.

UN, U. N. (2024). *Assessing the status of implementation of the Programme of Action of the International Conference on Population and Development and its contribution to the follow-up and review of the 2030 Agenda for Sustainable Development during the decade of action and delivery for sustainable development*. https://www.un.org/development/desa/pd/sites/www.un.org.development.desa.pd/files/undesa_pd_2024_e_cn.9_2024_2_advance-unedited.pdf

Vaze, J., & Chiew, F. H. (2002). Experimental study of pollutant accumulation on an urban road surface. *Urban Water*, *4*(4), 379-389.

Vo, H. C., & Pham, M. H. (2021). Ecotoxicological effects of microplastics on aquatic organisms: a review. *Environmental Science and Pollution Research*, *28*, 44716-44725.

Waara, S., & Johansson, F. (2022). Ecological risk assessment of trace elements accumulated in stormwater ponds within industrial areas. *Environmental Science and Pollution Research*, *29*(18), 27026-27041.

Wagner, M., Scherer, C., Alvarez-Muñoz, D., Brennholt, N., Bourrain, X., Buchinger, S., Fries, E., Grosbois, C., Klasmeier, J., & Marti, T. (2014). Microplastics in freshwater ecosystems: what we know and what we need to know. *Environmental Sciences Europe*, *26*(1), 1-9.

Wang, S., Feng, L., & Min, F. (2023). Optimizing first flush diverter for urban stormwater pollution load reduction by most efficiently utilizing first flush phenomena. *Journal of Environmental Management*, *335*, 117563.

Wang, S., He, Q., Ai, H., Wang, Z., & Zhang, Q. (2013). Pollutant concentrations and pollution loads in stormwater runoff from different land uses in Chongqing. *Journal of Environmental Sciences*, *25*(3), 502-510.

Wang, S., Ma, Y., Zhang, X., & Shen, Z. (2022). Transport and sources of nitrogen in stormwater runoff at the urban catchment scale. *Science of the Total Environment*, *806*, 150281.

Wang, Y., Zhong, Z., Chen, X., Sokolova, I., Ma, L., Yang, Q., Qiu, K., Khan, F. U., Tu, Z., & Guo, B. (2024). Microplastic pollution and ecological risk assessment of Yueqing Bay affected by intensive human activities. *Journal of hazardous materials*, *461*, 132603.

Wei, L., Yue, Q., Chen, G., & Wang, J. (2023). Microplastics in rainwater/stormwater environments: Influencing factors, sources, transport, fate, and removal techniques. *TrAC Trends in Analytical Chemistry*, *165*, 117147.

Weibel, S. R., Anderson, R. J., & Woodward, R. L. (1964). Urban land runoff as a factor in stream pollution. *Journal (Water Pollution Control Federation)*, 914-924.

Welsh, K., & Sánchez-Murillo, R. (2020). Rainfall, groundwater, and surface water isotope data from extreme tropical cyclones (2016-2019) within the Caribbean Sea and Atlantic Ocean basins. *Data in Brief*, *30*, 105633.

Werbowski, L. M., Gilbreath, A. N., Munno, K., Zhu, X., Grbic, J., Wu, T., Sutton, R., Sedlak, M. D., Deshpande, A. D., & Rochman, C. M. (2021). Urban Stormwater Runoff: A Major Pathway for Anthropogenic Particles, Black Rubbery Fragments, and Other Types of Microplastics to Urban Receiving Waters. *ACS ES&T Water*, *1*(6), 1420-1428. https://doi.org/10.1021/acsestwater.1c00017

Wicke, D., Matzinger, A., Sonnenberg, H., Caradot, N., Schubert, R.-L., Dick, R., Heinzmann, B., Dünnbier, U., von Seggern, D., & Rouault, P. (2021). Micropollutants in urban stormwater runoff of different land uses. *Water*, *13*(9), 1312.

Wiseman, C. L. S., Levesque, C., & Rasmussen, P. E. (2021). Characterizing the sources, concentrations and resuspension potential of metals and metalloids in the thoracic fraction of urban road dust. *Science of the Total Environment*, *786*, 147467. https://doi.org/https://doi.org/10.1016/j.scitotenv.2021.147467

Wright, S. L., & Kelly, F. J. (2017). Plastic and human health: a micro issue? *Environmental science & technology*, *51*(12), 6634-6647.

Wróblewska, K., & Jeong, B. R. (2021). Effectiveness of plants and green infrastructure utilization in ambient particulate matter removal. *Environmental Sciences Europe*, *33*(1), 110.

Xia, J., Zhang, Y., Xiong, L., He, S., Wang, L., & Yu, Z. (2017). Opportunities and challenges of the Sponge City construction related to urban water issues in China. *Science China Earth Sciences*, *60*(4), 652-658.

Xiang, P., Zhang, Y., Zhang, T., Wu, Q., Zhao, C., & Li, Q. (2023). A novel bacterial combination for efficient degradation of polystyrene microplastics. *Journal of Hazardous Materials*, *458*, 131856.

Xie, N., Akin, M., & Shi, X. (2019). Permeable concrete pavements: A review of environmental benefits and durability. *Journal of Cleaner Production*, *210*, 1605-1621. https://doi.org/https://doi.org/10.1016/j.jclepro.2018.11.134

Xu, C., Zhang, B., Gu, C., Shen, C., Yin, S., Aamir, M., & Li, F. (2020). Are we underestimating the sources of microplastic pollution in terrestrial environment? *Journal of Hazardous Materials*, *400*, 123228.

Xu, K., Zhang, Y., Huang, Y., & Wang, J. (2021). Toxicological effects of microplastics and phenanthrene to zebrafish (Danio rerio). *Science of the Total Environment*, *757*, 143730.

Xu, P., Peng, G., Su, L., Gao, Y., Gao, L., & Li, D. (2018). Microplastic risk assessment in surface waters: A case study in the Changjiang Estuary, China. *Marine pollution bulletin*, *133*, 647-654.

Xue, H., Zhao, L., & Liu, X. (2020). Characteristics of heavy metal pollution in road runoff in the Nanjing urban area, East China. *Water Science and Technology*, *81*(9), 1961-1971.

Yan, L., Chengqing, Y., & Wu, C. (2008). Application of grassed swales in urban non-point source pollution control. *Chinese Journal of Environmental Engineering*, *2*(3), 334-339.

Yang, Z., Wang, Y., Shen, Z., Niu, J., & Tang, Z. (2009). Distribution and speciation of heavy metals in sediments from the mainstream, tributaries, and lakes of the Yangtze River catchment of Wuhan, China. *Journal of Hazardous Materials*, *166*(2-3), 1186-1194.

Yano, K. A., Geronimo, F. K., Reyes, N. J., & Kim, L. H. (2021). Characterization and comparison of microplastic occurrence in point and non-point pollution sources. *Science of the Total Environment*, *797*, 148939.

Ying, J., Zhang, X., Zhang, Y., & Bilan, S. (2022). Green infrastructure: Systematic literature review. *Economic research-Ekonomska istraživanja*, *35*(1), 343-366.

Yonkos, L. T., Friedel, E. A., Perez-Reyes, A. C., Ghosal, S., & Arthur, C. D. (2014). Microplastics in four estuarine rivers in the Chesapeake Bay, USA. *Environmental science & technology*, *48*(24), 14195-14202.

Yuan, J., Passeport, E., & Hofmann, R. (2022). Understanding adsorption and biodegradation in granular activated carbon for drinking water treatment: A critical review. *Water Research*, *210*, 118026.

Yufen, R., Xiaoke, W., Zhiyun, O., Hua, Z., Xiaonan, D., & Hong, M. (2008). Stormwater runoff quality from different surfaces in an urban catchment in Beijing, China. *Water Environment Research*, *80*(8), 719-724.

Zacharias, J. (2021). Pedestrian dynamics on narrow pavements in high-density Hong Kong. *Journal of Urban Management*, *10*(4), 409-418.

Zgheib, S., Moilleron, R., & Chebbo, G. (2012). Priority pollutants in urban stormwater: Part 1–Case of separate storm sewers. *Water Research*, *46*(20), 6683-6692.

Zhai, W., Bai, L., Zhou, R., Fan, X., Kang, G., Liu, Y., & Zhou, K. (2021). Recent progress on wear‐resistant materials: designs, properties, and applications. *Advanced Science*, *8*(11), 2003739.

Zhang, H. Z., & Li, H. M. (2014). Influencing factors analysis on sunken Greenbelt design of urban road. *Applied Mechanics and Materials*, *638*, 1158-1161.

Zhang, J., Ding, W., Zou, G., Wang, X., Zhao, M., Guo, S., & Chen, Y. (2023). Urban pipeline rainwater runoff is an important pathway for land-based microplastics transport to inland surface water: A case study in Beijing. *Sci Total Environ*, *861*, 160619. https://doi.org/10.1016/j.scitotenv.2022.160619

Zhang, K., Xu, S., Zhang, Y., Lo, Y., Liu, M., Ma, Y., Chau, H. S., Cao, Y., Xu, X., & Wu, R. (2022). A systematic study of microplastic occurrence in urban water networks of a metropolis. *Water Research*, *223*, 118992.

Zhang, K., Yong, F., McCarthy, D. T., & Deletic, A. (2018). Predicting long term removal of heavy metals from porous pavements for stormwater treatment. *Water Research*, *142*, 236-245.

Zhang, M., Chen, H., Wang, J., & Pan, G. (2010). Rainwater utilization and storm pollution control based on urban runoff characterization. *Journal of Environmental Sciences*, *22*(1), 40-46.

Zhang, P., Dong, Y., Guo, Y., Wang, C., Wang, G., Ma, Z., Zhou, W., Zhang, D., Ren, Z., & Wang, W. (2023). Urban forest soil is becoming alkaline under rapid urbanization: A case study of Changchun, northeast China. *Catena*, *224*, 106993.

Zhang, Q., Wang, X., Hou, P., Wan, W., Ren, Y., Ouyang, Z., & Yang, L. (2013). The temporal changes in road stormwater runoff quality and the implications to first flush control in Chongqing, China. *Environmental monitoring and assessment*, *185*(12), 9763-9775.

Zhang, W., Li, J., Sun, H., & Che, W. (2021). Pollutant first flush identification and its implications for urban runoff pollution control: a roof and road runoff case study in Beijing, China. *Water Science and Technology*, *83*(11), 2829-2840. https://doi.org/10.2166/wst.2021.157

Zhang, W., Qu, P., Sun, H., & Che, W. (2023). Assessing the characteristics of different-sized particles in the first flush of roof runoff. *Water Science & Technology*, *87*(9), 2265-2276.

Zhang, Y., Jiang, H., Bian, K., Wang, H., & Wang, C. (2021). A critical review of control and removal strategies for microplastics from aquatic environments. *Journal of Environmental Chemical Engineering*, *9*(4), 105463.

Zhang, Z., Qi, H., Chen, H., Zhang, X., Tan, C., Bai, X., Gong, Y., & Li, H. (2023). The control efficiency and mechanism of heavy metals by permeable pavement system in runoff based on enhanced infiltration materials. *Journal of Environmental Management*, *329*, 117042.

Zhao, H., Ma, Y., Fang, J., Hu, L., & Li, X. (2022). Particle size distribution and total suspended solid concentrations in urban surface runoff. *Science of the Total Environment*, *815*, 152533.

Zhao, J.-w., Shan, B.-q., & Yin, C.-q. (2007). Pollutant loads of surface runoff in Wuhan City Zoo, an urban tourist area. *Journal of Environmental Sciences*, *19*(4), 464-468.

Zhao, M., Cheng, C., Zhou, Y., Li, X., Shen, S., & Song, C. (2021). A global dataset of annual urban extents (1992–2020) from harmonized nighttime lights. *Earth System Science Data Discussions*, *2021*, 1-25.

Zhong-hua, D. (2016). The Application of the Concept of Sponge City on Urban Road Engineering. *Construction & Design for Engineering*.

Zhou, Y., Wang, J., Zou, M., Jia, Z., Zhou, S., & Li, Y. (2020). Microplastics in soils: A review of methods, occurrence, fate, transport, ecological and environmental risks. *Science of the Total Environment*, *748*, 141368.